ON WESTERN JUNIPER CLIMATE RELATIONS

by

SCHYLER AINSWORTH REIS

A DISSERTATION

Presented to the Environmental Studies Program
and the Division of Graduate Studies of the University of Oregon
in partial fulfillment of the requirements
for the degree of
Doctor of Philosophy

September 2022

DISSERTATION APPROVAL PAGE

Student: Schyler Ainsworth Reis

Title: On Western Juniper Climate Relations

This dissertation has been accepted and approved in partial fulfillment of the requirements for the Doctor of Philosophy degree in the Environmental Sciences, Studies, and Policy by:

Lucas Silva	Chairperson
Dan Gavin	Core Member
Carolyn Fish	Core Member
Peter Ralph	Institutional Representative

and

Krista Chronister   Vice Provost for Graduate Studies

Original approval signatures are on file with the University of Oregon Division of Graduate Studies.

Degree awarded September 2022

DISSERTATION ABSTRACT

Schyler Ainsworth Reis

Doctor of Philosophy

Environmental Sciences, Studies, and Policy

September 2022

Title: On Western Juniper Climate Relations

Western juniper woodlands are highly sensitive to climate in terms of tree-ring growth, seedling establishment and range distribution. Understanding the dynamics of western juniper woodlands to changes in precipitation, temperature, and atmospheric CO_2 levels is an important component in the development of the next generation of ecological models, natural resource policies, and land management actions. Increased atmospheric CO_2 has been hypothesized to reduce the impact of drought through an increase in intrinsic water use efficiency. However, whether this increase in drought tolerance will mitigate predicted increases in temperature and decreases in precipitation in poorly understood. Additionally, potential geospatial patterns of changes in sensitivity to climate, and differential responses of competing plant species warrants further investigation.

Recent projection models focused on the rangelands of Oregon retain a high level of uncertainty regarding the dynamics of western juniper woodlands. My dissertation reduces this uncertainty by quantifying the impacts of increased atmospheric CO_2 on the sensitivity of western juniper tree-ring growth to precipitation and temperature. In Chapter II, I applied a method for quantifying changes in tree-ring sensitivity to climate variables under changing CO_2 values to thirteen previous dendrochronological studies. I

discovered that climate sensitivity dynamics of western juniper woodlands follow a pattern of increasing baseline sensitivity, and greater recent reductions in sensitivity, as site aridity increase across climate-space. Additionally, I developed a permutation model to assess the coverage of site locations across western juniper climate-space. In Chapter III, I applied the same analytical method on western juniper and ponderosa pine trees I sampled in the Chewaucan river basin. I discovered that western juniper are more sensitive to precipitation, and ponderosa pine are more sensitive to temperature. Also, including a long-term precipitation variable in tree-ring growth models improved model fit. In Chapter IV, I compared sensitivity trends from Chapter II with trends from bootstrapped moving window correlation and response functions and found strong agreement between model types. Throughout these chapters I infer how changes in climates sensitivity of western juniper trees may impact the future range and distribution of western juniper woodlands along with the potential impacts on policy and land management actions.

CURRICULUM VITAE

NAME OF AUTHOR: Schyler Ainsworth Reis

GRADUATE AND UNDERGRADUATE SCHOOLS ATTENDED:

University of Oregon, Eugene
Oregon State University, Corvallis
Oregon State University, Corvallis

DEGREES AWARDED:

Doctor of Philosophy, Environmental Sciences, Studies and Policy, 2022
University of Oregon
Master of Science, Wildlife Science, 2017, Oregon State University
Batchelor of Science, Bioresource Research, 2014, Oregon State University

AREAS OF SPECIAL INTEREST:

Biogeography of Semi-Arid Ecosystems
Dendrochronology
Climate Sensitivity of Western Juniper Woodlands
Rangeland Ecology

PROFESSIONAL EXPERIENCE:

Graduate Teaching Fellow, University of Oregon 2016-2022

Graduate Research Fellow, University of Oregon 2016-2022

GRANTS, AWARDS, AND HONORS:

Water in the Pacific Northwest, Past and Future. 8th Annual Grad Forum, Eugene Oregon. Panel Presentation. Winner: 1st place, Best Panel Presentation. 2019

PUBLICATIONS:

Reis, S.A., Silva L (2022) Non-stationary in western juniper growth and climate relationships. Accepted by Ecology and Evolution.

Reis, S. A., Ellsworth, L. M., Kauffman, J. B., & Wrobleski, D. W. (2018). Long-Term Effects of Fire on Vegetation Structure and Predicted Fire Behavior in Wyoming Big Sagebrush Ecosystems. Ecosystems.

Ellsworth, L.M., Reis, S.A., Kauffman, J.B, Kendra Mosely & Sapsis, D. (2020) Repeated fires altered succession and increased fire behavior in basin big sagebrush-native grasslands. Ecosphere, 11(5).

Ellsworth, L. M., Wrobleski, D. W., Kauffman, J. B., & Reis, S. A. (2016). Ecosystem resilience is evident 17 years after fire in Wyoming big sagebrush ecosystems. Ecosphere, 7(12), e01618.

Reis, S.A., Silva L (2022) Climate tree-ring growth relationships of Western Juniper and
Ponderosa Pine trees in Chewuacan River Basin. In prep for Northwest Science Journal.

ACKNOWLEDGMENTS

I would like to acknowledge my friends and family, in particular my mother Sarah Reis and my father Jeff Reis for their love and support. I would like to acknowledge my committee members, Lucas Silva, Dan Gavin, Carolyn Fish and Peter Ralph, for their input on this manuscript. My colleges Mike Farinacci, Paul Reed and Toby Maxwell helped with brainstorming and study design. Undergraduates Alexia Gee, Aaron LeFore, and Davis Lamb helped with fieldwork and with geospatial analysis.

TABLE OF CONTENTS

Chapter Page

Chapter Page

LIST OF FIGURES

Figure Page

LIST OF TABLES

Table Page

CHAPTER I

INTRODUCTION

Western juniper (*Juniperus occidentallis*) woodlands (WJW) are located at the upper elevational ranges of the cool semi-arid sagebrush ecosystems of the American West. Over the past century WJW have expanded rapidly into adjacent shrub and grass dominated communities (Rowland et al., 2011). Similar expansion of woody species has been observed in cool semi-arid ecosystems (CSAEs) around the world. Currently WJW are the second most expansive tree-dominated ecosystem in eastern Oregon, and cover ~3.6 million ha (The Gymnosperm Database, 2021), which represents nearly a six-fold increase in area in less than 100 years (Azuma et al., 2005).

Often this expansion is attributed primarily to increased cattle grazing and a concomitant reduction in fire frequency. However, recently more attention has been paid to the role that climate and increased atmospheric CO_2 have played in the increase in area occupied by WJW and the growth rates of western juniper trees (Soulé et al., 2004; Soulé & Knapp, 2019). In WJW, elevated CO2 can influence tree growth by impacting physiological processes such as water-use efficiency, an important characteristic of drought responses (Knapp et al., 2001a; Knapp & Soulé, 1996; Soule & Knapp, 1999).

Isotope chronologies in tree rings across a wide range of tree species have suggested that increases in water use efficiency — the ratio of carbon fixed due to assimilation to water lost through stomatal conductance — have occurred at a widespread scale over the last 200 years (Franks et al., 2013). *In situ* studies and meta-analyses addressing the effects of elevated CO_2 on tree-ring growth in other forested ecosystems are prevalent in the literature (De Kauwe et al., 2013; Franks et al., 2013; Silva & Anand, 2013), but the impacts and geo-ecological patterns of such impacts are still inconclusive (Geldof & Berg 2010; Peñuelas et al., 2011). Additionally, there is a paucity of studies addressing this issue in CSAEs around the globe, and particularly in WJW.

Given the potentially contrasting positive and negative effects of elevated CO_2 and changes to climate on WJ growth, respectively, this interaction needs to be explored further from the perspective of sensitivity to climate and CO_2 as well as their interactions. Ideally, an improvement in our understanding of the impacts of elevated CO_2 and changes to climate on WJ growth can improve the posterity of modeling efforts focused on dynamics of both WJW, adjacent ecosystems, and CSAEs around the world.

Cool Semi-Arid Ecosystems and Ecological Models

Cool semi-arid ecosystems are located on every continent except Antarctica. In general, most CSAEs could be classified as steppes: areas dominated by grasses, shrubs, and intermittent trees that are too arid to support dense forests, but not arid enough to be considered deserts. The responses of these ecosystems to climate change are likely to be varied due to the predicted asymmetric changes in global temperature and precipitation patterns. In addition, these ecosystems have experienced different management histories over the past millennia and centuries. Increased atmospheric CO_2 concentrations will affect all these ecosystems in several ways, but the specifics are still unknown. It has been shown that increased CO_2 concentrations can increase plant vegetative growth; can ameliorate the effects of disturbances like drought by increasing plants' water use efficiency;and that individual plant species and plant functional groups will respond differentially to increases in CO_2 concentrations, thus resulting in potential shifts in plant community composition particularly between C3 and C4 plants (Polley et al. 2013). However, most CSAEs are dominated by C3 plants with very little of their flora consisting of C4 plants (Still et al. 2003). Therefore, it is important to conduct research specifically aimed at elucidating responses of the dominant plant species and the potential differential responses multiple species have to changes in CO_2 concentrations in CSAEs.

A better understanding of such phenomena is critical for the next generation of ecological forecasting models in CSAEs (Tietjen and Jeltsch, 2007), and as I will further explain in subsequent portions of this chapter, an understanding of past processes can inform our understanding of current and future processes. This is true for tree rings, ecosystems, and the models used to describe their dynamics. An often-used model for understanding and predicting ecological dynamics in such ecosystems are state and transition models (STM). Most of the STM modeling efforts have been conducted in North America, therefore increased efforts are needed to link ecological process across time and space via the generation and refinement of ecological theory. Results from this dissertation can be incorporated into the development of the next generation of ecological forecast models that have moved beyond mere STMs by linking them with future climate scenarios, topographic and edaphic properties, dynamic global vegetation models, and proposed management scenarios, as seen in Halofsky et al. (2013) and Creutzburg et al. (2015).

When an ecological model can no longer make accurate predictions of an ecosystem's responses to management actions or natural disturbances it must be either adapted or abandoned. Such was the case with the Clementsian climax model, a model based on traditional climax theory that,when applied to rangelands, assumes that successional tendency and above-average rainfall drive a plant community towards a favorable condition and climax, and conversely that grazing pressure and drought drive that community towards poor condition and early successional composition. However, during the 1970s and 1980s this model was under scrutiny (Stringham et al., 2003; Walker and Westoby, 2011), leading to a change. By incorporating an ecological theory alternative to those presented by Clements (e.g., alternative stable states, discontinuous and irreversible transitions, nonequilibrium communities, and stochastic effects on succession) and packaging them in a simplified, practical, and organized manner, Westoby et al. (1989) developed a new type of model that would be adopted and utilized by land managers and scientists across the world. Thus, STMs were born. Fourteen years later Stringham et al. (2003) recognized the need to formalize the nomenclature with universally-accepted definitions and to refine the model and its associated theories. This cleared up some of the confusion and therefore criticism of STMs, but in doing so they defined the temporal scale of STMs as existing within a permanent climate regime, and therefore STMs alone are incapable of dealing with issues such a climate change.

Climate change has altered the rangelands of CSAEs around the world in many ways, but, how and to what degree a changing climate interacts with land management and natural systems differs between the planet's various CSAEs. Rangelands are semi-natural areas that are grazed by domestic livestock. Although not all rangelands are semi-arid, and not all semi-arid lands are used for grazing, there is a strong association between the two. Arid and semi-arid rangelands support around half of the world's livestock production, and all the CSAEs that I will be discussing are actively managed as rangelands. Also, climate classification is strongly linked to the vegetation communites that grow within a given climate. Köppen, being a botanist, defined the climatic categories in his climate classification system based on vegetation variation patterns and not vice versa. Although there are many methods for defining climate and the associated vegetation, the Köppen system is still the most frequently used climate classification system (Kottek et al., 2006; Huang et al., 2015).

Three major consequences of climate change are elevated CO_2 levels, climate warming, and precipitation variability, yet how these factors have and will continue to change CSAEs around the world is not fully understood. In a review of available models set in semi-arid rangelands, Tietjen and Jeltsch (2007) identified six major criteria that a model must address to make predictions in system dynamics because of climate change. They are: intra-annual precipitation, soil moisture, temperature/evapotranspiration, changes in CO_2 concentration, and the influence of vegetation on both water infiltration and on fire. They also determined that, as of 2007, no models incorporated all six criteria and that none of the models they analyzed addressed rising CO_2 levels.

Although more recent linked modeling efforts by Halofskey et al (2013) and Creutzberg et al. (2015) have incorporated many of the criteria set forth by Tietjen and Jeltsch (2007), and have even included additional criteria such as potential management scenarios into their predictions, conflicting results over the same study area in central Oregon highlight the need for further refinement of included and excluded parameters. For instance, Halofsky et al. (2013) did not include species-specific impacts of increasing atmospheric CO_2 in their model, and Creutzberg et al. (2015) did not include the impacts of increased CO_2 in their model at all.

Enhanced levels of CO_2 have been shown to increase plant growth in numerous controlled experiments; however, the overall effects of elevated CO_2 and warming on semi-arid ecosystems are still being determined. For instance, Blumenthal et al. (2013) found that invasive forbs increased in biomass and productivity due to elevated CO_2, whereas heating had no effect. They hypothesized that this was due to the invasive species' aggressive use of available water in the soil due to the increased water-use efficiency of native plants under conditions of elevated CO_2. In contrast, Blumenthal et al. (2016) found that heating treatments tripled biomass and seed production of cheatgrass (Bromus tectorum), a widespread and ecologically-devastating annual grass that has invaded tens of millions of hectares of the semi-arid American West. These contrasting results suggest that more species-specific and community-level experiments must be conducted and synthesized.

It is important to understand that the consequences of climate change may not affect semi-arid ecosystems around the world in the same way. The northern hemisphere is warming faster than the southern hemisphere (Freidman et al., 2013). Semi-arid climate regions are expanding across the globe, with the weakening of the Asian summer monsoon leading to the expansion of semi-arid climate regions into sub-humid climate regions in the eastern hemisphere. In contrast, a weakening of the Aleutian Low, enhanced westerlies, and warming Atlantic Sea surface temperatures that modulate the El Niño-Southern Oscillation is causing semi-arid climate regions to expand into once-arid climate regions (Huang et al., 2016).

In addition, the current and past socio-political climates and management histories will also impact the future of CSAE ecosystems as well. North and South America and Australia have ecosystems in cool semi-arid climates that have a relatively short history of grazing by domestic livestock (e.g., 1880s in Patagonia, the mid 1800s in the semi-arid American West and the early 1800s in Australia; Oliva et al., 2016; Beschta et al., 2012; McAlister et al., 2006). On the other hand, areas in Europe, Asia, and Africa were occupied by nomadic pastoralists for over 4 millennia (Sasaki et al., 2007; Jamiyansharav et al., 2018). The ecological narratives of post-Soviet and post-Soviet-linked countries, such as Uzbekistan, Kazakhstan, and Mongolia provide us with a glimpse of how societal changes can dramatically affect ecological processes. Mongolia's rangelands have become severely degraded due in part to a doubling of stocking rates after transitioning to a market economy in the early 1990s (Jamiyansharav et al., 2018). Uzbekistan was exploited under Soviet rule, when the widespread and rapid conversion of land into irrigated cotton fields (0.42 million ha of cotton fields in 1960 to 4 million ha of cotton fields in 1990) led to the collapse of Aral Sea fisheries and to widespread salinization of soils across the landscape (Schlüter and Herrfhrdt-Pähle, 2011). In Kazakhstan, the post-Soviet government, focused on decentralization and liberalization, severely cut funding to agricultural monitoring, and created an environment of hostility towards the collective actions needed for pest control. This contributed to the largest and most severe locust plague Kazakhstan had faced in a century (Toleubayev et al., 2007).

Other CSAEs around the world face similar changes to those in the American West. Australian rangelands are being invaded by native woody species, resembling the encroachment of the western juniper and sagebrush in North America (Tighe et al., 2009). In Patagonia, as in the American West, non-native species and intensive grazing practices are contributing to more frequent fires, leading to the transition to fire-prone alternative stable states (Raffael et al., 2011).

Ideally, the research I conducted and present in this dissertation can be incorporated into future studies conducted in CSAEs around the world through a better understanding of the responses of WJW to climate change at a mechanistic level, and perhaps influence future management actions and policy by improving the performance of future linked-modeling efforts, and with the effective communication of the benefits of understanding WJW climate dynamics through a more scientifically-informed lens.

Western Juniper Woodlands and Conceptual Models

I have heard it said that all models are wrong, but some can be useful. In the first paragraph of this introductory chapter, I briefly touched on the prevailing conceptual model of WJW expansion that has been primarily driven by the interaction between overgrazing by domestic livestock and therefore the reduction of fire frequency to fuel reduction through herbivory. Although I do not think that concept isn't true, more factors need to be addressed to make that conceptual model useful regarding ecological forecasting and potential management actions.

Soulé et al. (2004) offers a more complicated and complex hypothesis for the expansion of WJW since Euro-American settlement of the American West. By examining growth rates and establishment dates of 2,000 juniper trees at five match-paired (historically disturbed by livestock and historically undisturbed) study sites across Oregon, Soulé et al. (2004) were able to provide insight into detailed patterns of western juniper expansion dynamics, with and without grazing pressure. They also address the ecological causes of this expansion. Their conceptual model accounts for the following. (1) Biological inertia: as juniper woodlands expand in range, they also infill with more juniper, which results in increased seed rain over time and therefore increased rates of expansion. (2) Biotic interaction: grazing tends to increase shrub cover; these shrubs act as nurse plant for western juniper seedlings, creating favorable microclimates. (3) Increased atmospheric CO_2 levels: the direct and indirect benefits of elevated CO_2 on WJW expansion and juniper seedling establishment are: directly, an increase in available soil water by increasing the water use efficiency of juniper themselves; and indirectly, a reduction in the water use of other plants due to their increase in water-use efficiency. (4) Influences of seasonal temperature and precipitation on both seed production and seedling establishment: high levels of winter and springtime precipitation lead to reduced stress in adult western juniper trees, resulting in increased growth that year and an increase in the production of viable seeds. High levels of seedling establishment were associated with years of high levels of summer precipitation and years with above-average annual and summer temperatures; juniper seedlings are subject to freeze kill, and freezing events during the growing season are less likely to have occurred in years with above average annual/summer temperatures. (5) Topographic positioning and soil properties: seedling establishment may be favored in the deep, less well-drained soils of valley bottoms, whereas growth in established trees may be favored by shallow, well drained soils at higher elevations. Additionally, Soulé et al. (2004) found a significant correlation between decadal periods of increased western juniper tree-ring growth and western juniper seedling establishment, leading credence to the theory that dendrochronological studies of western juniper growth and climate relationships from the perspective of sensitivity to climate and CO_2 as well as their interactions, not only can be used to improve future modeling efforts, but also have a direct linkage to the demography and range dynamics of western juniper trees and WJW.

Dendrochronological Meta-Analysis and Ecological Forecasting

Recent studies have demonstrated the utility of combining *in situ* measurements, climate data, and ecological data bases to expand spatial and temporal inference beyond what would be possible with a single methodological approach (Correa-Díaz et al., 2019; Gu et al., 2007; Krofcheck et al., 2015; Snyder et al., 2019). These emerging integrated approaches can provide new insight into complex spatial and temporal patterns of key ecosystem functions and landscape dynamics (Pasquarella et al., 2016). However, upscaling data generated via a traditional dendrochronological sampling regime can potentially result in contrasting errors in future forest behavior. Klesse et al., (2018) warns that the utilization of dendrochronological databases can result in an overestimation of forest responses to predicted changes in climate because these targeted sampling methods are aimed at amplifying the climate response signals of tree-ring chronologies. However, in contrast, reducing noise caused by variation of individual trees, when analyzed across a broad scale, may inhibit our ability to detect early warning signals of possible regime shifts (Bauch et al., 2016).

Data generated to answer specific research questions must be examined critically before they are applied to other inquires, and traditionally dendrochronological studies have been used to enhance our understanding of the past, not the future. If data are taken out of context, statistical methods are inappropriately applied, or models generated are not evaluated sufficiently, then erroneous conclusions might be drawn (Benestad et al., 2016). Even a minimal amount (< 3%) of incorrect conclusions based on improperly conducted scientific studies can contribute to large discrepancies in the general public's understanding and perception of global climate change (Benestad et al., 2016). That being said, one way to better inform our understanding of likely responses of organisms and ecosystems to changes in climate is to study how they reacted to climate variation in the past. Tree annual growth rings act as high-resolution natural archives of past climate conditions (Hughes et al., 2011; Swetnam et al., 1999); this is because the annual growth of a tree is influenced by many factors, both biological and climatic (Speer, 2010).

According to Speer (2010), the concept that trees produce annual rings was first described by the Greek philosopher and botanist Theophrastus (born 371 BC), and perhaps the first to describe the relationship between annual variation of tree-rings and climate was Leonardo da Vinci. The first recorded discovery of a marker ring occurred in the mid-1700s, when two French naturalists, Henri Louis Duhamel du Monceau and George Louis Leclerc de Buffon, discovered that many trees showed evidence of frost damage in rings that corresponded with the winter of 1709. Marker rings are a key component of one of the most important and basic tenets of dendrochronology: cross-dating. Cross-dating is the matching of patterns of ring widths between tree cores, thus reducing potential errors due to locally absent or false rings. Additionally, when cross-dating is used to link overlapping tree core specimens, a continuous tree-ring chronology may be extended for thousands of years into the past. There are now dozens of such continuous tree-ring chronologies. These multi-millennial chronologies played an important role in the development and refinement of radio carbon-dating methods, by providing annually resolute empirical data used to create 14C calibration curves (Brinks et al., 2012). Because dendrochronological studies often aim to maximize climate signal in tree-width variation, site selection—macro (e.g., ecotonal boundaries) and micro (e.g., rocky outcroppings)—is not done at random. The selection of trees within sites is also biased, with older, larger, and more dominant trees being preferred (Hughes et al., 2011; Klesse et al., 2018; Speer, 2010). Additionally, the act of averaging multiple tree cores, and the choice of standardization techniques, can both further dampen variation due to climate change or biological effects. However, Soulé and Knapp (2019) found that all tree-ring standardization options produced identical annual growth values in western juniper trees in central Oregon.

Trees growing near the margins of their species' climatic range are often under greater stress than trees growing within the center of said range; therefore, dendrochronologists often sample trees from sites in or around ecotonal boundaries. Klesse et al. (2018) tested how these sampling biases influence projections of future tree growth across the southwestern U.S. They compared growth variability and climate sensitivity of three tree species: Douglas-fir (Pseudotsuga menziesii), ponderosa (Pinus ponderosa) and pinyon (Pinus edulis) pine, from two data sets. The targeted (i.e., biased) samples came from the International Tree-Ring Databank (ITRDB), and the random (i.e., unbiased, representative) samples came from the USFS Forest Inventory and Analysis database. Targeted samples showed higher growth variability and were more responsive to climate variation than representative samples, and therefore yielded different projections of tree growth in response to climate change. Klesse et al. (2018) cautions that artifacts of sampling bias may hinder the ability of ITRDB chronologies to inform accurate projections of forest response to future climate scenarios at a species-distribution or regional scale. However, in chapter II of this dissertation we will present a novel approach towards assessing and quantifying the coverage of a series of ecological sampling site locations or "constellation," with a newly developed permutation model aimed at quantifying the Representation of Ecological Inter-Space-- the REIS method.

Dissertation Research

The overarching aim of this dissertation is to examine how the response of western juniper tree rings to precipitation, temperature and increases in atmospheric CO_2 has or has not changed since 1896 at site and regional scales. Specifically, I investigate this through 1) analyzing 13 past western juniper tree-ring studies with a recently-developed modeling approach similar to that developed by Zuidema et al. (2020) to create site specific and reginal models, 2) exploring spatial patterns of changes in western juniper climate sensitivity over climate-space, 3) assessing the coverage of the western juniper climate-space of the 13 study-site locations with a novel "Representation of Ecological Inter-Space" permutation model, 4) validating my findings with data I collected in the Chewaucan River Basin of southern central Oregon, and by 5) validating my findings by reanalyzing my results with a more commonly-used bootstrapped moving-window correlation and response functions.

Chapter II of my dissertation, entitled "Nonstationarity in western juniper growth and climate relationships," has been accepted by *Ecology and Evolution* and is coauthored by me and Lucas Silva. We construct and analyze multiple linear and mixed-effects models of western juniper tree-ring responses to precipitation, temperature and atmospheric CO_2 constructed from 13 previous tree-ring studies. In addition, we use a novel permutation model to determine the spatial coverage of those study site locations within the climate-space of western juniper woodlands.

Chapter III is entitled "Climate tree-ring growth relationships of western juniper and ponderosa pine trees in the Chewaucan River Basin." In this chapter I focus on applying the modeling methodology refined in chapter II to quantitatively compare the changes in responses of western juniper and ponderosa pine to precipitation and temperature as atmospheric CO_2 has increased over time.

Chapter IV is entitled "Comparison of evaluations of western juniper tree-ring climate sensitivity between mixed-effects models and bootstrapped moving-window correlation and response functions." This chapter compares results from the mixed-effects models constructed in chapter II to the more commonly used method of analysis of tree ring climate sensitivity, the bootstrapped moving window correlation and response function.

Chapter V is a summary of the preceding chapter's results, and a discussion of the potential future research and management implications.

References

Azuma, D. L., Hiserote, B. A., & Dunham, P. A. (2005). *The western juniper resource of eastern Oregon, 1999.* (PNW-RB-249). U.S. Department of Agriculture, Forest Service, Pacific Northwest Research Station. https://doi.org/10.2737/PNW-RB-249

Bauch, C. T., Sigdel, R., Pharaon, J., & Anand, M. (2016). Early warning signals of regime shifts in coupled human–environment systems. *Proceedings of the National Academy of Sciences*, *113*(51), 14560–14567. https://doi.org/10.1073/pnas.1604978113

Benestad, R. E., Nuccitelli, D., Lewandowsky, S., Hayhoe, K., Hygen, H. O., van Dorland, R., & Cook, J. (2016). Learning from mistakes in climate research. *Theoretical and Applied Climatology*, *126*(3–4), 699–703. https://doi.org/10.1007/s00704-015-1597-5

Beschta, R. L., Donahue, D. L., DellaSala, D. A., Rhodes, J. J., Karr, J. R., O'Brien, M. H., Fleischner, T. L., & Deacon Williams, C. (2013). Adapting to Climate Change on Western Public Lands: Addressing the Ecological Effects of Domestic, Wild, and Feral Ungulates. *Environmental Management*, *51*(2), 474–491. https://doi.org/10.1007/s00267-012-9964-9

Blumenthal, D. M., Kray, J. A., Ortmans, W., Ziska, L. H., & Pendall, E. (2016). Cheatgrass is favored by warming but not CO_2 enrichment in a semi-arid grassland. *Global Change Biology*, *22*(9), 3026–3038. https://doi.org/10.1111/gcb.13278

Blumenthal, D. M., Resco, V., Morgan, J. A., Williams, D. G., LeCain, D. R., Hardy, E. M., Pendall, E., & Bladyka, E. (2013). Invasive forb benefits from water savings by native plants and carbon fertilization under elevated CO_2 and warming. *New Phytologist*, *200*(4), 1156–1165. https://doi.org/10.1111/nph.12459

Correa-Díaz, A., Silva, L. C. R., Horwath, W. R., Gómez-Guerrero, A., Vargas-Hernández, J., Villanueva-Díaz, J., Velázquez-Martínez, A., & Suárez-Espinoza, J. (2019). Linking Remote Sensing and Dendrochronology to Quantify Climate-Induced Shifts in High-Elevation Forests Over Space and Time. *Journal of Geophysical Research: Biogeosciences*, *124*(1), 166–183. https://doi.org/10.1029/2018JG004687

Creutzburg, M. K., Halofsky, J. E., Halofsky, J. S., & Christopher, T. A. (2015). Climate Change and Land Management in the Rangelands of Central Oregon. *Environmental Management*, *55*(1), 43–55. https://doi.org/10.1007/s00267-014-0362-3

De Kauwe, M. G., Medlyn, B. E., Zaehle, S., Walker, A. P., Dietze, M. C., Hickler, T., Jain, A. K., Luo, Y., Parton, W. J., Prentice, I. C., Smith, B., Thornton, P. E., Wang, S., Wang, Y.-P., Wårlind, D., Weng, E., Crous, K. Y., Ellsworth, D. S., Hanson, P. J., … Norby, R. J. (2013). Forest water use and water use efficiency at elevated CO_2: A model-data intercomparison at two contrasting temperate forest FACE sites. *Global Change Biology*, *19*(6), 1759–1779. https://doi.org/10.1111/gcb.12164

Franks, P. J., Adams, M. A., Amthor, J. S., Barbour, M. M., Berry, J. A., Ellsworth, D. S., Farquhar, G. D., Ghannoum, O., Lloyd, J., McDowell, N., Norby, R. J., Tissue, D. T., & Caemmerer, S. (2013). Sensitivity of plants to changing atmospheric CO_2 concentration: From the geological past to the next century. *New Phytologist*, *197*(4), 1077–1094. https://doi.org/10.1111/nph.12104

Friedman, A. R., Hwang, Y.-T., Chiang, J. C. H., & Frierson, D. M. W. (2013). Interhemispheric Temperature Asymmetry over the Twentieth Century and in Future Projections. *Journal of Climate*, *26*(15), 5419–5433. https://doi.org/10.1175/JCLI-D-12-00525.1

Global Ecology and Biogeography—2010—Pe uelas—Increased water-use efficiency during the 20th century did not (1).pdf. (n.d.).

Gu, Y., Brown, J. F., Verdin, J. P., & Wardlow, B. (2007). A five-year analysis of MODIS NDVI and NDWI for grassland drought assessment over the central Great Plains of the United States. *Geophysical Research Letters*, *34*(6). https://doi.org/10.1029/2006GL029127

Halofsky, J. E., Hemstrom, M. A., Conklin, D. R., Halofsky, J. S., Kerns, B. K., & Bachelet, D. (2013). Assessing potential climate change effects on vegetation using a linked model approach. *Ecological Modelling*, *266*, 131–143. https://doi.org/10.1016/j.ecolmodel.2013.07.003

Huang, J., Ji, M., Xie, Y., Wang, S., He, Y., & Ran, J. (2016). Global semi-arid climate change over last 60 years. *Climate Dynamics*, *46*(3–4), 1131–1150. https://doi.org/10.1007/s00382-015-2636-8

Hughes, M. K., Swetnam, T. W., & Diaz, H. F. (Eds.). (2011). *Dendroclimatology: Progress and prospects*. Springer.

Jamiyansharav, K., Fernández-Giménez, M. E., Angerer, J. P., Yadamsuren, B., & Dash, Z. (2018). Plant community change in three Mongolian steppe ecosystems 1994-2013: Applications to state-and-transition models. *Ecosphere*, *9*(3), e02145. https://doi.org/10.1002/ecs2.2145

Klesse, S., DeRose, R. J., Guiterman, C. H., Lynch, A. M., O'Connor, C. D., Shaw, J. D., & Evans, M. E. K. (2018). Sampling bias overestimates climate change impacts on forest growth in the southwestern United States. *Nature Communications*, *9*(1). https://doi.org/10.1038/s41467-018-07800-y

Knapp, P. A., & Soulé, P. T. (1996). Vegetation Change and the Role of Atmospheric CO2 Enrichment on a Relict Site in Central Oregon: 1960–1994. *Annals of the Association of American Geographers*, *86*(3), 387–411. https://doi.org/10.1111/j.1467-8306.1996.tb01759.x

Knapp, P. A., Soulé, P. T., & Grissino-Mayer, H. D. (2001a). Detecting potential regional effects of increased atmospheric CO2 on growth rates of western juniper. *Global Change Biology*, *7*(8), 903–917.

Knapp, P. A., Soulé, P. T., & Grissino-Mayer, H. D. (2001b). Post-drought growth responses of western Juniper (*Juniperus occidentals var. Occidentalis*) in central Oregon. *Geophysical Research Letters*, *28*(13), 2657–2660. https://doi.org/10.1029/2000GL012365

Kottek, M., Grieser, J., Beck, C., Rudolf, B., & Rubel, F. (2006). World Map of the Köppen-Geiger climate classification updated. *Meteorologische Zeitschrift*, *15*(3), 259–263. https://doi.org/10.1127/0941-2948/2006/0130

Krofcheck, D., Eitel, J., Lippitt, C., Vierling, L., Schulthess, U., & Litvak, M. (2015). Remote Sensing Based Simple Models of GPP in Both Disturbed and Undisturbed Piñon-Juniper

Woodlands in the Southwestern U.S. *Remote Sensing*, *8*(1), 20. https://doi.org/10.3390/rs8010020

McAllister, R. R. J., Abel, N., Stokes, C. J., & Gordon, I. J. (2006). Australian Pastoralists in Time and Space: The Evolution of a Complex Adaptive System. *Ecology and Society*, *11*(2). https://doi.org/10.5751/ES-01875-110241

Oliva, G., Ferrante, D., Paredes, P., Humano, G., & Cesa, A. (2016). A conceptual model for changes in floristic diversity under grazing in semi-arid Patagonia using the State and Transition framework. *Journal of Arid Environments*, *127*, 120–127. https://doi.org/10.1016/j.jaridenv.2015.10.018

Pasquarella, V. J., Holden, C. E., Kaufman, L., & Woodcock, C. E. (2016). From imagery to ecology: Leveraging time series of all available Landsat observations to map and monitor ecosystem state and dynamics. *Remote Sensing in Ecology and Conservation*, *2*(3), 152–170. https://doi.org/10.1002/rse2.24

Polley, H. W., Briske, D. D., Morgan, J. A., Wolter, K., Bailey, D. W., & Brown, J. R. (2013). Climate Change and North American Rangelands: Trends, Projections, and Implications. *Rangeland Ecology & Management*, *66*(5), 493–511. https://doi.org/10.2111/REM-D-12-00068.1

Raffaele, E., Veblen, T. T., Blackhall, M., & Tercero-Bucardo, N. (2011). Synergistic influences of introduced herbivores and fire on vegetation change in northern Patagonia, Argentina: Herbivore and fire influences on vegetation. *Journal of Vegetation Science*, *22*(1), 59–71. https://doi.org/10.1111/j.1654-1103.2010.01233.x

Rowland, M. M., Suring, L. H., Tausch, R. J., Geer, S., & Wisdom, M. J. (2011). *Dynamics of western juniper woodland expansion into sagebrush communities in central Oregon*. *16*, 12.

Sasaki, T., Okayasu, T., Jamsran, U., & Takeuchi, K. (2007). Threshold changes in vegetation along a grazing gradient in Mongolian rangelands. *Journal of Ecology*, *0*(0), 071106211313003-??? https://doi.org/10.1111/j.1365-2745.2007.01315.x

Schlüter, M., & Herrfahrdt-Pähle, E. (2011). Exploring Resilience and Transformability of a River Basin in the Face of Socioeconomic and Ecological Crisis: An Example from the

Amudarya River Basin, Central Asia. *Ecology and Society*, *16*(1). https://doi.org/10.5751/ES-03910-160132

Silva, L. C. R., & Anand, M. (2013). Probing for the influence of atmospheric CO_2 and climate change on forest ecosystems across biomes: Changes in growth and iWUE across biomes. *Global Ecology and Biogeography*, *22*(1), 83–92. https://doi.org/10.1111/j.1466-8238.2012.00783.x

Snyder, K. A., Evers, L., Chambers, J. C., Dunham, J., Bradford, J. B., & Loik, M. E. (2019). Effects of Changing Climate on the Hydrological Cycle in Cold Desert Ecosystems of the Great Basin and Columbia Plateau. *Rangeland Ecology & Management*, *72*(1), 1–12. https://doi.org/10.1016/j.rama.2018.07.007

Soule, P. T., & Knapp, P. A. (1999). Western Juniper Expansion on Adjacent Disturbed and Near-Relict Sites. *Journal of Range Management*, *52*(5), 525. https://doi.org/10.2307/4003782

Soulé, P. T., & Knapp, P. A. (2019). Radial Growth Rate Responses of Western Juniper (Juniperus occidentalis Hook.) to Atmospheric and Climatic Changes: A Longitudinal Study from Central Oregon, USA. *Forests*, *10*(12), 1127. https://doi.org/10.3390/f10121127

Soulé, P. T., Knapp, P. A., & Grissino-Mayer, H. D. (2004a). HUMAN AGENCY, ENVIRONMENTAL DRIVERS, AND WESTERN JUNIPER ESTABLISHMENT DURING THE LATE HOLOCENE. *Ecological Applications*, *14*(1), 96–112. https://doi.org/10.1890/02-5300

Soulé, P. T., Knapp, P. A., & Grissino-Mayer, H. D. (2004b). HUMAN AGENCY, ENVIRONMENTAL DRIVERS, AND WESTERN JUNIPER ESTABLISHMENT DURING THE LATE HOLOCENE. *Ecological Applications*, *14*(1), 96–112. https://doi.org/10.1890/02-5300

Speer, J. H. (n.d.). *Fundamentals of Tree-Ring Research*. 86.

Still, C. J., Berry, J. A., Collatz, G. J., & DeFries, R. S. (2003). Global distribution of C_3 and C_4 vegetation: Carbon cycle implications: C_4 PLANTS AND CARBON CYCLE. *Global Biogeochemical Cycles*, *17*(1), 6-1-6–14. https://doi.org/10.1029/2001GB001807

Stringham, T. K., Krueger, W. C., & Shaver, P. L. (n.d.). *State and Transition Modeling: An Ecological Process Approach*. 9.

Swetnam, T. W., Allen, C. D., & Betancourt, J. L. (1999). Applied Historical Ecology: Using the Past to Manage for the Future. *Ecological Applications*, *9*(4), 1189. https://doi.org/10.2307/2641390

Tietjen, B., & Jeltsch, F. (2007). Semi-arid grazing systems and climate change: A survey of present modelling potential and future needs: Grazing systems and climate change. *Journal of Applied Ecology*, *44*(2), 425–434. https://doi.org/10.1111/j.1365-2664.2007.01280.x

Tighe, M., Reid, N., Wilson, B., & Briggs, S. V. (2009). Invasive native scrub and soil condition in semi-arid south-eastern Australia. *Agriculture, Ecosystems & Environment*, *132*(3–4), 212–222. https://doi.org/10.1016/j.agee.2009.04.001

Toleubayev, K., Jansen, K., & van Huis, A. (2007). Locust Control in Transition: The Loss and Reinvention of Collective Action in Post-Soviet Kazakhstan. *Ecology and Society*, *12*(2). https://doi.org/10.5751/ES-02229-120238

Walker, B., & Westoby, M. (2011). States and transitions: The trajectory of an idea, 1970-2010. *Israel Journal of Ecology & Evolution*, *57*(1–2), 17–22. https://doi.org/10.1560/IJEE.57.1-2.17

Westoby, M., Walker, B., & Noy-Meir, I. (1989). Opportunistic Management for Rangelands Not at Equilibrium. *Journal of Range Management*, *42*(4), 266. https://doi.org/10.2307/3899492

Zuidema, P. A., Heinrich, I., Rahman, M., Vlam, M., Zwartsenberg, S. A., & Sleen, P. (2020). Recent CO_2 rise has modified the sensitivity of tropical tree growth to rainfall and temperature. *Global Change Biology*, *26*(7), 4028–4041. https://doi.org/10.1111/gcb.15092

CHAPTER II

NON-STATIONARITY IN WESTERN JUNIPER GROWTH AND CLIMATE RELATIONSHIPS

Introduction

Western Juniper Woodlands (WJW) are a vast, semi-arid ecosystem that have historically occupied areas between 34° N to 47° N and 124° W to 111° W (https://www.fs.fed.us/database/feis/plants/tree/junocc/all.html#DistributionAndOccurrence). Recent analyses of WJW range indicate that this ecosystem has been expanding rapidly into adjacent shrub and grass dominated communities (Rowland et al., 2011), a process that has been described since the mid-19th century in the Great Basin of the western United States (Figure 1). Today, the extent of WJW is ~3.6 million ha (The Gymnosperm Database, 2021), which represents nearly six-fold increase in less than 100 years, making WJW the second most expansive tree-dominate ecosystem in eastern Oregon(Azuma et al., 2005).

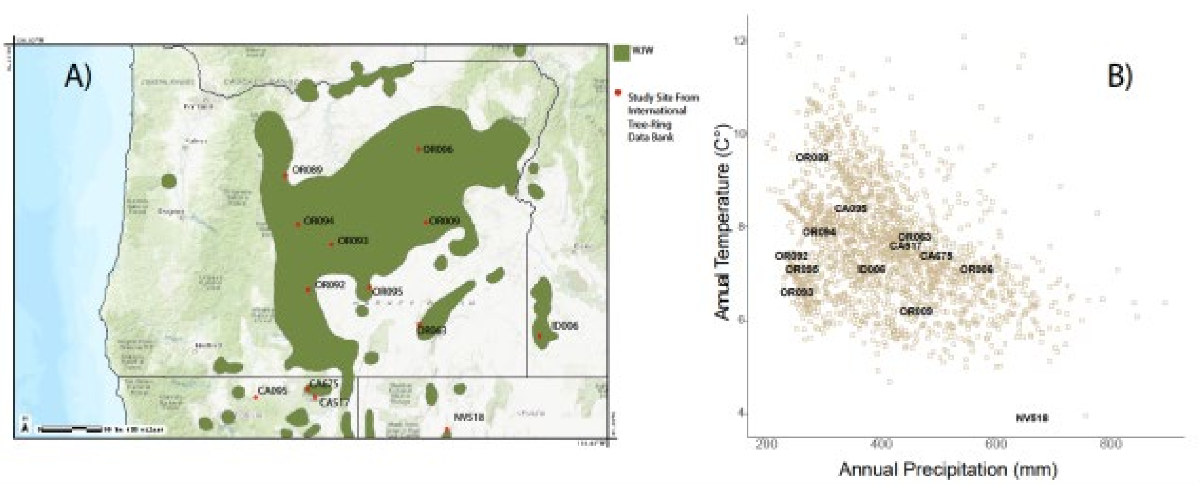

Figure 1- A) Western Juniper Woodlands and study sites from the International Tree-Ring Data Bank (red dots) in the states of Oregon, Washington, California, Idaho, and Nevada (left). B) Locations of those same study sites within the annual precipitation and mean annual temperature "climate-space" biplot occupied by western juniper woodlands within the state of Oregon (right).

The expansion of WJW into adjacent grass and shrub dominated rangelands has garnered much attention from land managers and scientists due to the impacts of its dominant tree species - western juniper (WJ): *Juniperus occidentalis* - on soil resources, availability of livestock forage, habitat for species of concern, and ecosystem carbon stocks (Abdallah et al., 2020; Bates, 2020; Chambers et al., 2017; Schroeder et al., 2004). The use of natural archives like lake pollen cores and pack rat middens have provided much insight into the prehistoric patterns and distributions of WJW in relation to changes in climate (Miller 2019). The recent expansion of WJW, however, has been mostly attributed to the interaction between fire suppression and livestock grazing with less attention and agreement over the role climate and of rising atmospheric CO_2 concentrations on the growth patterns of WJ trees (Miller et al 2008; Johnson and Miller 2008; Eddleman et al 1994; Burkhardt and Tisdale 1976). Therefore, the dynamics of recent WJW expansion, and their interaction with a changing climate under elevated CO_2, represent an important factor that can help improve models aiming to forecast future WJW range expansion and related changes in ecosystem structure and function (Charney et al., 2016; Creutzburg et al., 2015; Klesse et al., 2018; Polley et al., 2013; Tietjen & Jeltsch, 2007; Tredennick et al., 2021a)).

Approximately 7K-4K years before present, WJW were distributed ~500-640 km further south than where they are currently located (Mehringer & Wigand, 1987; Miller et al., 2000; Miller & Wigand, 1994b). The migration of WJW toward their current range coincided with the end of a period of extreme drought 8K-4.5K YBP and general cooling in the northwestern Great Basin (Miller & Wigand, 1994). Once WJW reached their current geographic range, their elevational-climatic relationship can generally be understood as follows: tree-cover expansion in its range at lower and upper elevations during wetter conditions; tree-cover decline at its upper elevational range during colder conditions; and/or retreat upslope during hotter and dryer conditions (Mehringer & Wigand, 1987; Miller & Wigand, 1994a) More recent analyses of the dynamics of WJW post Euro-American settlement attributes its expansion to three main factors: 1) cool and wet conditions at the turn to the 19th century that were favorable for WJ growth and WJ seed production; 2) a reduction in fire-return intervals due to the forced removal indigenous peoples from the landscape and; 3) overgrazing by domestic livestock that preferentially grazed non woody species, further reducing the fire-return interval due to a reduction of fine fuels (Johnson & Miller, 2008; Miller et al., 2000). Fire has often acted as a control on the lower elevational range of WJ, even during climate conditions favorable for expansion at lower elevations (Miller & Rose, 1999) However, beyond the drastic biomass removal caused by fire, the effects of climate and rising CO_2 levels on WJ tree growth remain poorly understood. In addition, although the analysis in this study pertains to WJ tree-ring growth and climate, it has been shown that WJ seed production, germination rates, and seedling survival are statistically correlated with climate and tree-ring growth (Soulé et al., 2004).

It has been hypothesized that elevated CO_2 levels played a role in WJ tree growth rates and WJW expansion over the 20th century (Soulé et al., 2004; Soulé & Knapp, 2019). Our study further explores this hypothesis from Soulé et al. (2004), and Soulé & Knapp (2019) by expanding the number of sites studied, and by applying a new analytical method for quantifying the impacts that elevated CO_2 has on tree-ring growth and sensitivity climate (Zuideman et al. 2020). Therefore, with the geographic and climatic range of study sites expanded we can examine the potential geospatial pattern associated with atmospheric CO_2 induced changes in tree-ring sensitivity to climate.

Isotope chronologies in tree-rings across a wide range of tree species have suggested that increases in water use efficiency — the ratio of carbon fixed due to assimilation to water lost through stomatal conductance — have occurred at a widespread scale over the last 200 years (Franks et al., 2013). In WJW, elevated CO_2 can influence tree growth by impacting physiological processes such as water-use efficiency, an important characteristic of drought responses (Knapp et al., 2001a; Knapp & Soulé, 1996; Soule & Knapp, 1999). *In situ* studies and meta-analyses addressing the effects of elevated CO_2 on tree-ring growth in other forested ecosystems are prevalent in the literature(De Kauwe et al., 2013; Franks et al., 2013; Silva & Anand, 2013). However, there is a paucity of studies addressing this issue in cool semi-arid ecosystems around the globe, and particularly in WJW. Given the potentially contrasting positive and negative effects of elevated CO_2 and changes to climate on WJ growth, respectively, this interaction needs to be explored further from the perspective of sensitivity to climate and CO2 as well as their interactions.

The impacts of climate variables (precipitation and temperature) of WJ growth rates and the effects of rising CO_2 on drought tolerance of WJ has been investigated with tree-ring analysis in a limited number of studies (Knapp et al., 2001a, 2001b; Knapp & Soulé, 1996; Knutson & Pyke, 2008; Soulé & Knapp, 2019). Although these studies provide evidence of increased drought tolerance due to increased CO_2 concentrations in the early 20th century, a more comprehensive examination of the recent impacts of increased atmospheric CO_2 on WJ growth in relation to climate is warranted. For instance, Knapp et al. (2001b) only produced bivariate models to describe the relationship between WJ tree-ring growth and precipitation using regionally resolute climate data, and therefore would not be suitable to use in projection models of future climate scenarios where not just inter-annual but intra-annual precipitation patterns are predicted to change. Knutsnon and Pyke (2008) did provide insight into the role that soil subsurface texture plays in the growth response of WJ tree-rings to drought conditions, with trees growing on sandy and rocky soils being more negatively impacted by drought than those on more fine textured soils, however they also only produced bivariate tree-ring climate relation models. Knapp and Soulé (1996) drew their conclusions from plant cover data collected in 1960 and 1994 at a single site in central Oregon. Soulé and Knapp (2019) explored the relationship between climate and WJ tree-ring growth at four sites in central Oregon and produced both bivariate and multi-variate models of tree-ring growth, but did not include CO_2 climate interactions, a method for assessing the change in climate sensitivity as atmospheric CO_2 has increased (Zuideman et al. 2020).

In particular, to the best of our knowledge, no studies have yet examined the interactions between climate variables and rising CO_2 levels across the geographic and climatic range of WJW. Similarly, we know of no studies that examined these relationships at an intra-year resolution necessary to explore the impacts that future climate change will have on WJW ecosystem functions across geographic ranges. To address this knowledge gap, here we develop several related lines of inquiry leveraging thirteen previous WJ tree-ring studies.

First, we investigate WJ tree-ring growth to sensitivity to precipitation and temperature for all 13 study sites, then we evaluate whether increased atmospheric CO_2 has changed that sensitivity at the site and regional levels. We define sensitivity as the resultant coefficient of linear models examining the response of WJ tree-rings to climate variables. Change in sensitivity is explored by examining the coefficient of the interaction between climate variables and CO_2 (figure 2). In a similar fashion to Zuidema et al (2020) we compare models of tree-ring growth and climate relations, with and without interaction terms (i.e. climate * CO_2 interactions on tree growth), to determine if and to what degree increased CO_2 has changed WJ sensitivity to climate. Furthermore, we perform several post hoc exploratory analyses to determine if sensitivity of WJ tree-ring growth to climate and CO_2 produce significant patterns across the climate space of WJW in the Great Basin. Additionally, we investigate both 1) how well our study sites represent the expanse of WJW climate space, and 2) the site distribution patterns of our study sites, both these factors are needed to represent an environmental system such as the climate-space of WJW and factors that are often unaccounted for with dendrochronological sampling networks (Babst et al., 2018) To this end, we use a novel permutation model that accounts for three metrics of climate representation (area of coverage, evenness of site distribution, and representation of site density) to compare between our site locations and randomly selected hypothetical site locations within the climate-space of WJW.

Figure 2 Conceptual figure of A) hypothesized western juniper tree-ring responses to climate variables at site and regional level. At lower atmospheric CO_2 levels (solid lines) tree-rings respond positively to precipitation and negatively to summer temperatures. At higher CO2 levels the sign of responses is the same but the slope of the response (dashed line) is lower in magnitude. This represents a reduction in sensitivity to climate variables at high vs low CO2 levels. B) hypothesized changes in site level tree-ring sensitivity across the regional climate gradient at both high and low CO2 levels. Solid red lines represent the site level responses of tree-rings to climate variables, with steeper lines representing higher levels of sensitivity. As annual precipitation increases, moving from left to right along the x-axis site level sensitivity to climate variables decreases (solid black line). The dashed lines represent what we hypothesis to observe at high atmospheric CO2 levels. At high CO2 levels there will still be a relationship between site level annual precipitation levels and tree-ring sensitivity, but overall sensitivity will be decreased (proximity of dashed black line compared to solid black line) along the y-axis, additionally the slope of that relationship will be decreased, meaning that drier sites will have a greater reduction to climate variable sensitivity than less dry sites.

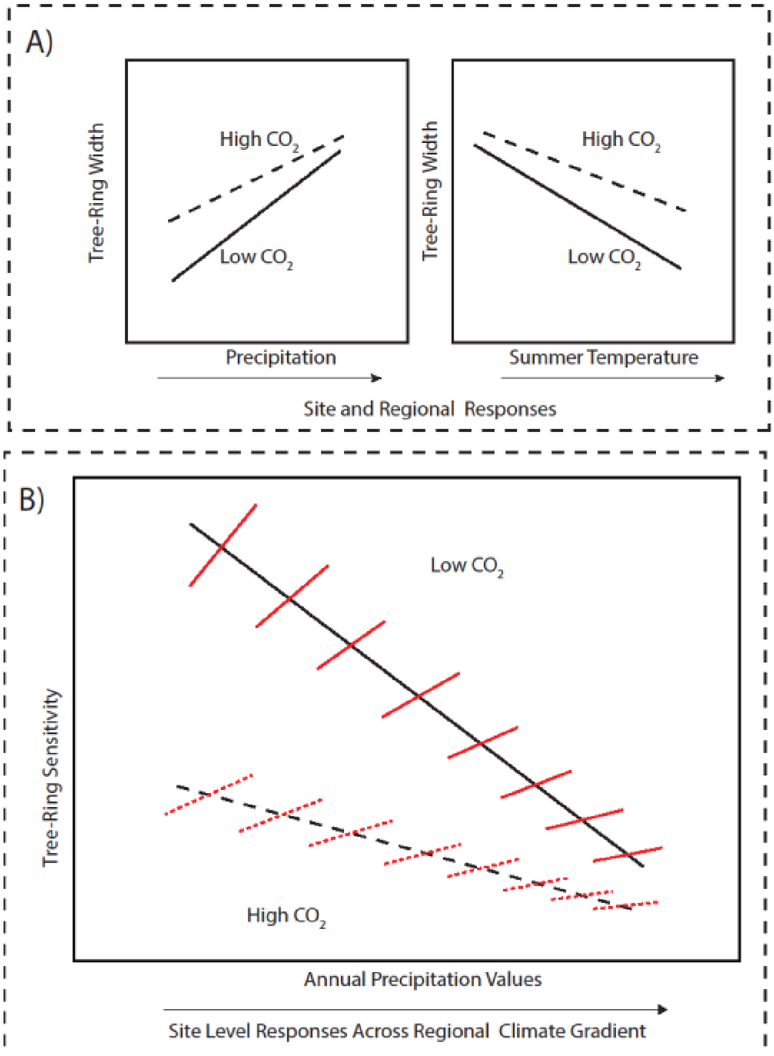

Our overarching hypothesis is that if increases in atmospheric CO_2 are increasing the iWUE of western juniper trees we will observe non-stationary, but predictable, trends in tree growth emerge over space and time as a result of interactions between climate (seasonal and annual), atmospheric CO_2 levels, and site conditions. The results from our analyses are used to explore three specific categories: 1) site specific responses, 2) regional responses, and 3) patterns of sensitivity change across regional climate gradients. Our specific hypotheses are as follows. If increases in atmospheric CO_2 are increasing the iWUE of western juniper trees: 1a), we will observe that at the site level WJ tree growth will have a positive response to seasonal precipitation and a negative response summer temperature with significant interactions arising from seasonal climate and CO_2 levels (figure 2a); 1b) Site level multiple linear regression models that include climate variable * CO_2 interactions will have a better fit than multiple linear regression models without such interaction terms 2a) At the regional level WJ tree growth will have a positive response to seasonal precipitation and a negative response summer temperature with significant interactions arising from seasonal climate and CO_2 levels (figure 2a); 2b) Regional level mixed effects models that include climate variable * CO_2 interactions will have a better fit than mixed effects models without such interaction terms. 3a) WJ tree-ring sensitivity to climate variables will vary across a climate gradient of annual precipitation and temperature with drier sites being more sensitive to precipitation than wetter sites (figure 2b) and 3b) the impact of elevated CO_2 will decrease WJ tree-ring sensitivity to climate variables to a greater degree at drier than at wetter sites (figure 2b).

Methods

Study Sites, Data Sources and Climate Trends:

To test our three hypotheses, we searched for all available WJ tree width data in the Great Basin, which we interpret as a proxy for tree growth across space and time (Figure 1A). We used tree-ring data gathered from the international tree-ring database (ITRDB), querying the database for *Juniperus occidentallis*. Our initial search rendered 51 dendrochronological studies. We then filtered these studies to only include the most recent timeseries, which represent the entirety of WJW climate space in Oregon, USA (Figure 1B). We removed studies that sampled Sierra juniper (*Juniperus grandis*) in the same region, which left us with 13 sites where master chronologies, each comprised of numerous individual trees, for our analysis of responses to rising CO_2 levels and climate variability. The number of trees sampled at each of the 13 study sites ranged from 14 to 32 with a mean sampling size of 25 trees per site. The studies used for our analysis were conducted on varying dates, therefore, the latest tree-ring sampled from each site varies by location, from 1980 to 2010. Locations were based on the GPS coordinates provided within the meta data from the ITRDB, where the citations to the original studies can also be found https://www.ncei.noaa.gov/products/paleoclimatology/tree-ring (Holmes 2002 a,b,c,d,e; Knapp and Soulé 2008; Malevich 2013 a,b,c,d,e; Meko 2002; Meko 2013).

For all study sites, climate data was collected at an 800m resolution for monthly values starting in January 1895 and ending in the last year sampled at each site using interpolated spatial data products of all available observations from a wide range of monitoring networks (PRISM climate group). The location of study sites (Figure 1A) and their corresponding climate space (Figure 1B) span the current WJ range from which we gathered monthly and annual climate data to test our three hypotheses based on sensitivity relationships over space and interactions with atmospheric CO_2 over time. In all case, we used average estimates of atmospheric CO_2 concentrations from NASA reconstructions (1850-1958) http://data.giss.nasa.gov/modelforce/ghgases/Fig1A.ext.txt. and direct measurements available at NOAA (1958-2016) ftp://aftp.cmdl.noaa.gov/products/trends/co2/co2_annmean_mlo.txt.

We created plots of seasonally aggregated mean precipitation and temperature values at the regional level. Additionally, we calculated the rates of change for precipitation and temperature for the three 4-month seasons for the time period of 1980-2010 using the lm function from the stats package (R core team, 2021) (figure 3 and figure 4).

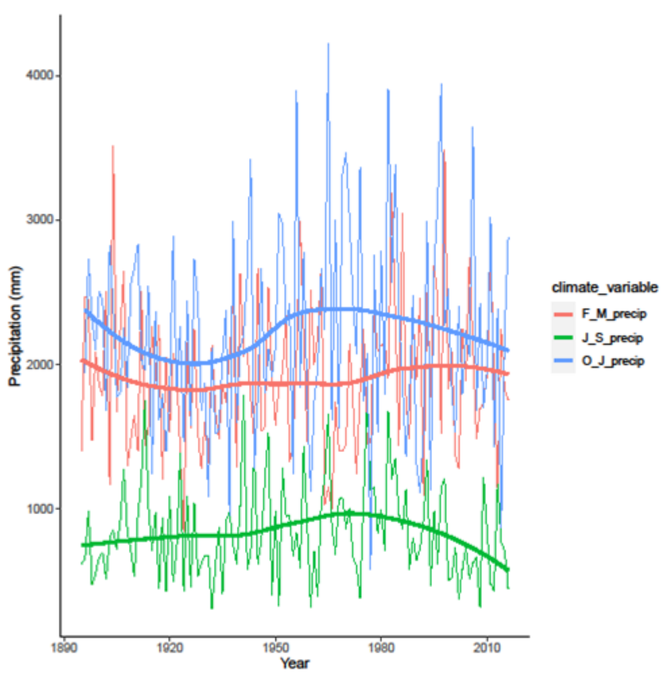

Figure 3- Mean seasonal precipitation values of all sites

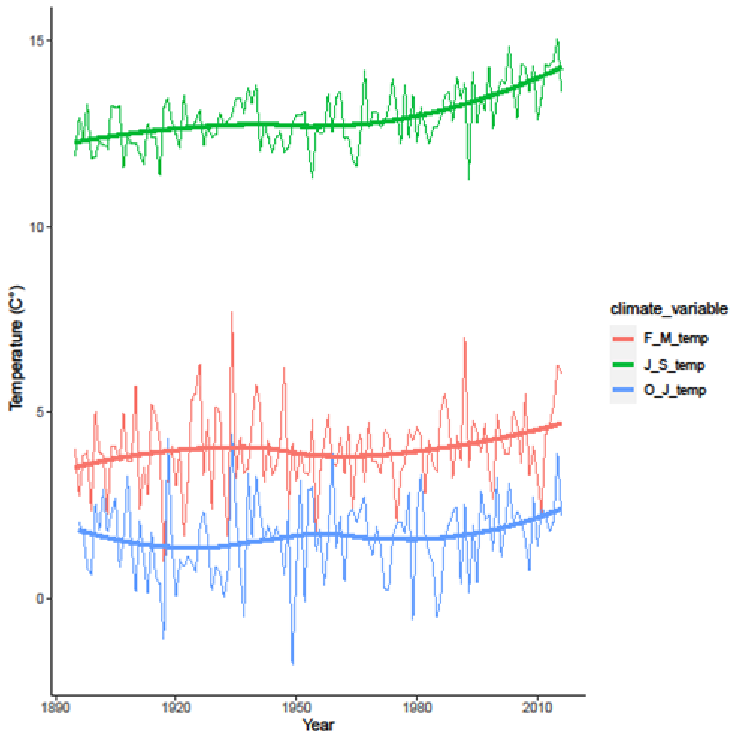

Figure 4- Mean seasonal temperature values for all sites

Data Standardization:

For all sites tree-ring widths were detrended using a modified negative exponential curve to account for the ontogenetic effect of tree size on ring width (Speer, 2010.)(figure 5a). Individual trees were then aggregated into a mean ring width index, or master chronology, at the site level to avoid interdependence of the climate predictor variables that were collected at the site level (Walker 2020) (figure 5b). Climate data was standardized at each site (mean=0 SD=1) to allow us to directly compare effect, size, and significance of resultant coefficients (figure 5f). Additionally, we aggregated monthly climate variables into consecutive equally sized multi-month “seasons” (figure 5e) To determine season size and calendar location we tested several variations of these “seasons” (two 6-month seasons, three 4-month seasons, and four 3-month seasons). We determined that three-4 month seasons was the most appropriate season length based on comparing AIC scores of linear models for each season size per site, and the general shape of climographs we produced show three potential seasons. These seasons are as follows: previous year October to current year January (O_J), current year February to current year May

(F_M) and current year June to current year September (J_S). We chose to include the preceding year's precipitation and temperature starting in October as a predictor variable in our study because previous studies found that precipitation from the previous year's October through the current year is the strongest single predictor of a current year's ring-width growth in our study species (Knapp et al., 2001b; Knutson & Pyke, 2008; Soulé & Knapp, 2019).

Figure 5- Flow chart of data processing, model selection and evaluation. Panels A-C represent the data flow of data processing for three-ring data. A) Raw tree-ring data from site OR089 series TRJ01B, black line shows tree ring variation from the pith of the tree to the year it was cored, yellow line shows the modified negative exponent used to detrend the series and account for the ontogenetic effect of tree age on ring width; B) The now unitless ring width index plotted against the age of tree at ring formation; C) The master chronology for site OR089, this is the mean RWI for all tree series at this site (n=19). Panels D-F represent the flow of data processing for climate data gathered from the PRISM climate group for each site. A) Monthly climate data for each year (1895-2016), this panel only shows monthly precipitation data, but monthly mean temperature data was also used in analysis; D) The same climate data but aggregated into three 4-month seasons: the preceding year's October through current year's January, current year's February through current years May, and current year's June through current year's September; E) The same seasonal aggregated data but scaled to have a mean of 0 and an SD of 1. Panels G-I represent the model selection, evaluation and visualization flow chart. G) The Dredge function is used to generate the most parsimonious model based on two global models (w/o climate CO_2 interactions & w/ climate CO_2 interactions); H) the adjusted r-squared value for the most parsimonious models (w/o climate CO_2 interactions & w/ climate CO_2 interactions) are compared to determine what one provides a better fit and more predictive power J) The best fitting model is displayed with significant covariates (y-axis) and their resulting coefficients (x-axis).

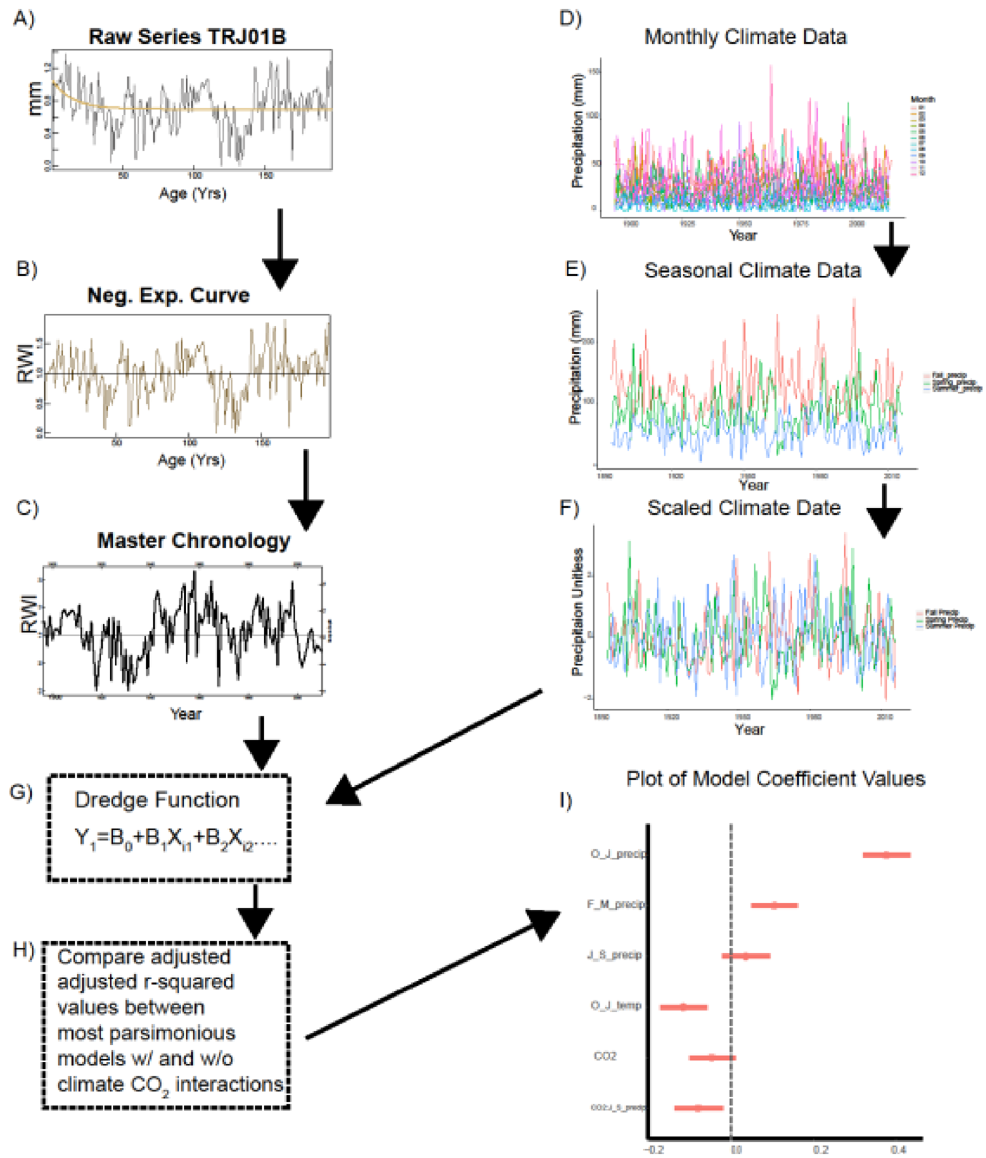

Testing Site Specific Responses:

For each individual site we constructed four multiple linear regression models using the lm function from the stats package (R core team, 2021). One model including just climate variables as predictor variables, one model including CO_2 and its interaction with climate variables as predictor variables, and a simplified version of each model using a dredge function from the MuMln stats package (R core team, 2021). (figure 5g). The dredge function works by conducting repeated evaluations of all possible iterations of predictor variables and then ranks all possible models based on AIC score. We then selected each model with the lowest AIC score for each model group and each site. By comparing the two sets of models (with and without climate * CO_2 interactions) inference on to what degree increased CO_2 levels have been modifying the effects of climate on tree-ring growth is possible (figure 5h).

Testing Regional Responses:

We used mixed-effects models to evaluate the significance and magnitude of increased atmospheric CO_2 and climate variables on WJ tree-ring growth at a regional scale with the lme function from the nlme package (Pinheiro et al, 2021). For the entirety of our data set we constructed four mixed effects models: a model consisting of just the climate variables as predictor variables, a model that included the climate variables and climate variable * CO_2 interactions, and a dredged version of each of the aforementioned models. For these mixed effects models, we included site a random intercept term.

Patterns of Sensitivity Across Regional Climate Gradients:

In order to further expand our understanding of the relationships between the growth of WJ tree-rings, climate, and increasing CO_2 levels we found it prudent to proceed with an explicitly exploratory examination of the resultant coefficients produced in our previously described site-specific modeling efforts. An exploratory approach is particularly useful when searching for relationships between climate and ecological processes and is less statistically restrictive than models aimed specifically at prediction or inference (Tredennick et al., 2021) To accomplish this, we used a mixed-effects model in a similar method to what was done in the 'Testing Site Specific Response' methods subsection. We included all climate variable predictors and climate variable * CO_2 interaction terms, however, instead of using a dredge function which determines what coefficient terms should be included to produce the most parsimonious model with the most predictive power; all climate variables, and their interactions with CO_2 were included. By including all predictive variables, we were then able to examine all resulting coefficients organized along gradients of annual precipitation and temperature. We then performed linear regressions using site mean annual precipitation or temperature as the predictor variable, and coefficient values from the previous model as the response variable. The approach allowed us to explore linear relationships between the sensitivity of WJ tree-ring growth to climate variables and the changes in that sensitivity as CO_2 levels have increased over time, across the annual precipitation and annual temperature gradients of our study sites.

Representation of our Regional Model in Western Juniper Climate-Space:

To explore how well the sites of our regional model represent the climate-space of WJW, we constructed a permutation model that compared the proximity of our 13 sites in the climate-space of WJW to 100 randomly selected 13 sites subsamples from within WJW climate-space. This comparison was based on three geospatial factors: the area of the convex-hull created by the site locations in climate-space (Area Score) (figure 6b), the dispersal of those sites in climate-space via an average Ripley's K function score for the sample sites (Dispersal Score) (figure 6c), and the proximity of the sites in climate-space to areas in climate-space with a high density of WJW locations, via the sum of site values in correspondence to a 2-D density plot or heat map (Density Score) (figure 6a). We chose these three geospatial factors because we hypothesize that a set of sample points will be well representative of a climate-space if they 1) cover a large area of that climate space, 2) are evenly distributed throughout that climate-space, and 3) the sites are within close proximity to areas in that climate-space where there is a high density of occurrence of the species of interest.

Figure 6 Conceptual figure of methods for determining how well all 13 sites from our study represented the climate space of western juniper woodlands. The upper panels (a, b, c) represent the three geospatial factors we used to quantify representation; proximity to high density potential plot locations (a), the total convex area of climate space covered by the constellation of plot locations (b), Rippley's K function to determine the dispersal of plot locations in climate space (c). In the middle panel (d, e, f) are corresponding density curves of scores (vertical dashed lines) for each geospatial factor compared to results from permutations of 13 randomly selected potential sites from within the climate space of western juniper woodlands. The bottom figure (f) is the density of scores of the composite score of all three factors (Density percentile score * Area percentile score * Dispersal percentile score), the vertical dotted line represents the three-factor score for our configuration of sites.

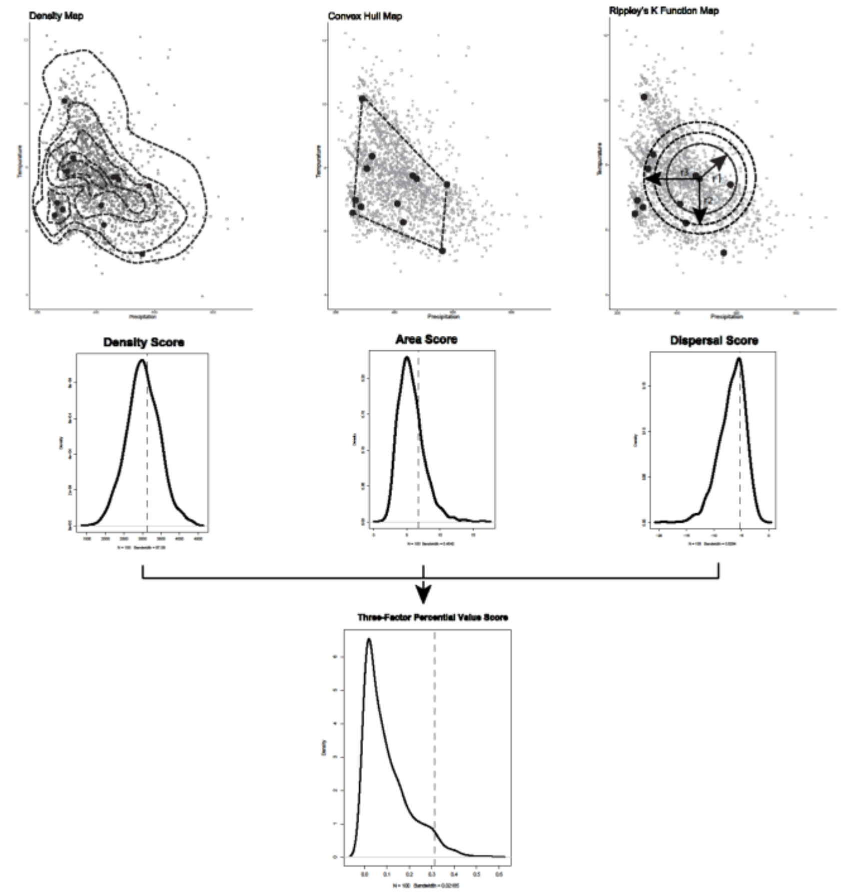

To determine the climate-space of WJW, we used a raster map of western-juniper woodlands in Oregon then filtered annual precipitation and temperature values gathered from the PRISM climate group, through the presence of WJW, leaving us with 2189 points (4km resolution) with annual precipitation and annual temperature values that represent the climate space of WJW in Oregon. To calculate the overall climate-space representation score we first individually calculated the score for each factor (Area Score, Dispersal Score, and Density Score) (figure 6 e,f,g) in our model for the set of our existing site locations. Area Score was determined using the convhulln function from the geometry package in r studio. Distribution Score was determined by using the Rippley's K function with the Kest function from the spatstat r package. Density Score was determined by calculating the sum score of the 13 points based on an overlayed density plot created using the density function with a sigma score of 0.15 from the raster package. We then selected 100 sets of 13 randomly selected points within the WJW climate-space that we will refer to as subsamples. For each of those subsamples we calculated their scores for each of our three model factors.

Based on the scores from the 100 sub samples we created empirical cumulative distribution functions and calculated the percentile value for each factor in our model for our sites and each subset (percentile scores) (figure 6g) . We then multiplied each percentile score together to calculate a single three-factor value for our sites and each subsample. These three-factor values were then used to compute another empirical cumulative distribution function. The three-factor value generated from our sites was then used as an input for this function to determine a single percentile value score. We then iterated the previous process 100 times in order to generate 100 percentile value scores from which we could generate statistics about dispersion and variation of percentile value scores from our set of sites (Figure 6).

Results

Climate Trends:

Seasonally aggregated precipitation and temperature values show a high degree of interannual variation (figure 4 and figure 5). Thirty-year climate annuals per site range from 250-669 mm (mean = 402 mm, sd=127) and 3.9-9.5C^{o} (mean=7.24 C^{o}, sd = 1.24) for precipitation and temperature respectively. Across all sites Summers are dry and warm, with the Fall, Winter, and Springs seasons being cool and wet with 45% (41-48%) of precipitation occurring from October to January and 38% (32-44%) of precipitation occurring from February to May. Results from linear models of annual values and seasonally aggregated climate variables from 1980-2010 indicate that precipitation and temperature patterns are changing with annual precipitation decreasing, and annual temperature increasing. October through January precipitation showed no significant trend, October through January temperature increasing, February through May precipitation decreasing, February through May temperature showing no significant trend, June through September precipitation decreasing, and June through September temperature increasing (table 1).

Table 1 Results of linear regression model for changes in climate at all sites (n=13) from years 1980-2010, including angular coefficients (i.e. slope) and significance level of each regression. Precipitation and Temperature values are aggregated into three 4-month "seasons" starting with the precedent year's October through current year's January (O_J), the current year's February through May (F_M) and the current year's June through September (J_S).

Climate Trends 1980-2010

Climate Variable	*Coefficient*	*p-value*
Annual Precip	-2.3436	<0.01
O_J Precip	-0.5174	0.1618
F_M Precip	-0.8193	<0.05
J_S Precip	-1.0068	<0.001
Annual Temp	0.0290	<0.001
O_J Temp	0.1191	<0.001
F_M Temp	0.0503	0.108
J_S Temp	0.1791	<0.001

Site Specific Responses:

Our set of site specific multiple linear models show a positive response of WJ tree-ring growth to seasonal precipitation and negative response to summer temperature for the majority of sites, supporting hypothesis 1a (table 2, figure 7). Tree-ring sensitivity to precipitation varied between seasons, in terms of magnitude of coefficient values and inclusion in models. Sensitivity to October to January precipitation had the greatest mean coefficient value (0.203) but was only an included covariate in 8 out of 13 site specific models (table 1). Sensitivity to February to March precipitation had the next highest mean coefficient value (0.088) and was included as a covariate in all site specific models. Sensitivity to June to September precipitation had a mean coefficient of 0.063 and was included in 12 of 13 site specific models. Seven out of 13 site specific models included June to September as a model covariate, with each resulting coefficient being negative in sign with a mean value of -0.06.

Table 2- Resultant coefficient values from site specific multiple linear models including climate variables and CO2 interactions. Models were created using the dredge function to determine the most parsimonious model per site.

	OR092	**OR093**	**OR095**	**OR089**	**OR094**	**CA095**	**ID006**	**CA517**	**OR063**	**OR009**	**CA675**	**OR006**	**NV518**
(Intercept)	1.12	1.01	1.04	1.01	0.98	1.00	1.06	1.01	1.03	1.08	1.04	1.02	1.09
O_J_precip	0.30	0.21	0.20	0.38	0.22	0.12		0.14					0.05
F_M_precip	0.17	0.13	0.11	0.11	0.14	0.10	0.08	0.06	0.09	0.05	0.04	0.09	0.06
J_S_precip	0.08	0.07	0.04	0.04		0.06	0.08	0.04	0.07	0.08	0.06	0.09	0.12
O_J_temp	-0.03	-0.04		-0.12	-0.06		0.06	0.01		0.07	0.05	0.05	
F_M_temp	-0.05		-0.04		-0.06								
J_S_temp			-0.05		-0.08	-0.07		-0.04	-0.07	-0.05	-0.06		
CO2	-0.02	0.09	0.12	-0.05	0.11	0.10		-0.06	0.09	0.03	0.03		
CO2*O_J_precip	-0.07		-0.07										
CO2*F_M_precip		0.04	0.04							-0.05	0.05		
CO2 * J_S_precip				-0.08				0.04			-0.04		
CO2 * O_J_temp	-0.05							-0.07					
CO2 * F_M_temp			0.04		0.07								
Observations	115	115	115	101	115	87	89	85	103	87	115	87	103
R^2 / R^2 adjusted	0.631 / 0.603	0.530 / 0.504	0.532 / 0.491	0.558 / 0.530	0.492 / 0.459	0.439 / 0.404	0.275/ 0.249	0.456 / 0.399	0.488 / 0.462	0.314 / 0.263	0.268 / 0.220	0.243 / 0.215	0.234 / 0.210

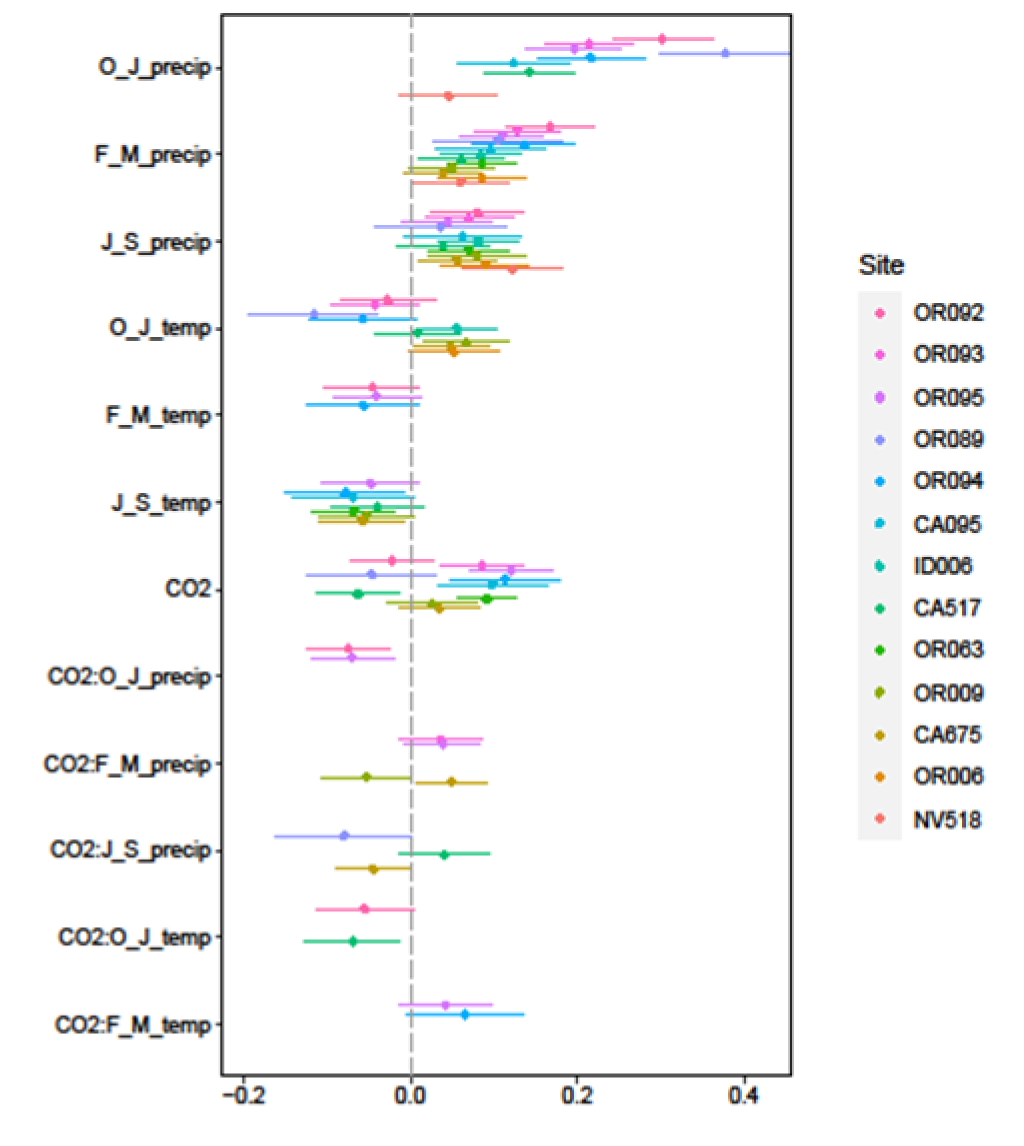

Figure 7- Site specific results from dredged linear models with climate * CO_2 interactions. On the Y-axis are the coefficient terms and on the X-axis are the coefficient values. These coefficient values represent the sensitivity of WJ tree-rings to these terms. Sites are arranged in the legend and values for sites are arranged in the figure descending from lowest annual precipitation values (OR092) to highest annual precipitation values (NV518).

By comparing the adjusted r-squared value between models with and without climate * CO_2 interactions, we can infer the effect of increased atmospheric CO_2 on WJ climate-growth relationships at a site level. At 10 of 13 sites, the model with the highest adjusted r-squared value, and therefore highest amount of model fit, and variance explained, included climate * CO_2 interaction terms, supporting hypothesis 1b (table 3). Mean values for adjusted r-squared values were 0.385 and 0.330 for models with and without climate x CO_2 interactions, respectively. When examining the resultant coefficients and annual precipitation of each site we see a pattern of decreasing coefficient values, as mean annual precipitation increases for fall-winter precipitation (Multiple R-squared: 0.5702, Adjusted R-squared: 0.4986, F-statistic: 7.961 on 1 and 6 DF, p-value: 0.0303) and winter-spring precipitation (Multiple R-squared: 0.5898, Adjusted R-squared: 0.5525, F-statistic: 15.81 on 1 and 11 DF, p-value: 0.002171). There is also a trend of decreasing r-squared values of our linear models for individual sites as annual precipitation increases across an annual precipitation gradient (Multiple R-squared: 0.7071, Adjusted R-squared: 0.6805, F-statistic: 26.56 on 1 and 11 DF, p-value: 0.0003167). Additional trends of sensitivity of tree-ring growth to climate variables is further explored in the section 'Patterns of Sensitivity Across Regional Climate Gradients.'

Table 3 Comparisons of adjusted r-squared values from two linear models, with and without climate *CO_2 interactions for all 13 study sites.

	Adjusted r-squared	
Site	*with interaction terms*	*without interaction terms*
OR092	0.6027	0.5679
OR093	0.5041	0.4446
OR095	0.4914	0.332
OR089	0.5298	0.5164
OR094	0.459	0.3907
CA095	0.4039	0.3498
ID006	0.2494	0.2494
CA517	0.3991	0.3249
OR063	0.4619	0.2954
OR009	0.2627	0.2422
CA675	0.2197	0.1492
OR006	0.2154	0.2154
NV518	0.2105	0.2105

Regional Responses:

Results from our regional model show that precipitation from the previous year's October until the current year's January (O_J_precip) had the greatest positive influence on tree-ring growth for WJ trees within our study sites, followed by February through march precipitation (F_M_precip), then June through September precipitation (J_S_precip). Finally, June through September (J_S_temp) temperature has a negative influence on WJ tree-ring growth with a magnitude that is lower than the climate variables that have a positive influence (Figure 8). This supports our hypothesis 2a), that at the regional level WJ tree growth will have a positive response to seasonal precipitation and a negative response summer temperature with significant interactions arising from seasonal climate and CO_2 levels.

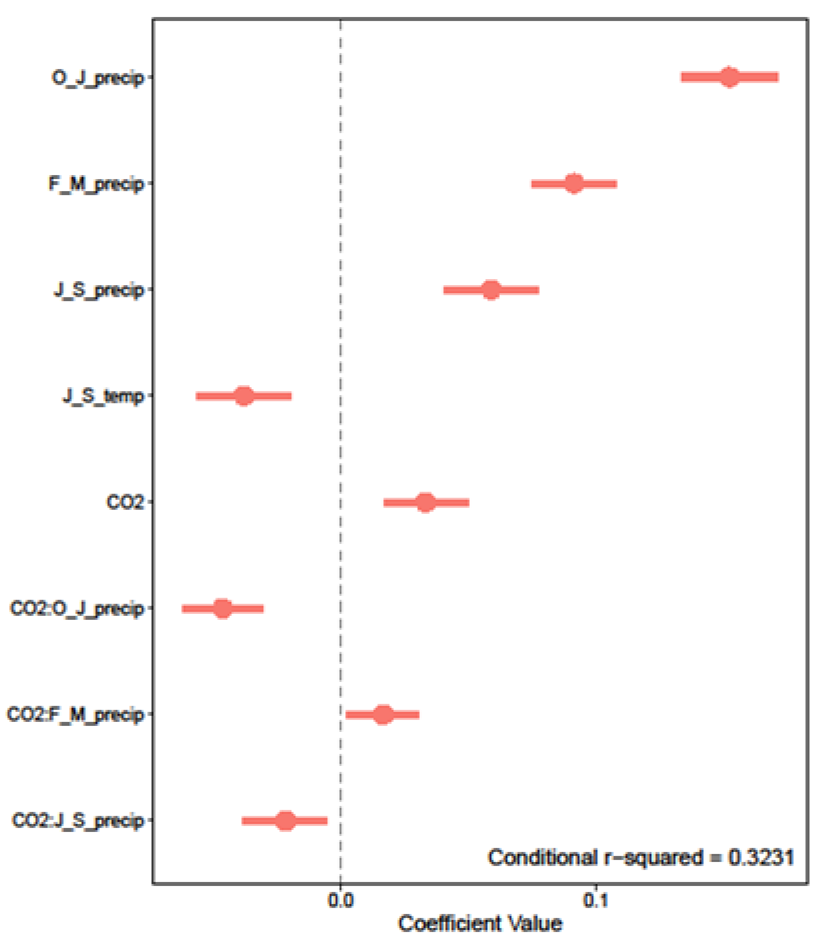

Figure 8- Coefficient values (x-axis) and predictor variables (y-axis) from dredged regional mixed effects model.

Comparison of the marginal and conditional r-squared values for our regional model for with and without climate * CO_2 interactions show that the model with climate * CO_2 interactions explains more of the variance and has a better fit (0.3232 and 0.2866, respectively) and therefore our hypothesis 2b) is supported that our model will have a better fit and stronger predictive power when CO_2 x climate variable interactions are included (Table 4).

Table 4- Results from our regional mixed effects model of western juniper woodlands

	Ring Width Index		
Predictors	*Estimates*	*CI*	*p*
(Intercept)	1.05	1.03 – 1.07	**<0.001**
CO2	0.03	0.02 – 0.05	**<0.001**
F_M_precip	0.09	0.07 – 0.11	**<0.001**
J_S_precip	0.06	0.04 – 0.08	**<0.001**
J_S_temp	-0.04	-0.06 – -0.02	**<0.001**
O_J_precip	0.15	0.13 – 0.17	**<0.001**
CO2 * F_M_precip	0.02	0.00 – 0.03	**0.022**
CO2 * J_S_precip	-0.02	-0.04 – -0.01	**0.010**
CO2 * O_J_precip	-0.05	-0.06 – -0.03	**<0.001**
Random Effects			
σ^2	0.09		
$\tau_{00\ Site}$	0.00		
ICC	0.00		
N_{Site}	13		
Observations	1317		
Marginal R^2 / Conditional R^2	0.321 / 0.323		

When examining predicted and observed values from our regional model plotted per year we can see that both series show a large degree of annual variation, which is highly correlated

(R=0.78) (Figure 9). Our model tends to under predict for years of either extremely large or small observed ring-widths.

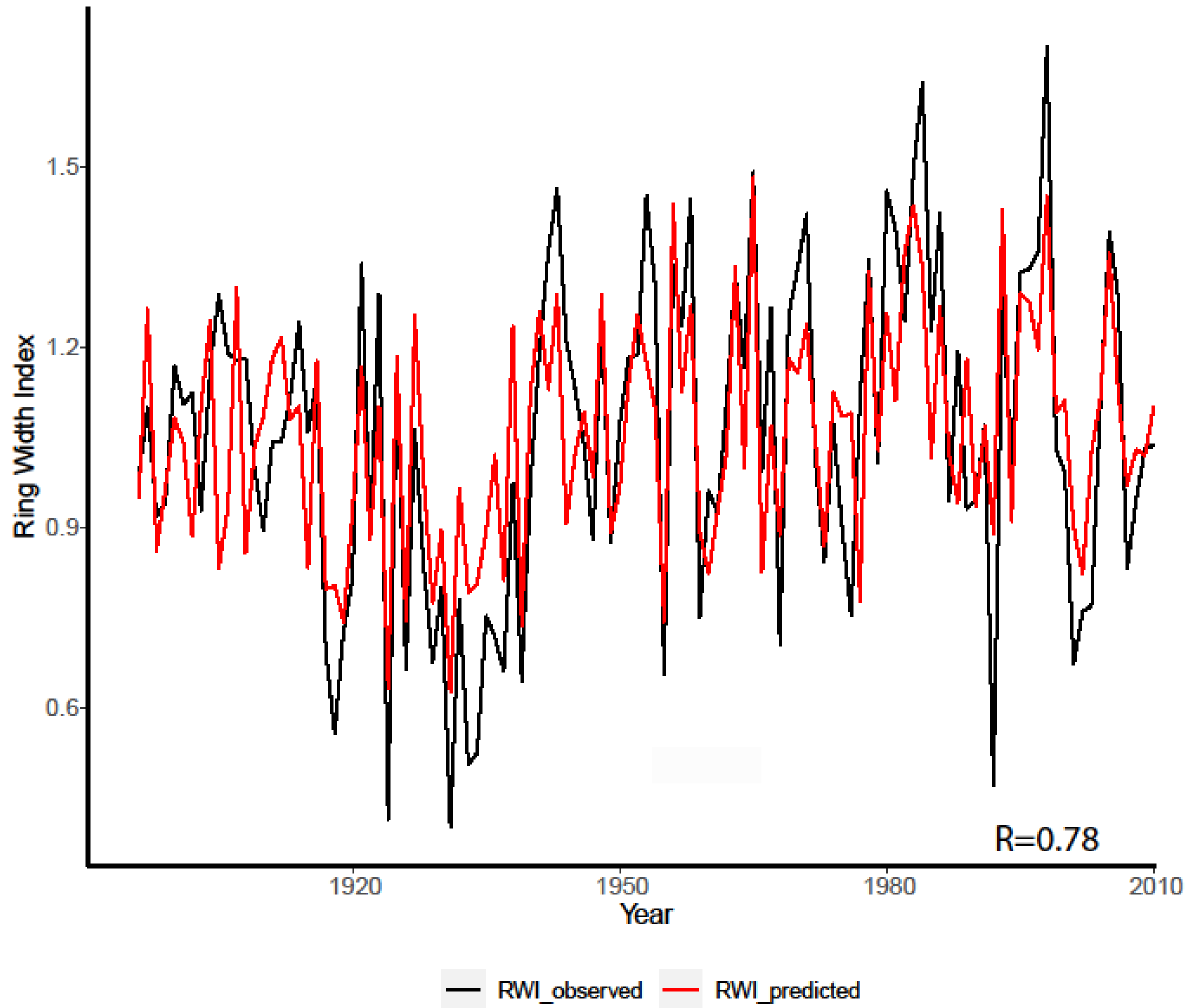

Figure 9- Observed (black) and predicted (red) average regional tree growth, inferred from tree ring width, using master chronologies of western juniper woodlands based on 13 different study sites, for years 1896-2010.

Our regional model contains three climate variable x CO_2 interaction terms. Fall-winter precipitation and summer precipitation that are both negative in sign, and winter-spring precipitation that is positive in sign. This indicates that WJ ring-widths have been becoming less sensitive to fall-winter precipitation and summer precipitation, while becoming more sensitive to winter-spring precipitation. These significant interactions between climate variables provides both support and counter evidence for our hypothesis 2) that elevated CO_2 levels will result in an increase in drought tolerance for WJ trees as evidenced by statistically significant and negative CO_2 x precipitation coefficient values.

Patterns of Sensitivity Across Regional Climate Gradients:

Out of the 14 potential resultant coefficient terms that could have linear relationships with site level annual precipitation, between 7 and 4 of them produced significant results (figure 10). The number of significant results is dependent on if and what type of correction for multiple comparisons is used (Bonferroni, Holm). Since this is a model explicitly used for data exploration, the consequences of spurious relationships are minimized (Tredennick et al 2021), therefore we will report results as being either non-spurious or possibly spurious (figure 10).

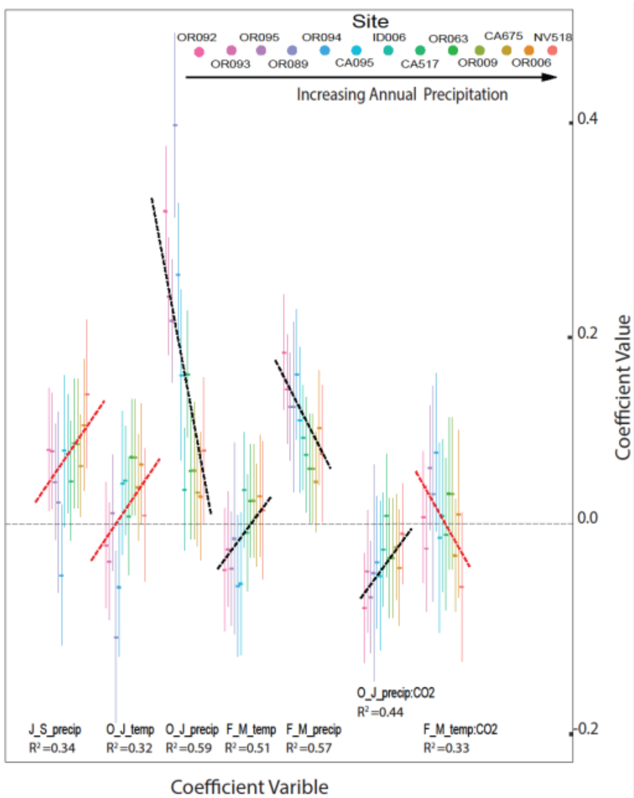

Figure 10- Representation of post-hoc data exploration of linear relationships between resultant coefficients of climate variables and climate variable CO_2 interactions and site level annual precipitation values. Mean coefficient values are shown (small colored rectangles) with standard error values (colored vertical bars). Bold dashed lines represent linear relationships, red dashed lines are possible spurious results, and black dashed lines are non-spurious. Site coefficient values are organized for each climate variables along an annual precipitation gradient, with more arid sites on the left side, and less arid sites on the right.

The four non-spurious relationships are between site annual precipitation and: O_J_Precip, F_M_Temp, F_M_Precip, and O_J Precip:CO_2. The three possibly spurious relationships are between site annual precipitation and J_S precip, J_S temp, and F_M Temp: CO_2. Results from this analysis show us that tree-ring sensitivity to O_J Precip and F_M Precip is positive for all sites and decreases as annual precipitation increases across sites. However, the resultant coefficients, or sensitivity to F_M Temp is negative at drier sites and positive at wetter sites, with increasing sensitivity as annual precipitation increases. This indicates that annual tree-ring width of WJ trees are negatively impacted by warmer spring temperatures at drier sites, but positively impacted by warmer spring temperatures at wetter sites. The only non-spurious relationship that contains a climate variable * CO_2 interaction is the positive relationship between O_J Precip:CO_2 coefficients and annual precipitation. The coefficient term for O_J Precip:CO2 is negative for 12 of 13 sites and increases (becomes less negative) as annual precipitation increases across sites. This indicates that as CO_2 concentrations have increased, the decrease in sensitivity to O_J precipitation is more pronounced at more arid sites than at less arid sites. Additionally, there may be positive relationship between sensitivity to J_S prrecipitation and annual precipitation, along with J_S Temp and annual precipitation. Their also may be a negative relationship between F_M Temperature :CO_2 and annual precipitation, with a decrease in sensitivity to F_M Temp as CO_2 has increased at both more arid and less arid sites (figure 10).

Representation of our Regional Model in Western Juniper Climate-Space:

To explore how well the site locations used in this study represent the climate-space occupied by WJW (Figure 1B), we developed a permutation model that accounts for three factors: 1) the area of a convex hull created by the locations of our sites in climate-space, 2) the evenness of the distributions of our sites in climate- space, and 3) the proximity to areas of high-density WJW locations in climate-space (Figure 6). For this analysis, we define climate space as a two-dimensional plane of annual precipitation and annual temperature (Figure 1B). The precipitation range of climate space occupied by WJW is 208mm to 900mm with a mean value of 414mm. Mean annual temperature ranges from 3.96 C^o to 12.15 C^o with a mean value of 7.59 C^o. Our sites had a mean Area Score percentile of 0.736 (SD=0.043), a mean Dispersal Score percentile of 0.6811 (SD=0.044) and a mean Heat Score percentile of 0.6209 (SD=0.05). When these three factors were composited and compared to the scores of the composite scores of 100 subsamples 100 times, our results show us that our sites our in the 93.91 (SD=2.63) percentile of representativeness of 13 site plot locations.

Discussion

Here we provide evidence for this non-stationarity of climate-juniper-woodland relationships. Global CO_2 concentrations have increased by 38% over the course of this study (333ppm in 1895 to 404 ppm in 2016). Our analysis of WJ tree-rings show that this CO_2 rise has resulted in temporal non-stationarity in WJ growth and climate relationships at both a site a regional level. We identified shifts in juniper tree growth sensitivity to climate and CO_2 over space and time which supports our overarching hypothesis that predictable trends in tree growth emerge as a result of interactions between climate (seasonal and annual), atmospheric CO_2 levels, and site conditions.

Specifically, we find support to hypothesis 1a) and 1b) that WJ tree ring growth will have a positive response to precipitation and a negative response to summer temperature at a site level and that models including CO_2 climate interactions will have a better fit and more predictive power than models that do not include that interaction (table 3, figure 7).We also find support for hypothesis 2a) and 2b) that at the regional level WJ tree growth will have a positive response to precipitation and a negative response to summer temperature with models having a better fit and more predictive power when CO_2 climate interactions were included (figure 8). Finally, we found partial support for h3a) and h3b) We did discover patterns of WJ tree ring sensitivity varying across a climate gradient of annual precipitation, with a greater reduction in sensitivity at drier sites at elevated CO_2 levels. However, no such patterns we detected for across a climate gradient of annual temperature (figure 10).In summary, we show that tree-ring growth models have a better fit and more predictive power when $CO2_2$ * climate variable interactions are included.

Even though the number of site locations in this study (n=13) was limited, by taking an exploratory analytical approach to WJ growth responses across geographic and climatic space we are able to recognize and reflect on several noticeable geographic and climatic patterns, that should prove useful in producing future hypotheses and informing future research avenues.

Additionally, our permutation model for assessing representativeness of site locations within environmental space could provide a framework for assessing existing research networks or for selecting future sampling locations. Furthermore, investigating the impact of increased atmospheric CO_2 on tree-ring growth climate relations should be applied to a wider range of ecosystems with an emphasis on exploring patterns of differential change in sensitivity across the climate space of the ecosystem or species of interest.

Site Specific Responses:

When examining the adjusted r-squared values from the individual site models we see, for 11 of the 13 sites, that tree-ring growth is better explained when CO_2 * climate variable interactions are included in the models. No sites however, had models that provided more explanatory power when CO_2 x climate variable interactions were not included. The sites NV518, OR006, and ID006 have the same adjusted r-squared values for both models with and without CO_2 * climate variable interactions. This is because the dredge function selected the same explanatory variables for each model set and these models did not include CO_2 * climate variable interactions for these sites. However, this may be an artifact of the temporal limitations of those data sets and/or related to an actual climate tree-ring relationship. Sites OR006 and ID006 only have tree-ring data that extends to 1982, and 1984 respectively; and NV518 and OR006 have the highest and second highest annual precipitation for all sites in this study. It seems reasonable to hypothesize that the explanatory value of CO_2 * climate variable interactions would be greater in more recently sampled sites, and also in more arid sites. The results from our individual site models, along with our regional model analysis provide further evidence that CO_2 increases impacting the relationships between WJ tree-ring growth and climate relationships.

Regional Responses:

Our regional model provides insight about how climate variables aggregated into three 4-month "seasons" affect tree-ring growth for WJ trees. Previous studies have identified that precipitation from the previous October to the current year June to be the strongest predictor variable for WJ tree-ring growth and that summer temperature can have a negative impact on WJ tree-ring growth (Soulé and Knapp, 2019; Knutson and Pike, 2008). When we convert the coefficients for each of the precipitation variables into the proportion of the sum of these coefficients, we see that 50% of the explanation due to precipitation is due to O_J precipitation (coefficient=0.15), 30% is due to F_M precipitation (coefficient= 0.09) and 20% is due to J_S precipitation (coefficient= 0.06). These proportions of the sum of precipitation coefficients are similar to the percentages of precipitation for those same three 4-month seasons; with O_J precipitation at 45% of the total, F_M precipitation at 38% of the total and J_S precipitation at 17% of the total. O_J and J_S both have coefficient percentages that are slightly higher than total precipitation percentages (50% vs 45% and 20% vs 17%) and F_M has a the opposite with a coefficient percentage that is slightly lower than its precipitation percentage (30% and 38%). This could mean that precipitation in the O_J season and the J_S season play a more important role in WJ tree-ring formation and growth that F_M precipitation when compared to the proportion of precipitation in each of those seasons.

Additionally, when we examine the CO_2 * climate variables interactions from our regional model and recent climate trends, we see that the climate for this region is changing, and the relationship between climate and tree-ring growth is also changing. Included in the regional model are three CO_2 * climate variables interaction terms, CO_2 * F_M_precip, CO_2 * J_S_precip, and CO_2 * O_J_precip. The inclusion of these CO_2 * climate variable interaction terms means that the relationship between WJ tree-ring growth and these climate variables has changed as CO_2 has increased over the last century. Specifically, the negative coefficients for CO_2 * J_S_precip, and CO_2 * O_J_precip means that tree-ring growth in WJ trees have been becoming less sensitive to J_S precipitation, and less sensitive to O_J precipitation. Conversely, the positive coefficient for CO_2 * F_M_precipitation implies that WJ tree-ring growth has become more sensitive to F_M precipitation since 1896.

Since F_M_precipitation has decreased significantly by 0.82 mm per year over the last 30 years, this decrease could be the cause of the perceived increase in tree-ring sensitivity to F_M_precipitation that we see in our model, via a positive F_M_precipitation * CO_2 interaction term. However, the decrease in tree-ring sensitivity to O_J_precipitation and J_S_precipitation as CO_2 increases occurred while O_J_precipitation did not change significantly and J_S_precipitation decreased significantly, supporting the hypothesis that increased atmospheric

CO_2 increases drought tolerance in WJ trees due to an increase in intrinsic water use efficiency (iWUE).

Patterns of Sensitivity Across Regional Climate Gradients:

The results from our post hoc data exploration of pattern of sensitivity across regional climate gradients support our hypothesis 3a) -that the sensitivity of WJ trees to climate variables varies across a climate gradient- and hypothesis 3b) that the impact of elevated CO_2 will decrease WJ tree-ring sensitivity to climate variables to a greater degree at drier than at wetter sites. Our findings from hypothesis 3a) are similar to phenomena that have been observed in adjacent ecosystems (Adler et al., 2018; Kleinhesselink & Adler, 2018; Klesse et al., 2020; Renwick et al., 2018). The meta-analyses conducted by Kleinhesselink and Adler (2018), and Renwick et al (2018) observed the responses of big sagebrush (*Artemisia tridentata*) to interannual climate variation from 1994-2006 at over 100 study plots. Big sagebrush is a woody perennial shrub that occupies the interspace of WJW, and dominates the plant communities directly downslope of WJW.

Based on our post hoc data exploration of tree-ring sensitivities organized along climate gradients, and similar findings from Kleinhesselink and Adler (2018) we can postulate how climate variation might impact relative production of these often competing and interacting plant species where they co-occur. Where we found that WJ tree-ring growth was most sensitive to precipitation variables with several significant trends of sensitivity when sites were organized along an axis of annual precipitation, we found no significant trends of sensitivity when organized along an axis of annual temperature. However, according to Kleinhesselink and Adler (2018), big sagebrush foliage cover was most sensitive to growing season temperatures, with a positive response to warmer than average years at colder sites and a negative response to warmer than average years at hot sites. The inflection point for the impact of temperature on big sagebrush growth was at a mean annual temperature of 10 degrees Celsius, a mean annual temperature higher than any of our sites. Since J_S Temperature, and F_M Temperature, both have negative impact on WJ tree-ring growth at arid sites, but a positive impact at less arid sites (figure 10), perhaps, where WJ and big sagebrush coexist, warmer than average years might favor increased sagebrush growth with negative impacts on WJ growth at arid sites, and positive impacts on WJ growth at less arid sites. Meaning that increasing temperatures might favor big sagebrush over WJ at more arid locations, but perhaps not at less arid locations. The study by Kleinhesselink and Alder (2018) did not explicitly address the impacts of increasing CO_2 levels on the sensitivities of big sagebrush to climate, their study years were relatively recent (1994-2006) but we do not know if and in what direction increased CO_2 has and/or will shift big sagebrush climate sensitivities.

Representation of our Regional Model in Western Juniper Climate-Space:

In order for dendrochronology to be useful in producing accurate projections of future tree and woodland function and distribution there is a need to focus on the spatial representativeness tree-ring sampling networks (Babst et al., 2018), specifically the spatial representativeness within n-dimesional hypervolume that represents niche space (Perret & Fox, 2022). Perret and Fox (2022) examined the coverage of niche space for 64 conifer species between a geographic sampling grid and a niche space grid and discovered that a niche grid covers more area of a specie's niche space than a geographic grid.

However, Perret and Fox (2022), only assessed spatial coverage via one metric, minimum convex polygon. Our permutation model considers three metrics of spatial coverage: area covered, evenness of site distribution, and proximity of sites to densely populated areas of climate space. We believe our permutation model could provide future researchers with avenues of exploration in the refinement of such niche representation models. In addition, our method for exploring this problem might prove helpful in the selection of sampling site areas used to augment an existing sampling network, where the formation of a site network gridded in niche space may not be feasible.

Results from our permutation model provide evidence that the locations of sites in this study represent the climate-space of WJW better than 93% ±2.63% of 13 hypothetical sites selected randomly from WJW climate-space. Although this score provides evidence that the site locations from this study represent the climate space of WJW well, based on our three selected metrics (Area, Dispersal, and Density) several lines of inquiry remain to be explored related to our model of representativeness of climate-space. Firstly, a network of tree-ring site locations should attempt to represent more than just climate-space and should move beyond a two-dimensional climate bi-plot for score evaluation (Klesse et al., 2018). Ideally, our representativeness model could expand its score evaluations into an n-dimensional climate/ecological/management hyper-space, that accounts for variables such as: land use history and ownership; edaphic properties like soil type and parent material; plant community composition; geomorphic properties like, elevation, slope, aspect, and topographic wetness index; disturbance and fire history, and stand age, and stand structure. This would make our permutation model transcend the representation of climate-space to the representation of meta-ecological hyper-space. Beyond the inclusion of meta-ecological variables, our permutation model would then need to be calibrated using a network of existing tree-ring studies that contains enough study sites to determine what variables and spatial metrics create correlation between tree-ring growth models constructed from the entire data set and a subsample of sites.

Inclusion in Subsequent Future Projection Models:

Efforts over the last decade to model future extent and abundance of WJW and adjacent ecosystems can show a high level of uncertainty, and inconsistency; with Creutzburg et al. (2015) predicting WJW expanding from three to five-fold in area over the 21st century in central and eastern Oregon. In contrast, Zimmer et al (2021), and Gibson (2011), predict widespread declines in WJ vegetation over the same time period and region. Inclusion of our findings in subsequent future projection models should reduce this uncertainty, because from what we have gathered recent models either do not account for the impacts of increased CO_2 on WJ climate relations (Creutzburg et al., 2015) or do not account for the idiosyncratic responses of WJW to climate changes because of the broad vegetation categories of Dynamic Global Vegetation Models (Jiang et al., 2013; Notaro et al., 2012; Rehfeldt et al., 2012; Zimmer et al., 2021).

Declining of CO_2 Stimulation of Tree Growth and Broader Implications:

How WJW will respond in the future depends greatly on future management, disturbance regimes, climate scenarios, and the impact and persistence of the CO_2 fertilization effect. There is high confidence that drought and fire prone weather will continue to increase in Western North America under future climate scenarios (IPCC 2021). Fire regimes and both patterns of precipitation and temperature are two mitigating factors of WJW distributions at both large and small spatiotemporal scales (Miller, 2019), however recent increases in temperature and decreases in precipitation have not had the negative impacts on WJ tree-ring growth as one would expect compared to the historical records, perhaps due to a reduction in drought sensitivity due to an increase in iWUE due to an increase in atmospheric CO_2 levels, as evidenced by our study. The temporal persistence, and spatial patterns of the potential drought mitigating effect of increased atmospheric CO_2 levels is still uncertain. It is generally agreed upon that the CO_2 fertilization effect will vary across biomes (Charney et al., 2016; Donohue et al., 2013), be limited by nutrients related to edaphic properties (Norby et al., 2010), and eventually be overtaken by a continued decreased precipitation or increased temperatures (Sperkich et al., 2020; Charney et al. 2016). Results from our study will help to elucidate some of these questions.

However, we recommend that similar analysis be applied to all existing tree-ring data sets. It has been predicted that the drought mitigating effect of increased atmospheric CO_2 will be greater in arid ecosystems (Donohue et al. 2013), additionally from our study we see a similar pattern with in the WJW ecosystem. As seen by our permutation model for the representation of the sites from our study within the climate space of WJW, our study site locations do good job of representing said climate space in an expansive, inclusive, and evenly distributed manner. However, it has been noted that models derived exclusively from dendrochronological studies can be biased towards more sensitive trees (Babst et al., 2018; Brienen et al., 2012; Klesse et al., 2018). Therefor, it would be beneficial to sample additional sites that allow for a sampling regime that goes beyond climate-space representation to a more meta-ecological representation of WJW. Additionally, sampling younger trees would help quantify the impacts of climate variables and CO_2 interactions on younger vs older trees, and perhaps capture non-linear relationships between climate and CO_2 level interactions (Andreson-Texera et al. 2021).

References

Allen, C. D., Macalady, A. K., Chenchouni, H., Bachelet, D., McDowell, N., Vennetier, M., Kitzberger, T., Rigling, A., Breshears, D. D., Hogg, E. H. (Ted), Gonzalez, P., Fensham, R., Zhang, Z., Castro, J., Demidova, N., Lim, J.-H., Allard, G., Running, S. W., Semerci, A., & Cobb, N. (2010). A global overview of drought and heat-induced tree mortality reveals emerging climate change risks for forests. Forest Ecology and Management, 259(4), 660–684. https://doi.org/10.1016/j.foreco.2009.09.001

Anderson-Teixeira, K. J., Herrmann, V., Rollinson, C. R., Gonzalez, B., Gonzalez-Akre, E. B., Pederson, N., Alexander, M. R., Allen, C. D., Alfaro-Sánchez, R., Awada, T., Baltzer, J. L., Baker, P. J., Birch, J. D., Bunyavejchewin, S., Cherubini, P., Davies, S. J., Dow, C., Helcoski, R., Kašpar, J., … Zuidema, P. A. (2021). Joint effects of climate, tree size, and year on annual tree growth derived from tree-ring records of ten globally distributed forests. Global Change Biology, 28, 245– 266. https://doi.org/10.1111/gcb.15934

Azuma, D. L., Hiserote, B. A., & Dunham, P. A. (2005). The western juniper resource of eastern Oregon, 1999. (PNW-RB-249). U.S. Department of Agriculture, Forest Service, Pacific Northwest Research Station. https://doi.org/10.2737/PNW-RB-249

Babst, F., Bodesheim, P., Charney, N., Friend, A. D., Girardin, M. P., Klesse, S., Moore, D. J. P., Seftigen, K., Björklund, J., Bouriaud, O., Dawson, A., DeRose, R. J., Dietze, M. C., Eckes, A. H., Enquist, B., Frank, D. C., Mahecha, M. D., Poulter, B., Record, S., … Evans, M. E. K. (2018). When tree rings go global: Challenges and opportunities for retro- and prospective insight. Quaternary Science Reviews, 197, 1–20. https://doi.org/10.1016/j.quascirev.2018.07.009

Baddeley A, Rubak E, Turner R (2015). Spatial Point Patterns: Methodology and Applications with R. London: Chapman and Hall/CRC Press, 2015. URL https://www.routledge.com/Spatial-Point-Patterns-Methodology-and-Applications-with-R/Baddeley-Rubak-Turner/9781482210200/

Barton K (2020). MuMIn: Multi-Model Inference. R package version 1.43.17. https://CRAN.R-project.org/package=MuMIn

Bates, J. D. (2020). Herbaceous Response to Cattle Grazing following Juniper Cutting in Oregon. 10.

Bazzaz, F. A. (1990). The Response of Natural Ecosystems to the Rising Global CO2 Levels. Annual Review of Ecology and Systematics, 21(1), 167–196. https://doi.org/10.1146/annurev.es.21.110190.001123

Belsky, A. J. (1996). Viewpoint: Western Juniper Expansion: Is It a Threat to Arid Northwestern Ecosystems? Journal of Range Management, 49(1), 53. https://doi.org/10.2307/4002725

Burkhardt, J. W., & Tisdale, E. W. (1976). Causes of Juniper Invasion in Southwestern Idaho. Ecology, 57(3), 472–484. https://doi.org/10.2307/1936432

Chambers, J. C., Maestas, J. D., Pyke, D. A., Boyd, C. S., Persistent Threats to Sagebrush Ecosystems and Greater Sage-grouse. Rangeland Ecology & Management, 70(2), 149–164. https://doi.org/10.1016/j.rama.2016.08.005

Charney, N. D., Babst, F., Poulter, B., Record, S., Trouet, V. M., Frank, D., Enquist, B. J., & Evans, M. E. K. (2016). Observed forest sensitivity to climate implies large changes in 21st century North American forest growth. Ecology Letters, 19(9), 1119–1128. https://doi.org/10.1111/ele.12650

Creutzburg, M. K., Halofsky, J. S., & Hemstrom, M. A. (2012). Using state-and-transition models to project cheatgrass and juniper invasion in southeastern Oregon sagebrush steppe. http://www.treesearch.fs.fed.us/pubs/42570

Creutzburg, M. K., Halofsky, J. E., Halofsky, J. S., & Christopher, T. A. (2015). Climate Change and Land Management in the Rangelands of Central Oregon. Environmental Management, 55(1), 43–55. https://doi.org/10.1007/s00267-014-0362-3

De Kauwe, M. G., Medlyn, B. E., Zaehle, S., Walker, A. P., Dietze, M. C., Hickler, T., Jain, A. K., Luo, Y., Parton, W. J., Prentice, I. C., Smith, B., Thornton, P. E., Wang, S., Wang, Y.-P., Wårlind, D., Weng, E., Crous, K. Y., Ellsworth, D. S., Hanson, P. J., … Norby, R. J. (2013). Forest water use and water use efficiency at elevated CO 2: A model-data intercomparison at two contrasting temperate forest FACE sites. Global Change Biology, 19(6), 1759–1779. https://doi.org/10.1111/gcb.12164

Donohue, R. J., Roderick, M. L., McVicar, T. R., & Farquhar, G. D. (2013). Impact of CO 2 fertilization on maximum foliage cover across the globe's warm, arid environments: CO 2 FERTILIZATION AND FOLIAGE COVER. Geophysical Research Letters, 40(12), 3031–3035. https://doi.org/10.1002/grl.50563

Eddleman, L., Miller, P., Miller, R. F., & Dysart, P. (1994). Western Juniper Woodlands (of the Pacific Northwest) Science Assessment. United States Forest Servise, 0(0), 1–132.

Franks, P. J., Adams, M. A., Amthor, J. S., Barbour, M. M., Berry, J. A., Ellsworth, D. S., Farquhar, G. D., Ghannoum, O., Lloyd, J., McDowell, N., Norby, R. J., Tissue, D. T., & Caemmerer, S. (2013). Sensitivity of plants to changing atmospheric CO 2 concentration:

From the geological past to the next century. New Phytologist, 197(4), 1077–1094. https://doi.org/10.1111/nph.12104

Gibson, J. R. (n.d.). Individualistic Response of Piñon and Juniper Tree Species Distributions to Climate Change in North America's Arid Interior West. 105.

The Gymnosperm Database. Available online: https://www.conifers.org/cu/Juniperus_occidentalis.php (accessed on 12 September 2021).

Habel K, Grasman R, Gramacy R, Mozharovskyi P and Sterratt D (2019). geometry: Mesh Generation and Surface Tessellation. R package version 0.4.5. https://CRAN.R-project.org/package=geometry

Holmes, R.L.; Adams, R.K.; Baker, L. (2002a): NOAA/WDS Paleoclimatology - Holmes - Sharp Mountain - JUOC - ITRDB CA095. NOAA National Centers for Environmental Information. https://doi.org/10.25921/cpat-kv17. Accessed [2015-09-09]

Holmes, R.L.; Adams, R.K.; Kirby, V.C.; Earle, C.J. (2002b): NOAA/WDS Paleoclimatology - Holmes - Grasshopper Trail - JUOC - ITRDB ID006. NOAA National Centers for Environmental Information. https://doi.org/10.25921/7bmv-2a15. Accessed [2015-09-09].

Holmes, R.L.; Adams, R.K. (2002c): NOAA/WDS Paleoclimatology – Holmes - Timbered Mountain - JUOC - ITRDB CA517. NOAA National Centers for Environmental Information. https://doi.org/10.25921/c8bz-vk30. Accessed [2015-09-09].

Holmes, R.L.; Adams, R.K.; Rose, M.R.; Wu, X.D. (2002d): NOAA/WDS Paleoclimatology - Holmes - Calamity Creek - JUOC - ITRDB OR009. NOAA National Centers for Environmental Information. https://doi.org/10.25921/pfn8-p790. Accessed [2015-09-09]

Holmes, R.L.; Adams, R.K.; Rose, M.R.; Wu, X.D. (2002e): NOAA/WDS Paleoclimatology - Holmes - Spring Canyon Oregon - JUOC - ITRDB OR006. NOAA National Centers for Environmental Information. https://doi.org/10.25921/qh3s-9804. Accessed [2015-09-09].

IPCC, 2021: Climate Change 2021: The Physical Science Basis. Contribution of Working Group I to the Sixth Assessment Report of the Intergovernmental Panel on Climate Change [Masson-Delmotte, V., P. Zhai, A. Pirani, S.L. Connors, C. Péan, S. Berger, N. Caud, Y. Chen, L. Goldfarb, M.I. Gomis, M. Huang, K. Leitzell, E. Lonnoy, J.B.R. Matthews, T.K. Maycock, T. Waterfield, O. Yelekçi, R. Yu, and B. Zhou (eds.)]. Cambridge University Press. In Press.

Inman, M. (2008). Carbon is forever. Nature Climate Change, 1(812), 156–158. https://doi.org/10.1038/climate.2008.122

Jiang, X., Rauscher, S. A., Ringler, T. D., Lawrence, D. M., Williams, A. P., Allen, C. D., Steiner, A. L., Cai, D. M., & McDowell, N. G. (2013). Projected Future Changes in Vegetation in Western North America in the Twenty-First Century. Journal of Climate, 26(11), 3671–3687. https://doi.org/10.1175/JCLI-D-12-00430.1

Johnson, D. D., & Miller, R. F. (2008). Intermountain Presettlement Juniper: Distribution, Abundance, and Influence on Postsettlement Expansion. Rangeland Ecology & Management, 61(1), 82–92. https://doi.org/10.2111/06-154.1

Kleinhesselink, A. R., & Adler, P. B. (2018). The response of big sagebrush (Artemisia tridentata) to interannual climate variation changes across its range. Ecology, 99(5), 1139–1149. https://doi.org/10.1002/ecy.2191

Klesse, S., DeRose, R. J., Guiterman, C. H., Lynch, A. M., O'Connor, C. D., Shaw, J. D., & Evans, M. E. K. (2018). Sampling bias overestimates climate change impacts on forest growth in the southwestern United States. Nature Communications, 9(1), 5336. https://doi.org/10.1038/s41467-018-07800-y

Klesse, S., DeRose, R. J., Babst, F., Black, B. A., Anderegg, L. D. L., Axelson, J., Ettinger, A., Griesbauer, H., Guiterman, C. H., Harley, G., Harvey, J. E., Lo, Y., Lynch, A. M., O'Connor, C., Restaino, C., Sauchyn, D., Shaw, J. D., Smith, D. J., Wood, L., … Evans, M. E. K. (2020). Continental-scale tree-ring-based projection of Douglas-fir growth: Testing the limits of space-for-time substitution. Global Change Biology, 26(9), 5146–5163. https://doi.org/10.1111/gcb.15170

Knapp, P. A., & Soulé, P. T. (1996). Vegetation Change and the Role of Atmospheric CO2 Enrichment on a Relict Site in Central Oregon: 1960–1994. Annals of the Association of American Geographers, 86(3), 387–411. https://doi.org/10.1111/j.1467-8306.1996.tb01759.x

Knapp, P. A., Soulé, P. T., & Grissino-Mayer, H. D. (2001). Post-drought growth responses of western Juniper (Juniperus occidentals var. Occidentalis) in central Oregon. Geophysical Research Letters, 28(13), 2657–2660. https://doi.org/10.1029/2000GL012365

Knapp, P.A.; Soulé, P.T. (2008): NOAA/WDS Paleoclimatology – Knapp - The Island Natural Research Area - JUOC - ITRDB OR089. NOAA National Centers for Environmental Information. https://doi.org/10.25921/e5pz-c150. Accessed [2015-09-09].

Knapp, P. A., Soulé, P. T., & Grissino-Mayer, H. D. (2001). Detecting potential regional effects of increased atmospheric CO2 on growth rates of western juniper. Global Change Biology, 7(8), 903–917

.Malevich, S.B.; Woodhouse, C.A.; Danloe, J.; Losleben, M.V. (2013a): NOAA/WDS Paleoclimatology - Malevich - Table Rock-Arrow Gap Update - JUOC - ITRDB OR092. NOAA National Centers for Environmental Information. https://doi.org/10.25921/a0ax-y007. Accessed [2015-09-09].

Malevich, S.B.; Woodhouse, C.A.; Losleben, M.V.; Danloe, J. (2013b): NOAA/WDS Paleoclimatology - Malevich - Frederick Butte Update - JUOC - ITRDB OR093. NOAA National Centers for Environmental Information. https://doi.org/10.25921/zcwf-rd08. Accessed [2015-09-09].

Malevich, S.B.; Woodhouse, C.A.; Danloe, J.; Losleben, M.V. (2013c): NOAA/WDS Paleoclimatology - Malevich - Little Juniper Mountain Update - JUOC - ITRDB OR095. NOAA National Centers for Environmental Information. https://doi.org/10.25921/c2ph-k818. Accessed [2015-09-09].

Malevich, S.B.; Woodhouse, C.A.; Danloe, J.; Losleben, M.V.; Faulstich, H.L. (2013d): NOAA/WDS Paleoclimatology - Malevich - Boles Creek Update - JUOC - ITRDB CA675. NOAA National Centers for Environmental Information. https://doi.org/10.25921/bgv6-gw03. Accessed [2015-09-09].

Malevich, S.B.; Woodhouse, C.A.; Danloe, J.; Losleben, M.V. (2013e): NOAA/WDS Paleoclimatology - Malevich - Horse Ridge Update - JUOC - ITRDB OR094. NOAA National Centers for Environmental Information. https://doi.org/10.25921/c6he-ad41. Accessed [2015-09-09].

Mehringer, P. J., & Wigand, P. E. (1987). Western Juniper In the Holocene, Proceedings—Pinyon- Juniper Conference, Reno, NV, January 13-16, 1986. https://doi.org/10.13140/2.1.1171.7442

Meko, D.M.; Baisan, C.H.; Funkhouser, G.; Dai, K. (2002): NOAA/WDS Paleoclimatology - Meko - Steens Mountain Recollection - JUOC - ITRDB OR063. NOAA National Centers for Environmental Information. https://doi.org/10.25921/6zc0-0127. Accessed [2015-09-09].

Meko, D.M.; Baisan, C.H.; Funkhouser, G. (2013): NOAA/WDS Paleoclimatology - Meko - Jackson Mountains Oct98 Re-collection - JUOC - NV518, PAGES North America 2K Version. NOAA National Centers for Environmental Information. https://doi.org/10.7289/V5CR5RP2. Accessed [2015-09-09]

Miller, R. F., Chambers, J. C., Evers, L., Jason, C., Snyder, K. A., Roundy, B. A., & Pierson, F. B. (2019). The ecology, history, ecohydrology, and management of pinyon and juniper woodlands in the Great Basin and Northern Colorado Plateau of the western United States. 292.

Miller 2005- Biology ecology and management of western juniper..

Miller, R. F., Svejcar, T. J., & Rose, J. A. (2000). Impacts of Western Juniper on Plant Community Composition and Structure. Journal of Range Management, 53(6), 574. https://doi.org/10.2307/4003150

Miller, R. F., & Rose, J. A. (1999). Fire History and Western Juniper Encroachment in Sagebrush Steppe. Journal of Range Management, 52(6), 550. https://doi.org/10.2307/4003623

Miller, R. F., & Wigand, P. E. (1994). Holocene Changes in Semiarid Pinyon-Juniper Woodlands. BioScience, 44(7), 465–474. https://doi.org/10.2307/1312298

Norby, R.J., Warren, J.M., Iversen, C.M., Medlyn, B.E. & McMurtrie, R.E. (2010). CO2 enhancement of forest productivity constrained by limited nitrogen availability. Proc. Natl Acad. Sci. USA, 107, 19368–19373.

Notaro, M., Mauss, A. and Williams, J.W. (2012), Projected vegetation changes for the American Southwest: combined dynamic modeling and bioclimatic-envelope approach. Ecological Applications, 22: 1365-1388. https://doi.org/10.1890/11-1269.1

Palmquist, K. A., Schlaepfer, D. R., Bradford, J. B., & Lauenroth, W. K. (2016). Mid-latitude shrub steppe plant communities: Climate change consequences for soil water resources. Ecology, 97(9), 2342–2354. https://doi.org/10.1002/ecy.1457

Perret, D. L., & Sax, D. F. (2022). Evaluating alternative study designs for optimal sampling of species' climatic niches. Ecography, 2022(1), ecog.06014. https://doi.org/10.1111/ecog.06014

Pinheiro J, Bates D, DebRoy S, Sarkar D, R Core Team (2021). _nlme: Linear and Nonlinear Mixed Effects Models_. R package version 3.1-152, <URL: https://CRAN.R-project.org/package=nlme>.

Polley, H. W., Johnson, H. B., & Marino, B. D. (1993). Increase in C3 plant water-use efficiency and biomass over Glacial to present CO2 concentrations. 361, 4.

Polley, H. W., Briske, D. D., Morgan, J. A., Wolter, K., Bailey, D. W., & Brown, J. R. (2013). Climate Change and North American Rangelands: Trends, Projections, and Implications. Rangeland Ecology & Management, 66(5), 493–511. https://doi.org/10.2111/REM-D-12-00068.1

PRISM Climate Group, Oregon State University, http://prism.oregonstate.edu, created 4 Feb 2018

R Core Team (2021). R: A language and environment for statistical computing. R Foundation for Statistical Computing, Vienna, Austria. URL https://www.R-project.org/.

Reeves, M. C., Moreno, A. L., Bagne, K. E., & Running, S. W. (2014). Estimating climate change effects on net primary production of rangelands in the United States. Climatic Change, 126(3–4), 429–442. https://doi.org/10.1007/s10584-014-1235-8

Rehfeldt, G. E., Crookston, N. L., Sáenz-Romero, C., & Campbell, E. M. (2012). North American vegetation model for land-use planning in a changing climate: A solution to large classification problems. Ecological Applications, 22(1), 119–141. https://doi.org/10.1890/11-0495.1

Renwick, K. M., Curtis, C., Kleinhesselink, A. R., Schlaepfer, D., Bradley, B. A., Aldridge, C. L., Poulter, B., & Adler, P. B. (2018). Multi-model comparison highlights consistency in predicted effect of warming on a semi-arid shrub. Global Change Biology, 24(1), 424–438. https://doi.org/10.1111/gcb.13900

Rowland, M. M., Suring, L. H., Tausch, R. J., Geer, S., & Wisdom, M. J. (2011). Dynamics of western juniper woodland expansion into sagebrush communities in central Oregon. 16, 12.

Sala, O. E., Gherardi, L. A., & Peters, D. P. C. (2015). Enhanced precipitation variability effects on water losses and ecosystem functioning: Differential response of arid and mesic regions. Climatic Change, 131(2), 213–227. https://doi.org/10.1007/s10584-015-1389-z

Schroeder, M. A., Aldridge, C. L., Apa, A. D., Bohne, J. R., Braun, C. E., Bunnell, S. D., Connelly, J. W., Deibert, P. A., Gardner, S. C., Hilliard, M. A., & others. (2004). Distribution of sage-grouse in North America. The Condor, 106(2), 363–376.

Silva, L. C. R., & Anand, M. (2013). Probing for the influence of atmospheric CO 2 and climate change on forest ecosystems across biomes: Changes in growth and iWUE across biomes. Global Ecology and Biogeography, 22(1), 83–92. https://doi.org/10.1111/j.1466-8238.2012.00783.x

Snyder, K. A., Evers, L., Chambers, J. C., Dunham, J., Bradford, J. B., & Loik, M. E. (2019). Effects of Changing Climate on the Hydrological Cycle in Cold Desert Ecosystems of the Great Basin and Columbia Plateau. Rangeland Ecology & Management, 72(1), 1–12. https://doi.org/10.1016/j.rama.2018.07.007

Sorte, C. J. B., Ibáñez, I., Blumenthal, D. M., Molinari, N. A., Miller, L. P., Grosholz, E. D., Diez, J. M., D'Antonio, C. M., Olden, J. D., Jones, S. J., & Dukes, J. S. (2013). Poised to prosper? A cross-system comparison of climate change effects on native and non-native species performance. Ecology Letters, 16(2), 261–270. https://doi.org/10.1111/ele.12017

Soulé, P. T., & Kna pp, P. A. (2019). Radial Growth Rate Responses of Western Juniper (Juniperus occidentalis Hook.) to Atmospheric and Climatic Changes: A Longitudinal Study from Central Oregon, USA. Forests, 10(12), 1127. https://doi.org/10.3390/f10121127

Speer, J. H. (2010). Fundamentals of Tree-Ring Research. 86.Sperlich, D., Nadal-Sala, D., Gracia, C., Kreuzwieser, J., Hanewinkel, M., & Yousefpour, R. (2020). Gains or Losses in Forest Productivity under Climate Change? The Uncertainty of CO2 Fertilization and Climate Effects. Climate, 8(12), 141. https://doi.org/10.3390/cli8120141

Swetnam, T. W., Allen, C. D., & Betancourt, J. L. (1999). Applied Historical Ecology: Using the Past to Manage for the Future. Ecological Applications, 9(4), 1189. https://doi.org/10.2307/2641390

Tietjen, B., & Jeltsch, F. (2007). Semi-arid grazing systems and climate change: A survey of present modelling potential and future needs: Grazing systems and climate change. Journal of Applied Ecology, 44(2), 425–434. https://doi.org/10.1111/j.1365-2664.2007.01280.x

Tredennick, A. T., Hooker, G., Ellner, S. P., & Adler, P. B. (2021). A practical guide to selecting models for exploration, inference, and prediction in ecology. Ecology, 102(6). https://doi.org/10.1002/ecy.3336

Tyrrell, T., Shepherd, J. G., & Castle, S. (2007). The long-term legacy of fossil fuels. Tellus B: Chemical and Physical Meteorology, 59(4), 664–672. https://doi.org/10.1111/j.1600-0889.2007.00290.x

Walker, J. A. (2020). Elements of Statistical Modeling for Experimental Biology. 522.

Williams, A. L., Wills, K.E., Janes. J. K., Vander Schoor, J.K., Newton, P.C.N, & Hovenden, M.J. (2007). Warming and free-air CO2 enrichment alter demographics in four co-occurring grassland species. New Phytologist, 10.

Zimmer, S. N., Grosklos, G. J., Belmont, P., & Adler, P. B. (2021). Agreement and Uncertainty Among Climate Change Impact Models: A Synthesis of Sagebrush Steppe Vegetation Projections. Rangeland Ecology & Management, 75, 119–129. https://doi.org/10.1016/j.rama.2020.12.006

Zuidema, P. A., Heinrich, I., Rahman, M., Vlam, M., Zwartsenberg, S. A., & Sleen, P. (2020). Recent CO 2 rise has modified the sensitivity of tropical tree growth to rainfall and temperature. Global Change Biology, 26(7), 4028–4041. https://doi.org/10.1111/gcb.15092

CHAPTER III

CLIMATE TREE-RING GROWTH RELATIONSHIPS OF WESTERN JUNIPER AND PONDEROSA PINE TREES IN CHEWAUCAN RIVER BASIN.

Introduction

The western juniper (*Juniperus occidentalis*) Woodlands (WJW) that occupy large portions of eastern Oregon are a highly dynamic ecosystem expanding in area by nearly six-fold over the last century (Azuma et al., 2005). Although numerous studies have assessed the impacts that factors such as overgrazing and reduction of fire have had on this expansion (Miller et al 2008; Johnson and Miller 2008; Eddleman et al 1994; Burkhardt and Tisdale 1976), there have been notably fewer studies regarding the role climate and rising CO_2 levels played on the growth rates on juniper trees in connection with spatiotemporal shifts in juniper populations (Miller et al 2021). This knowledge gap has hindered our ability to make predictions about the future of this system, especially under expected changes in climate sensitivity of western juniper tree-ring growth under rising atmospheric CO_2. Addressing this knowledge gap is the central motivation of this study.

Global meta-analyses show a clear effect of increased atmospheric CO_2 levels on tree-ring growth for many dominant tree species (Peñuelas et al 2011), in some cases attributed to a physiological shift in intrinsic water use efficiency (iWUE) ranging from ~10 to 60% over the past ~50 years (Silva & Anand, 2013) . Those same studies revealed large variation in tree growth responses to climate variability ranging to ~-30% to +45% in Mediterranean systems. In other words, changes in tree growth rates do not always correspond with increased iWUE, likely due to other environmental factors like nutrient limitation. Although, as seen in Zuidema et al. (2020) and Chapter 2 of this dissertation, changes in atmospheric CO_2 concentrations can impact the sensitivity of trees to seasonal fluctuations in temperature and precipitation variables. Here, we explore this concept by quantifying changes in sensitivity of juniper tree-rings to precipitation and temperature over the last century at sites in the Chewaucan River Basin of central, southern Oregon (Figure 1). To the best of our knowledge, our study region and target species have not been previously included in previous analyses of this kind, so we provide a novel contribution quantifying tree-ring sensitivity of both western juniper and (previously studied) *Pinus ponderosa* trees to climate and atmospheric CO_2 levels. Specifically, we 1) explore and refine empirical measurements and statistical modeling efforts set forth in chapter two, 2) provide a new data set for both intra and inter chapter model validation and 3) quantify the tree-ring sensitivity of the two species occupying the same geographic and climatic space, albeit at differing ends of their realized climatic niches (i.e. across a topographic gradient representative of in their respective distribution ranges). It is our hope that the information provided here will be of use in future research focused on ecological forecasting, under future climate scenarios, in semi-arid ecosystems of the Great Basin and beyond.

In addition, by refining our understanding of western juniper climate relations we hope to reduce uncertainty of forecasting models aimed at understanding the future distributions and abundances of semi-arid ecosystems of the great basin as seen in Creutzberg et al. (2015) and Halofsky et al (2013), because forecasting models play an important role in policy that can impact these ecosystems at vast scales as seen in the Oregon sage-grouse action plan (Sage-Grouse Conservation Partnership, 2015)

A major impact of the expansion of the western juniper woodlands in terms of land management actions was the implementation of the Sage Grouse Initiative (SGI). The greater sage grouse (*Centrocercus urophasianus*) was designated as a candidate species for possible listing under the Endangered Species Act in March of 2010. In response, the Natural Resource Conservation Service (NRCS) launched the SGI in an attempt to proactively conserve sage grouse habitat in order to prevent its listing as an endangered species. As of 2018, $760,000,000 was invested by the NRCS and private interest groups in an effort to conserve approximately 3.2 million ha across the American West. One of these conservation practices included removal, or “treatment,” of 163,995 ha of conifers woodlands. Approximately half of these conifer treatments were conducted in Oregon (NRCS, 2018).

Although, there is scientific evidence that the encroachment of juniper woodlands does have negative impacts on the survival of sage grouse (Coates et al., 2017; Bates et al., 2017, Boyd et al. 2017), the way in which the removal juniper woodlands affect other wildlife species is only now beginning to be understood (Bombaci and Pejchar, 2016). In addition, a study from

Dittel et al. (2018) found evidence of increased recruitment of juniper seedlings under juniper skeletons in recently treated areas, bringing into question the long-term efficacy of such treatments. In 2015, it was deemed that the greater sage grouse does not face the risk of extinction now or in the foreseeable future, and it was not listed under the Endangered Species Act. Ideally results from this study will be used to inform the next generation of projection models that will influence future policy and management actions aimed at conservation, fuels management and maximizing natural climate solutions regarding carbon sequestration.

Methods

Study Site:

We sampled juniper and pine trees at 12 plot locations across a topographic gradient in the Chewaucan River Basin, located near the town of Paisley in central, southern Oregon (Figure 1). The town of Paisley Oregon is a Bsk cool semi-arid climate according to the Köppen climate classification system. As one heads southwest into the Chewaucan river basin annual precipitation increases and annual temperature decreases as elevation increases. Paisley has an annual average precipitation of 257 mm per year with an average annual temperature of 9 degrees Celsius. Our site locations were all located off of county highway 2-08, and according to PRISM data have a 30 year normal of 579mm in precipitation and 5.5 degrees Celsius (Figures 2 and 3). The wooded portions of the Chewaucan river basin are dominated by ponderosa pine, with interspersed lodgepole pine, white fire, aspen, western juniper, mountain hemlock and sagebrush dominated meadows. The Chewaucan river basin could be considered the ecotone between cool dry montane forest and the cool semi-arid sagebrush steppe ecosystem to the east, and also represents some of the cooler wetter conditions of western juniper woodlands and conversely some of the drier portions of the range of ponderosa pine (McGowan 2003). Our study site being located at opposing ends of our study species' climate spaces allows us to explore the impacts of recent climate change on ecotonal climatic dynamics.

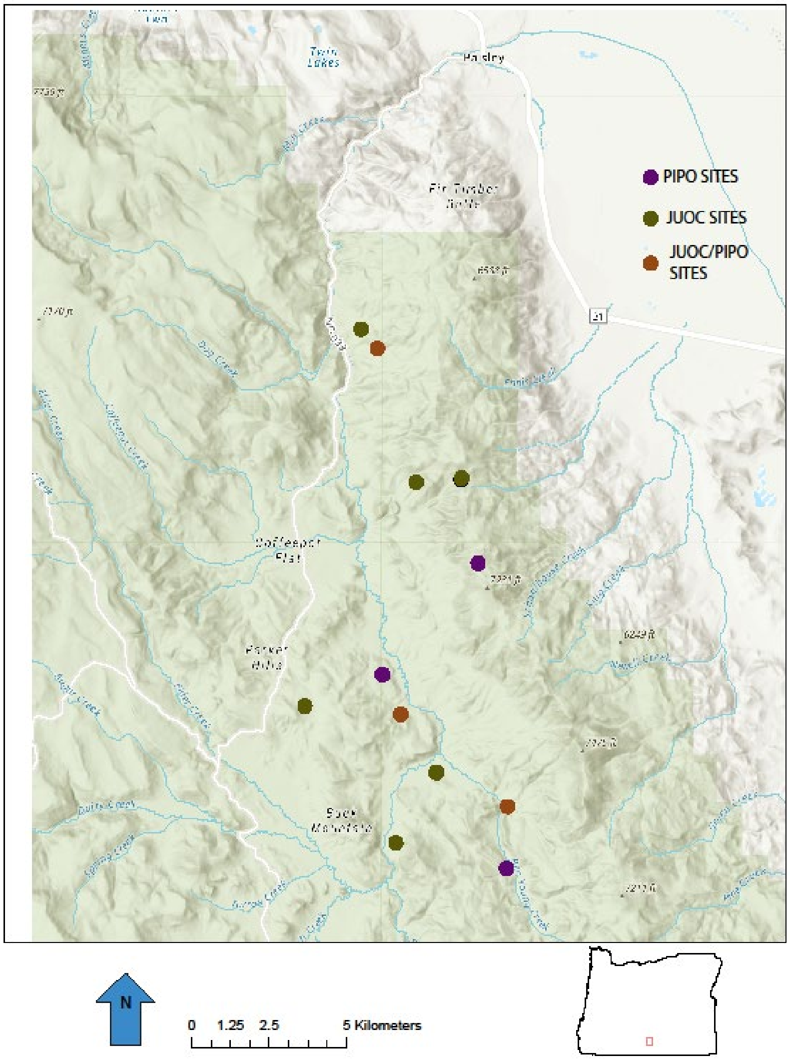

Figure 1- Map of study location and site locations. Purple dots represent locations where only ponderosa pine trees were sampled. Green dots represent locations where only western juniper trees were sampled. Brown dots represent locations where both ponderosa pine and western juniper tree were sampled.

Figure 2- Annual variation of Temperature by three 4-month “seasons” derived from PRISM climate data for our site in the Chewaucan River Basin, Oregon. The thicker line represents a smoothing spline and the grey bar represents standard error.

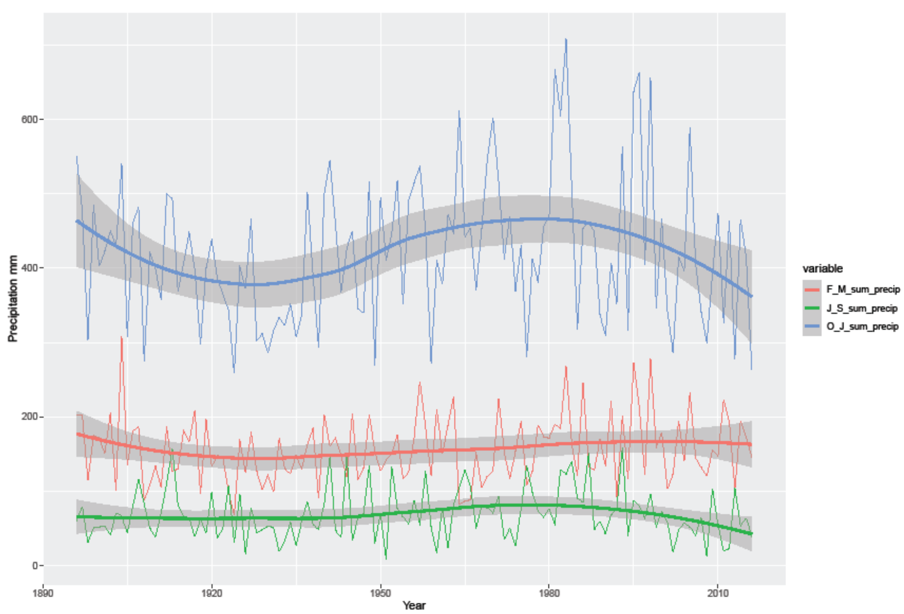

Figure 3- Annual variation of precipitation by three 4-month “seasons” derived from PRISM climate data for our site in the Chewaucan River Basin, Oregon. The thicker line represents a smoothing spline and the grey bar represents standard error.

Tree-Ring Collection and Processing:

All Tree cores were collected in the summer of 2017. A total of 63 tree cores were collected for this study (20 pine, 43 juniper) from 12 different plots throughout the Chewaucan river water shed (Figure 1). Plots were all located in areas with a southern to western aspect. Tree cores were collected with an increment borer at approximately 1.35 meters. Tree cores were mounted on wooden core mounts and sanded with sandpaper with increasing grit counts until a grit count of 1600 was achieved, cores were smooth and individual cell structure was visible under a microscope. Cores were then scanned, and tree-ring widths were measured digitally using imagej software. Prior to analysis several preprocessing steps are required for tree-ring data. These preprocessing procedures are necessary to account for the ontogenetic effect of tree age on ring width, and the inherent serial correlation of tree-ring widths (Speer, 2010; Cook 1985). As trees age and grow, the circumference of their trunk increases, therefore accumulation of the same amount of cross-sectional trunk area (Basal Area) will naturally produce thinner and thinner rings (Speer, 2010). To account for this ontogenetic effect, we standardized each tree-ring series by fitting a modified negative exponent, resulting in a tree-ring series in ring width index (RWI) instead of mm, these detrended series all having a mean of 1 (Figure4, Figure 5).

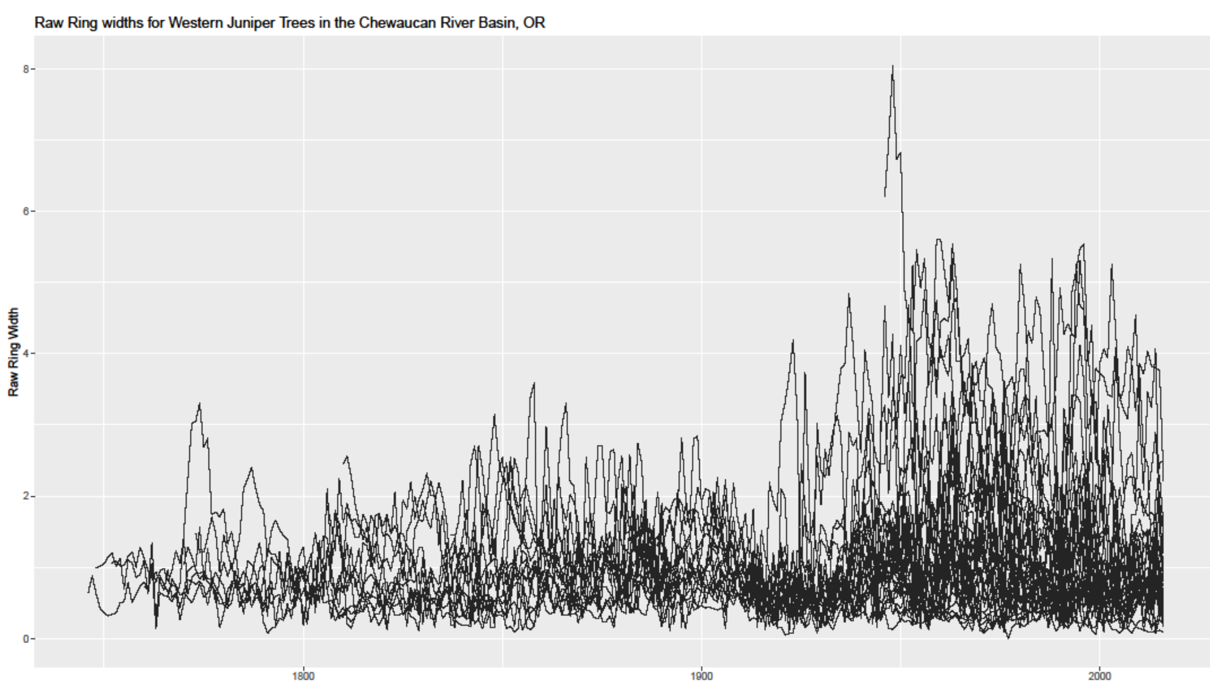

Figure 4- Raw tree-ring widths for western juniper tree in the Chewaucan River Basin.

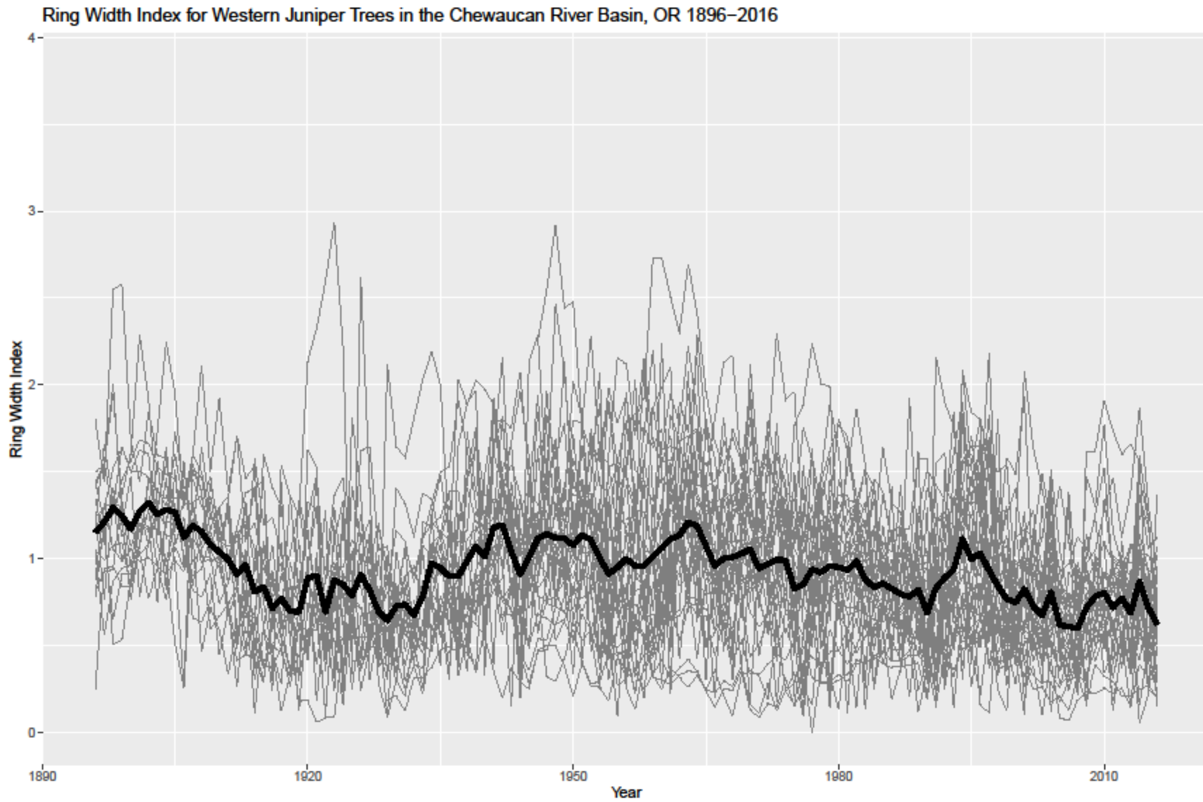

Figure 5- Ring width index for western juniper trees in the Chewaucan River Basin from 1896 to 2017

Additionally, tree-rings series often exhibit serial autocorrelation, meaning that the size of a tree-ring is dependent on the sized on the immediate previous rings. This is due to stored polysaccharides of previous growth (Cook 1985). To remove this serial autocorrelation the ring-width-indices were filtered through autoregressive standardization (ARSTAN). This double detrending method acts a compromise that removes the age-related growth trends and reduces the interdependence of serial autocorrelation, while retaining tree-ring climatic sensitivity (Cook 1985).

Climate data and Tree-Ring Width Over Time:

Climate data was acquired from the PRISM data group (PRISM) at a monthly temporal resolution and a spatial resolution of 4km. Monthly climate data was then aggregated into three 4-month seasons: the previous year's October to the current year's January (Fall), the current year's February to the current year's May (Spring) and the current year's June to the current year's September (Summer). Climate data was then standardized within season to a mean of 0 and a SD of 1, to allow for easy comparison of inter and intra seasonal impact of climate on tree-ring growth. Additionally, we constructed graphs of tree-ring growth at the site and individual tree level per species to aid in visually assessing patterns and congruency of tree-ring growth over time within and between study species.

Tree-Ring Response to Climate and Increasing Atmospheric CO_2 Levels:

To gain inference how western juniper and ponderosa pine tree-rings respond to seasonally resolute climate variables in the Chewaucan river basin, as atmospheric CO_2 has increased, we constructed two sets linear models for each species using standardized tree-ring width as the response variable and either climate variables or climate variables and climate variable * CO_2 interactions as predictor viable. Raw tree-rings were standardized to relative ring width (RWI) using a modified negative exponent via the detrend function from the dplR function in R (Bunn et al., 2022).We used global CO_2 averages from the Mauna Loa Observatory, located in Hawaii, USA. Models were created using the lm function from the stats package (Bartoń, 2022). In order to determine the most parsimonious model for each species and with or without CO_2 interactions we used the dredge function from the MuMln package stats package (Bartoń, 2022). The dredge function is an automated method for model selection and calculates the AIC score of all possible models from all possible combinations of predictor variables (Bartoń, 2022). The model with the lowest AIC score is considered the most parsimonious, meaning the simplest model with the greatest explanatory predictive power. Once the most parsimonious models were selected per species and CO_2 interaction type (with and without CO_2 interactions) we evaluated what model had the most predictive power by comparing the adjusted R squared values per model.

Model Validation:

In order to validate our models for western juniper and ponderosa pine tree-ring growth developed with the dredge function (both with and without CO_2 climate interactions), we then performed a k-folds cross validation. This method is performed by randomly assigning each year in our data set to one of 5 subsets, to be used for training the model and for model validation. These subsets constitute the "folds". One of the folds is then withheld from the analysis, and the model is fit on the remain k-1 (for our study k=5 and k-1 =4) folds. We then calculate the model fit on the withheld validation data set (Tredennick et al. 2021). This process is then repeated until each fold is used as the validation set. Model fit is then determined using the following metrices: Root mean squared error (RMSE), Rsquared, and Mean Absolute Error (MAE). When evaluating model fit with these metrics it is important to note that with RMSE, lower scores indicate greater predictive power of the model; with Rsquared, a higher score indicates greater predictive power of the model; and with MAE, a lower score indicates greater predictive power of the model (Tredennick et al. 2021).

In addition to validating our tree-ring growth models from the Chewaucan river basin by testing the model via k-folds cross validation. We also utilized the data set from this chapter to assess the regional western juniper growth model from the preceding chapter. Our regional model was generated using thirteen previous western juniper dendrochronological data sets from Oregon, Idaho, Nevada, and California. We then used the regional model to predict tree-ring growth based on the PRISM climate data from the Chewaucan river basin and assess the model by comparing the observed vs predicted values, via Multiple R-squared and root mean squared error.

Quantifying Interactions Among Multiple Drivers:

Several factors lead us to explore including long-term precipitation trends in our models. 1) Prolonged periods of below average precipitation can result in reduced ground water; 2) western juniper trees rely on both fine surface and deep lateral roots for water accumulation; 3) the long-term pattern of precipitation (particularly in October-January) matches the overall temporal pattern of RWI in western juniper trees, and ;4) our models that relied strictly on single year precipitation measurements failed to capture larger scale up-swings and down-swings in western juniper RWI, particularly in the time period around the 1930's, a time on widespread drought. Therefore, we explored how including a long-term precipitation trend would influence our model composition and fit. First to create a predictor variable we transformed October-January precipitation with a loess function with an alpha level of 0.75. A loess function in a local polynomial regression, that fits a smooth curve between two variables, in this case October-January precipitation and year. This smoothed precipitation variable was then scaled to have a mean of zero and a standard deviation of 1. This scaling was done to correspond with the scaling done for every possible predictor value in our model.

Results

Raw Tree Rings:

Mean raw tree-ring width for western juniper trees in our study site ranged from 0.01 to 3.1 mm. With a mean raw ring width for all trees and all years of 1.14 mm. The age of oldest tree-ring for western juniper per core ranged from 60 years to 272 years, however several of our oldest western juniper trees contained core rot, so age of establishment for older trees was often indeterminable. Mean raw tree-ring width for Ponderosa Pine trees in our study site ranges from 0.004 to 6.91 mm, with a mean raw tree-ring width of 1.44 mm.

Models of RWI with and without CO_2 Interactions:

For both western juniper and ponderosa pine, linear models that included climate*CO2 interactions produced better fit and more predictive power by all metrics. For western juniper our model with CO2 climate interactions compared to our model without CO2 climate interactions had a lower RMSE (0.27 vs 0.36), higher R-squared value (0.36 vs 0.14) and lower MAE (0.21 vs 0.25) (Tables 1&3). The same pattern is apparent when examining the model fit metrices for ponderosa pine (RMSE= 0.26 vs 0.27; R-squared= 0.26 vs 0.21; MAE= 0.211 vs 0.213) (Tables 2 & 3) (Figures 6 & 7).

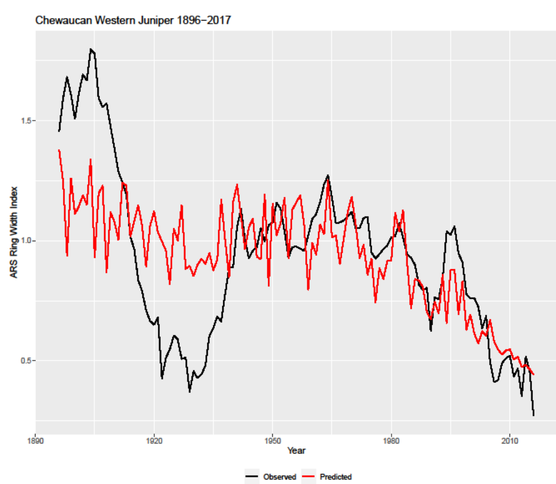

Figure 6- Observed (black) and Predicted (red) values for western juniper growth autoregressive standardized ring width index from years 1896-2016 Rsquared=0.386.

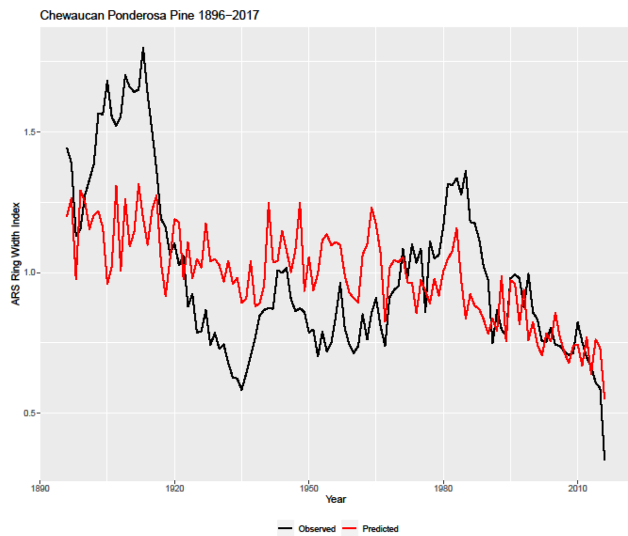

Figure 7- Observed (black) and Predicted (red) values for Ponderosa Pine growth autoregressive standardized ring width index from years 1896-2016, Rsquared=0.297.

For western juniper, three coefficients were included in the model with the highest adjusted r-squared value and therefore most predictive power; these include the sum of precipitation from the previous year's October to the current year's January, atmospheric CO_2 levels, and the interaction of CO_2 and the sum of precipitation from the previous year's October to the current year's January. October through January precipitation had a positive impact of western juniper tree-ring growth, atmospheric CO_2 levels had a negative impact, and the negative coefficient of the interaction term between CO_2 and October through January precipitation means that according to our model, at our site western juniper tree-ring growth is becoming less sensitive to October through January precipitation as CO2 has increased over the last century (Table 1).

Table 1- Results from the dredge derived most parsimonious ARS tree-ring width index (RWI) models with no CO_2*Climate interactions (No Interactions) and with CO_2*Climate interactions (Yes Interactions) for Western Juniper trees in the Chewaucan River Basin in southern, central Oregon. For each interaction type the model with the lowest AIC value was selected, and then R-squared values to compare what model produced a better fit, and therefore more predictive power.

Western Juniper

	No Interactions		Yes Interactions	
Predictors	*Estimates*	*p*	*Estimates*	*p*
(Intercept)	0.93	**<0.001**	0.94	**<0.001**
J S mean mean temp	-0.09	**0.003**		
O J sum precip	0.08	**0.008**	0.12	**<0.001**
CO2 scale			-0.19	**<0.001**
CO2 scale * O J sum precip			-0.05	0.075
Observations	121		121	
R^2 / R^2 adjusted	0.152 / 0.138		0.386 / 0.370	

For Ponderosa Pine four coefficients were included in the model with the highest r-squared values, the model with climate*CO_2 interactions. These variables were: atmospheric CO_2; June through September mean temperature, the previous year's October through the current year's January's precipitation and the interaction between CO_2 and June through September mean temperature. June through September mean temperature had a negative impact on Ponderosa Pine tree-ring growth. Ponderosa pine tree-ring growth was positively impacted by October through January precipitation. Additionally, the positive coefficient of CO_2 and June through September mean temperature indicates that ponderosa pine are becoming less sensitive to June through September mean temperatures as CO_2 has increased over the last century (Table 2).

Table 2 Results from the dredge derived most parsimonious ARS tree-ring width index (RWI) models with no CO2*Climate interactions (No Interactions) and with CO2*Climate interactions (Yes Interactions) for Ponderosa Pine trees in the Chewaucan River Basin in southern, central Oregon. For each interaction type the model with the lowest AIC value was selected, and then R-squared values to compare what model produced a better fit, and therefore more predictive power.

Ponderosa Pine

	No Interactions		**Yes Interactions**	
Predictors	*Estimates*	*p*	*Estimates*	*p*
(Intercept)	0.99	**<0.001**	0.97	**<0.001**
J S mean mean temp	-0.11	**<0.001**	-0.06	**0.017**
O J sum precip	0.04	0.119	0.06	**0.020**
CO2 scale			-0.13	**<0.001**
CO2 scale * J S mean mean temp			0.04	0.075
Observations	121		121	
R^2 / R^2 adjusted	0.174 / 0.160		0.297 / 0.273	

Comparison of Species by Basal Area Increment:

Tree-ring studies that exclusively rely on ring width index may fail to recognize growth trends and patterns that are evident in Basal Area Increment (BAI) curves (Johnson and Abrams 2016). This is because detrending raw tree-ring widths to ring-width index (RWI), via mathematical functions (e.g a smoothing spline, a modified negative exponent) by design remove a tree's natural biological growth trend. Therefore, exploring BAI can be of particular importance when comparing across species and climatic conditions (Johnson and Abrams 2016). When we investigate the BAI growth curves and ring width index of both western juniper and ponderosa pine, we see patterns of similarity and difference (Figure 8, Figure 9). For both species we see a basal area growth pattern that follows a sigmoidal curve, with a relatively shallow rate of growth followed by steep rate of growth and then a shallow rate of growth typical of most tree species. At a finer temporal scale both species also show oscillations in basal area growth rates indicating sensitivity to climate with considerable amounts of inter and intra species common growth variation. However, by 2010 ponderosa pine is increasing in basal area on average by about twice as much basal area per year than western juniper, approximately 20 cm squared compared to 10 cm squared respectively.

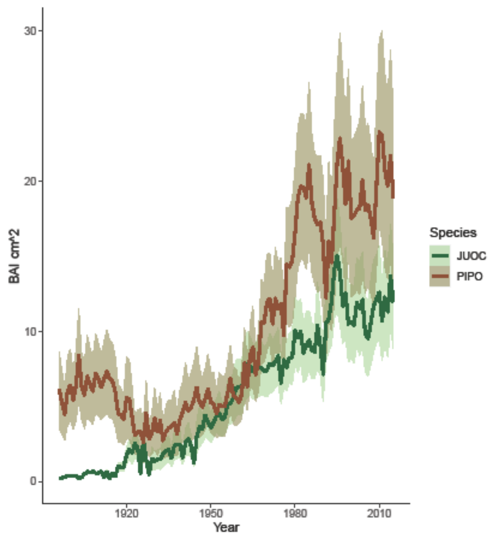

Figure 8- Basal area increase for western juniper and ponderosa pine trees in the Chewaucan River Basin, Oregon.

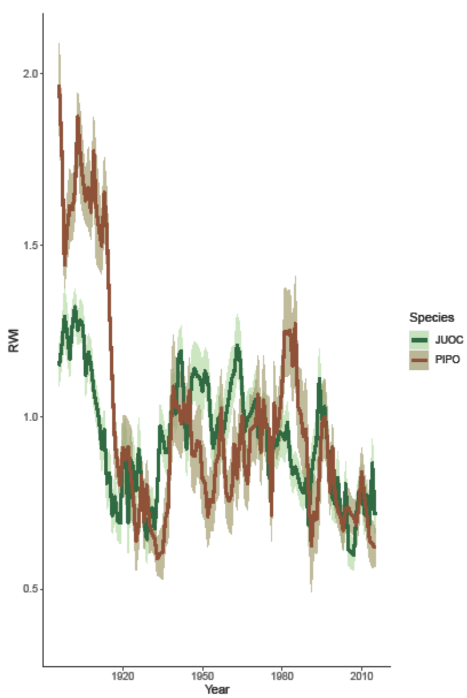

Figure 9- Ring Width Index for western juniper and ponderosa pine trees in the Chewaucan River Basin in Oregon.

Model Validation:

Results from our k-folds cross-validation of western juniper and ponderosa pine tree-ring growth indicate the same results metrics derived from the AIC value of the dredged models, that including CO2 and Climate interactions improves the fit and predictive power of our models (Table 3) For both western juniper and ponderosa pine, models that included CO2 and climate interactions had lower RMSE, higher R-squared values and lower MAE.

Table 3- Results from K-fold cross validation by species from the dredge derived models illustrated in table 1 and table 2

Climate Interaction	RMSE	Rsquared	MAE	Species
W/O	0.3263968	0.1405973	0.2518622	JUOC
W	0.2792367	0.3683395	0.2092757	JUOC
W/O	0.2748844	0.2060509	0.2130431	PIPO
W	0.2570397	0.2571298	0.2113303	PIPO

Chewaucan River Basin Western Juniper Tree-Ting Growth Model Compared to Regional Model:

Our site-specific model for the Chewaucan River Basin Western Juniper is much simpler than the regional model produced in chapter 2 based on 13 western juniper sites. However, the regional model performed well when implemented with our site specific data for this chapter, with a Multiple R-squared and Adjusted R-squared of 0.389 and 0.3461 respectively. The AIC of the regional model and the Chewaucan data set was 46.57, compared to 37.29, due to the greater parsimony of our local model.

Table 4. - Results from the dredge derived most parsimonious ARS tree-ring width index (RWI) models with no CO_2*Climate interactions (No Interactions) and with CO_2*Climate interactions (Yes Interactions) for Western Juniper trees in the Chewaucan River Basin in southern, central Oregon. These models include an alpha=0.75 smoothed spline of October-January precipitation as a predictor value. For each interaction type the model with the lowest AIC value was selected, and then R-squared values to compare what model produced a better fit, and therefore more predictive power.

Western Juniper Long-Term Precipitation Dredged

	No Interactions		**Yes Interactions**	
Predictors	*Estimates*	*p*	*Estimates*	*p*
(Intercept)	0.93	**<0.001**	0.94	**<0.001**
J S mean mean temp	-0.09	**0.001**		
OJPsmoothScale	0.17	**<0.001**	0.19	**<0.001**
O J sum precip			0.04	**0.028**
CO2 scale			-0.26	**<0.001**
OJPsmoothScale * CO2 scale			-0.12	**<0.001**
Observations	121		121	
R^2 / R^2 adjusted	0.327 / 0.315		0.667 / 0.656	

Inclusion of Long-Term Precipitation Trend:

When we included a long-term October-January precipitation trend as a predictor variable we produced the best fitting model in this study (table 4), with a Rsquared value of 0.67, with nearly twice the Rsquared value of 0.37 from our earlier modeling efforts for western juniper at this site. Comparing graphs of predicted vs observed values for the model with only annually resolute (figure 7) vs long-term precipitation values (figure 10) it is evident that visually that including a long-term climate trend improves model performance.

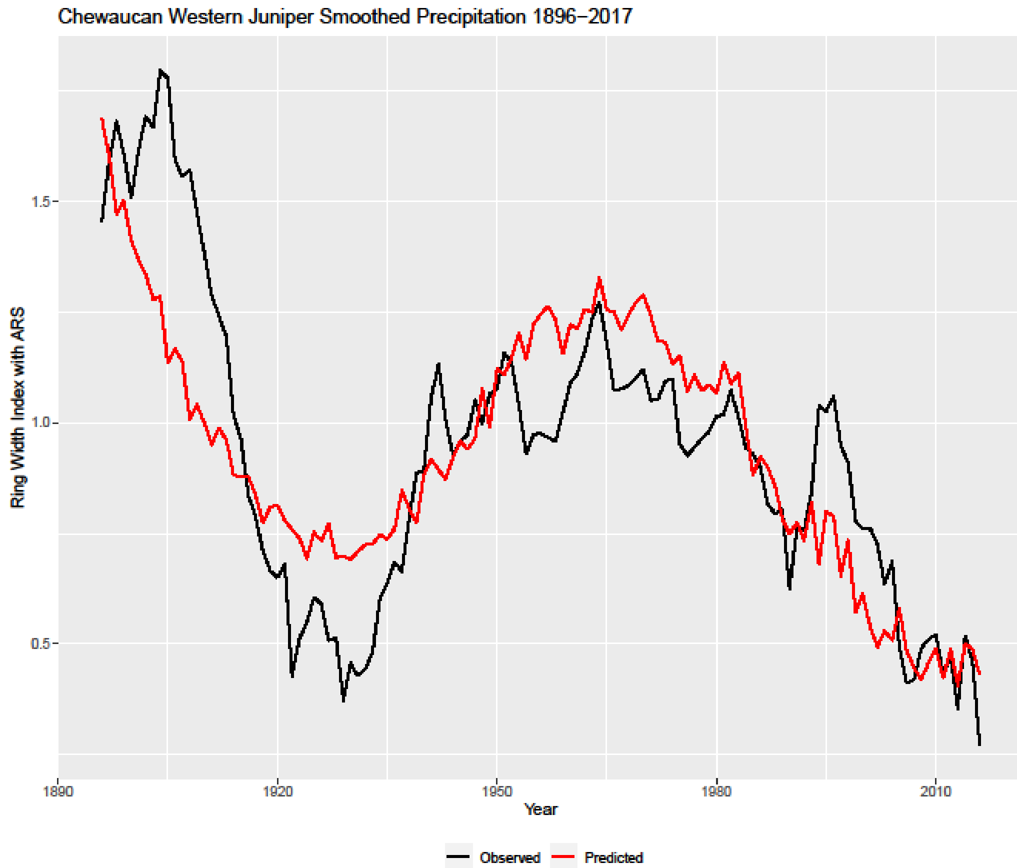

Figure 10- Observed (black) and Predicted (red) values for western juniper growth autoregressive standardized ring width index from years 1896-2016 with the inclusion of a long-term precipitation value as a predictor value, Rsquared=0.67.

Discussion

We discovered several important findings in this chapter. We provided further evidence that both western juniper and ponderosa pine tree-ring growth is modeled with more predictive power when CO_2 and Climate interaction are included in said model; adding to our theory that trees in semi-arid ecosystems are becoming more drought tolerant due to a CO_2 induced increase in iWUE. Additionally, we discovered that although western juniper and ponderosa pine exhibited similar standardized tree-ring growth in the Chewaucan River Basin from 1896-2017, the seasonally resolute specifics of their climate drivers are not identical. Ponderosa pine were equally sensitive to precipitation and temperature, whereas precipitation was the main climate driver of western juniper tree-ring growth. Similarities and differences between our study species growth patterns is also evident when investigating their growth over time in regards to their increase in basal area, with ponderosa pine adding on average nearly double that of Western Juniper over the course of this study.

The challenges facing those that aim to project future distributions of plant communities in semi-arid ecosystems are immense. Therefore, projections of the future production, function, and distributions of WJW are inconclusive; partially due to limited research on the topic, and specifically hindered by a lack of knowledge on: the relationships between tree-growth, range expansion, climate sensitivity, disturbance events, atmospheric CO_2, and uncertainty between future climate scenarios. Studies that aim to project future distributions of vegetation types must rely on assumptions to fill in knowledge gaps and simplifications of known concepts in order to function (Kerns, et al. 2018; Halofskey et al 2013; Creutzberg et al 2015). Kerns et al. (2018) holistically examined the results of several previous modeling efforts, paleo-records, autecology, and local knowledge to derive their conclusion that they are uncertain if western juniper will expand or contract in the Blue Mountains of Oregon under future climate scenarios. Creutzberg et al. (2015) and Halofsky et al (2013) relied on model linkage of state-and-transition models, dynamic global vegetation models, and future climate scenarios to determine that western juniper woodlands may or may not rapidly increase in area and then decline (Halofsky et al 2013) ; or may or may not continue to expand in area but at a slower pace than in the 20th century (Creutzberg et al. 2015). Both Halofsky et al. (2013) and Creutzberg et al. (2015) applied their modeling efforts to the same study area in central Oregon of approximately 1 million ha in size. Additionally, Creutzberg et al. (2015) did not incorporate the impacts of increased atmospheric CO_2 on plant growth in their model, or the impacts of changing climate variables on western juniper growth dynamics.

Halofsky et al (2013), did incorporate atmospheric CO_2 levels regarding plant growth by reducing the moisture constraint on plant growth, however this effect was implemented evenly for all species and was not geographically explicit. Additional studies are needed to provide further understanding of the impacts of climate and elevated CO_2 on multiple competing species within an area of interest in order to reduce the uncertainty of future distribution dynamics and these studies need to account for differential responses across space and time. I do not intend on criticizing the efforts of these past model based studies, but to emphasize the importance that quantifying the impacts of increased CO_2 on western juniper woodlands climate sensitivity could play in future modeling efforts. Furthermore, understanding the degree in which increased atmospheric CO_2 impacts trees' responses to climate variables under future climate scenarios is a recognized missing puzzle piece regarding future forest forecasting efforts, and is of particular importance in water-limited forests (Charney et al. 2016).

Another important way to test the likelihood of future climate scenarios on ecosystems is through multi-model comparisons. As long as the models compared have independent assumptions and parameters, this approach can help increase confidence of predicted outcomes and identify areas of uncertainty (Renwick et al., 2017). Renwick et al. (2017) tested four models that drew from different sources of information: spatial correlations, temporal correlations, and mechanistic representations of key processes (a seedling survival model and a dynamic global vegetation model [DGVM]) in order to improve our understanding of (1) how climate change will likely affect the persistence and abundance of big sagebrush (*Atremisia tridentata*) across its geographic range. They determined that big sagebrush is more sensitive to changes in temperature than precipitation, that the choice of model is the largest source of uncertainty in future projections, and that sagebrush is likely to increase in performance at the cooler end of its climatic range and decrease in performance at the warmer end of its' climatic range. According to Renwick et al. (2017) all sagebrush in Oregon falls within the cooler end of its climatic range. One might assume that the increase in performance of sagebrush might act to inhibit the performance and range of western juniper, however sagebrush often act as a shelter for western juniper seedlings (Soulé et al. 2004). Therefor as temperatures increase, the improved future performance of sagebrush may in fact positively impact the future of western juniper expansion into the sagebrush dominated ecosystems of eastern Oregon.

Although this study was relegated to one site, combining these findings with meta-analysis and future *In Situ* measurements could then be combined into a data set large enough to perform a study the explores geographic patterns of multi-species performance and demographics under future scenarios. Once applied at a vast enough spatial and temporal scale understanding the differential responses of two very important tree species in terms of economics and ecology in eastern Oregon will help inform land management actions aimed at conservation, fuels management and/or timber production. If the current paradigm of wide scale western juniper treatment is the goal, land managers may be able to work in tandem with future projection models to maximize WJW reduction at large time scales by focusing reduction treatments in areas where WJW are predicted to continue to expand and by foregoing areas where WJW are predicted to die off naturally. If fuels reduction is the primary goal, management actions may want to focus on both sides of the spectrum of future WJW performance, treating areas of predicted increases and decreases in performance, thus preemptively eliminating areas of predicted increased fuels from WJW expansion and preemptively eliminating areas of potential catastrophic fires due to large quantities of fuels accumulation due to drought induced tree death. Furthermore, we may be observing a larger scale elevational shift in WJW realized niche and allowing this shift to occur in a more "hands off" approach needs to be considered particularly in relations to carbon sequestration and storage as untreated WJW have been show to contain over 5 times the above ground carbon stocks as areas treated with juniper removal (Abdallah et al. 2019). All though as emphasized by Abdallah et al. (2019), further research is needed to understand the impacts of western juniper expansion and subsequent treatment on belowground carbon pools.

The more information we gather regarding western juniper and adjacent species climate and atmospheric CO_2 relations and interactions, the less uncertainty we can generate regarding the future performance and ranges of these species and ecosystem. Ideally this uncertainty will become reduced enough that land managers will be able to confidently make large scale, yet specific actions based on multiple and perhaps seemingly conflicting goals that will result in a swath desired outcomes with an overall success that is greater than the sum of the individual parts.

References

Abdallah, M. A. B., Mata-González, R., Noller, J. S., & Ochoa, C. G. (2020). Ecosystem carbon in relation to woody plant encroachment and control: Juniper systems in Oregon, USA. *Agriculture, Ecosystems & Environment*, *290*, 106762. https://doi.org/10.1016/j.agee.2019.106762

Azuma, D. L., Hiserote, B. A., & Dunham, P. A. (2005). *The western juniper resource of eastern Oregon, 1999.* (PNW-RB-249). U.S. Department of Agriculture, Forest Service, Pacific Northwest Research Station. https://doi.org/10.2737/PNW-RB-249

Bates, J. D., Davies, K. W., Hulet, A., Miller, R. F., & Roundy, B. (2017). Sage Grouse Groceries: Forb Response to Piñon-Juniper Treatments. *Rangeland Ecology & Management*, *70*(1), 106–115. https://doi.org/10.1016/j.rama.2016.04.004

Bombaci, S., & Pejchar, L. (2016). Consequences of pinyon and juniper woodland reduction for wildlife in North America. *Forest Ecology and Management*, *365*, 34–50. https://doi.org/10.1016/j.foreco.2016.01.018

Boyd, C. S., Kerby, J. D., Svejcar, T. J., Bates, J. D., Johnson, D. D., & Davies, K. W. (2017). The Sage-Grouse Habitat Mortgage: Effective Conifer Management in Space and Time. *Rangeland Ecology & Management*, *70*(1), 141–148. https://doi.org/10.1016/j.rama.2016.08.012

Burkhardt, J. W., & Tisdale, E. W. (1976). Causes of Juniper Invasion in Southwestern Idaho. *Ecology*, *57*(3), 472–484. https://doi.org/10.2307/1936432

Charney, N. D., Babst, F., Poulter, B., Record, S., Trouet, V. M., Frank, D., Enquist, B. J., & Evans, M. E. K. (2016). Observed forest sensitivity to climate implies large changes in 21st century North American forest growth. *Ecology Letters*, *19*(9), 1119–1128. https://doi.org/10.1111/ele.12650

Coates, P. S., Prochazka, B. G., Ricca, M. A., Gustafson, K. B., Ziegler, P., & Casazza, M. L. (2017). Pinyon and Juniper Encroachment into Sagebrush Ecosystems Impacts Distribution and Survival of Greater Sage-Grouse. *Rangeland Ecology & Management*, *70*(1), 25–38. https://doi.org/10.1016/j.rama.2016.09.001

Creutzburg, M. K., Halofsky, J. E., Halofsky, J. S., & Christopher, T. A. (2015). Climate Change and Land Management in the Rangelands of Central Oregon. *Environmental Management*, *55*(1), 43–55. https://doi.org/10.1007/s00267-014-0362-3

Dittel, J. W., Sanchez, D., Ellsworth, L. M., Morozumi, C. N., & Mata-Gonzalez, R. (2018). Vegetation Response to Juniper Reduction and Grazing Exclusion in Sagebrush-Steppe Habitat in Eastern Oregon. *Rangeland Ecology & Management*, *71*(2), 213–219. https://doi.org/10.1016/j.rama.2017.11.004

Eddleman, L., Miller, P., Miller, R. F., & Dysart, P. (1994). Western Juniper Woodlands (of the Pacific Northwest) Science Assessment. *United States Forest Servise*, *0*(0), 1–132.

Global Ecology and Biogeography—2010—Pe uelas—Increased water-use efficiency during the 20th century did not.pdf. (n.d.).

Halofsky, J. E., Hemstrom, M. A., Conklin, D. R., Halofsky, J. S., Kerns, B. K., & Bachelet, D. (2013). Assessing potential climate change effects on vegetation using a linked model approach. *Ecological Modelling*, *266*, 131–143. https://doi.org/10.1016/j.ecolmodel.2013.07.003

Johnson, D. D., & Miller, R. F. (2008). Intermountain Presettlement Juniper: Distribution, Abundance, and Influence on Postsettlement Expansion. *Rangeland Ecology & Management*, *61*(1), 82–92. https://doi.org/10.2111/06-154.1

Kerns, B. K., Powell, D. C., Mellmann-Brown, S., Carnwath, G., & Kim, J. B. (2018). Effects of projected climate change on vegetation in the Blue Mountains ecoregion, USA. *Climate Services*, *10*, 33–43. https://doi.org/10.1016/j.cliser.2017.07.002

Miller, R. F., Chambers, J. C., Evers, L., Jason, C., Snyder, K. A., Roundy, B. A., & Pierson, F. B. (n.d.). *The ecology, history, ecohydrology, and management of pinyon and juniper woodlands in the Great Basin and Northern Colorado Plateau of the western United States*. 292.

Miller, R. F., Tausch, R. J., McArthur, E. D., Johnson, D. D., & Sanderson, S. C. (2008). *Age structure and expansion of piñon-juniper woodlands: A regional perspective in the Intermountain West*. https://sagemap.wr.usgs.gov/Docs/Miller%20et%20al%202008.PDF

Renwick, K. M., Curtis, C., Kleinhesselink, A. R., Schlaepfer, D., Bradley, B. A., Aldridge, C. L., Poulter, B., & Adler, P. B. (2018). Multi-model comparison highlights consistency in predicted effect of warming on a semi-arid shrub. *Global Change Biology*, *24*(1), 424–438. https://doi.org/10.1111/gcb.13900

Silva, L. C. R., & Anand, M. (2013). Probing for the influence of atmospheric CO_2 and climate change on forest ecosystems across biomes: Changes in growth and iWUE across biomes.

Global Ecology and Biogeography, *22*(1), 83–92. https://doi.org/10.1111/j.1466-8238.2012.00783.x

Soulé, P. T., Knapp, P. A., & Grissino-Mayer, H. D. (2004). HUMAN AGENCY, ENVIRONMENTAL DRIVERS, AND WESTERN JUNIPER ESTABLISHMENT DURING THE LATE HOLOCENE. *Ecological Applications*, *14*(1), 96–112. https://doi.org/10.1890/02-5300

Speer, J. H. (n.d.). *Fundamentals of Tree-Ring Research*. 86.

Tredennick, A. T., Hooker, G., Ellner, S. P., & Adler, P. B. (2021). A practical guide to selecting models for exploration, inference, and prediction in ecology. *Ecology*, *102*(6). https://doi.org/10.1002/ecy.3336

Vold, S. (n.d.). *Oregon Department of Fish and Wildlife*. 129.

CHAPTER IV

COMPARISON OF EVALUATIONS OF WESTERN JUNIPER TREE-RING CLIMATE SENSITIVITY BETWEEN MIXED EFFECTS MODELS ANS BOOTSTRAPPED MOVING WINDOW CORRELATION AND RESPONSE FUNCTIONS

Introduction

One common way to asses changes in tree-ring sensitivity to climate variables is through the use of bootstrapped moving window correlation and response functions e.g. Árvai et al (2018); Bozkurt et al., (2021); Carrer and Urbinati, (2006); Lebourgeois et al., (2012); Marcinkowski et al., (2015); Wang et al., (2016) and others. These functions examine how tree-rings have responded overtime to climate variables via a moving time frame window (Guiot, 1991). For the time window of analysis of a given size the relationships between tree-rings and climate are quantified as regression coefficients (from here on referred to as sensitivity), then the earliest year of the window is removed and a succeeding year is added, then that process is repeated over the entire temporal period of interest. Usually, these analyses are conducted to examine how tree-ring climate relationships have or have not changed over time. Alternatively, we conducted mixed-effects models (MEMs) in chapter II and chapter III of this dissertation to explore a similar concept; how tree-ring climate relationships have changed as atmospheric CO_2 has increased over the last century. Our method of analysis from chapter II and chapter III was selected because MEMs allow for the testing of multiple and interacting explanatory variables at the same time (Zuidema et al 2020) and the explicitly produced mathematical parameters from such an analysis appear to be useful in climate impact modeling under future climate scenarios (Charney et al 2016; Lindner et al 2014). Therefore, we deem it prudent to compare our more novel regional climate sensitivity models from chapter II with this more commonly used approach. In addition, generally our understanding of complex ecological issues are better understood with ensembles of models each that draw attention to differing issues at hand, our models from chapter II and chapter III examined how western juniper tree-ring climate sensitivity changed in relation to atmospheric CO_2 concentration. Models from this chapter will explore how moving windows of tree-ring response to climate have changed over time, perhaps elucidating linear and non-linear trends and patterns. Hopefully the analysis from this chapter will further validate the findings from the precedent two chapters by expressing a similar phenomenon (non-stationarity in tree-ring climate sensitivity) across different model types (Lisciandra and Korbmacher 2021), and act as a "bridge" that links the relatively common moving window correlation and response function analyses with our previously executed more novel approach and explanation, allowing for further interpolation of our theory that increased atmospheric CO_2 influences tree-ring climate relations across species, biomes, and geographic space and time.

In order to achieve the goals of this chapter we conducted three main steps 1) we generated a response and correlation function analysis for each of our sites. 2) We fitted linear models to the outputs of our first moving-window response functions for the time periods of pre 1955 and post 1955. 3) We compared the results of our inter-chapter modeling efforts.

Methods

Details on study site locations and data acquisition are detailed in chapter II of this dissertation. Using the dcc function from the treeclim package in the r programing language we generated bootstrapped responses of detrended tree-ring growth to climate variables (Zang & Biondi, 2014). This function resamples the response of our tree-rings to climate by resampling from our data set 1,000 times for each time window. Our window size was set to 15 years. Climate variables included both monthly precipitation and mean temperature value for three 4-month "seasons", the previous October to the current January (Fall/Winter), February to May (Winter/Spring) and June to September (Summer). The results of such an analysis are coefficient values that represent the sensitivity of tree-ring growth to each climate variable.

Secondly, we conducted linear regression models using the mean correlation coefficient from our response function as our response variable and year as our predictor variable. This analysis was conducted twice per site, because we subdivided our years into to sets, pre-CO2 fertilization and post -CO_2 fertilization (pre 1955 and post 1955) the general period that CO_2 enhancement has been proposed to have stated (Kienast &Luxmoore 1988, Graumlich 1991). A difference in slopes of these regression line between pre and post 1955 represents a change in sensitivity. This change in slope was determined from the results of an analysis of variance tests (ANOVA) on each climate variable for each site. A significant interaction term between year and CO_2 fertilization category (per 1955 and post 1955) represented a significant difference in climate sensitivity. Types of changes in tree-ring sensitivity can be classified into a general biplot either positive (a positive coefficient of response to a given climate variable) or negative sensitivity (a negative coefficient of response to a given climate variable) and either increasing (diverging from a zero coefficient of response to a given climate variable) or decreasing sensitivity (converging on the zero coefficient of response to a given climate variable) (Figure 1).

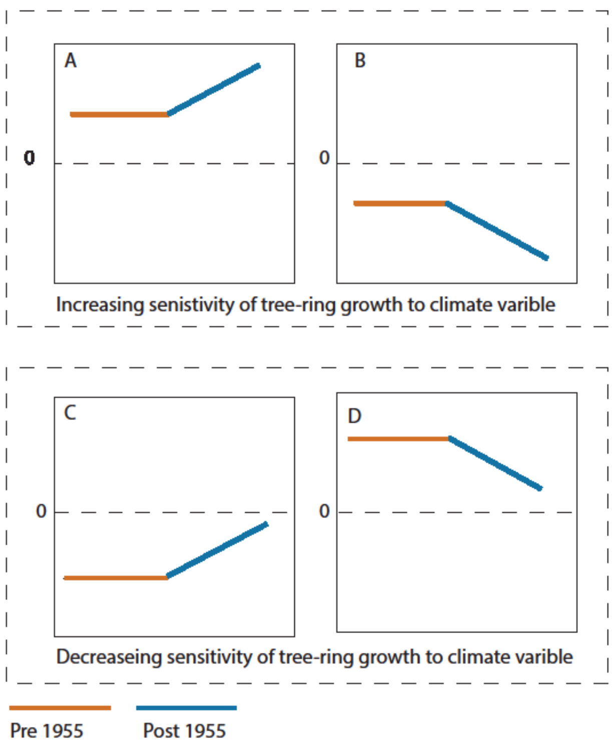

Figure 1.- Four hypothesized changes in sensitivity trends. Tree-ring sensitivity to various climate variables could hypothetically change in four-way A) Tree-rings could respond positively to a climate variable and become increasingly sensitive to that variable post 1955. B) Tree-rings could respond negatively to a climate variable and then become increasingly sensitive to that variable post 1955. C) Tree-rings could respond negatively to a climate variable and then become less sensitive to that variable post 1955, and D) tree-rings could respond positively towards a climate variable and then become less sensitive towards that variable post 1955.

When examining the outcomes of this analysis (figures 2-13) we identified several instances of what we are calling paradoxical changes in sensitivity mostly resulting in potential false positives. For instance, sensitivity to Winter/Spring temperature for OR009 shows a change in sensitivity pre and post 1955, but the regression lines both straddle the zero coefficient line but the mean sensitivity between those periods does not appear to be different in a linear fashion (Figure 10). However, we can also observe the opposite as in Winter/Spring temperature of CA095 where the means in sensitivity appear clearly different, with the signs of the coefficients abruptly changing from positive to negative around the 1955 mark, but the slopes of the regression lines not being significantly different (Figure 7).

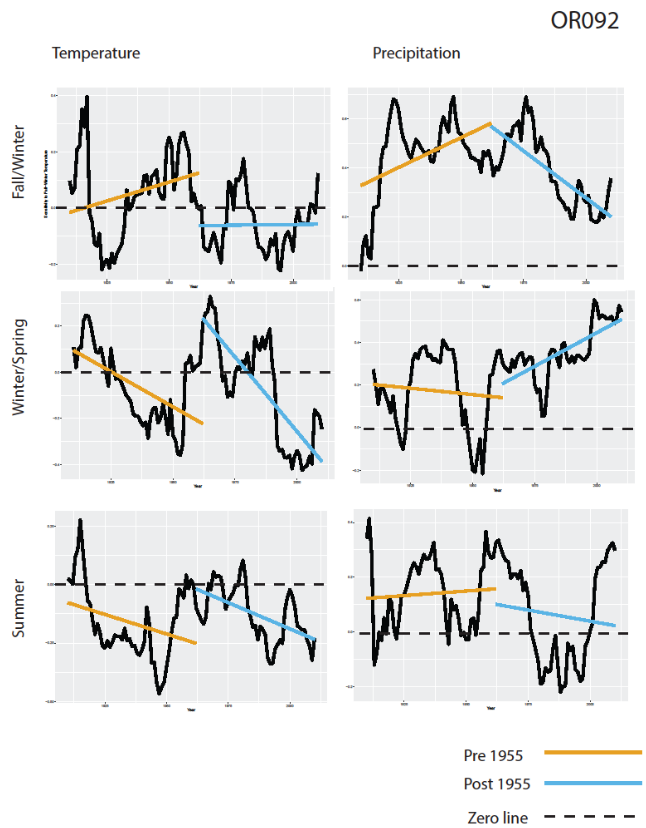

Figure 2- OR092 bootstrapped 15 year moving window response of western juniper tree-ring growth (solid black line) to three 4-month climate variables (Fall/Winter= previous year's October to current year's January, Winter/Spring= February to May, Summer= June to September) for temperature and precipitation. Solid gold and blue lines represent linear regression lines for time periods pre and post 1955. Dotted black line represents the zero line of the y-axis.

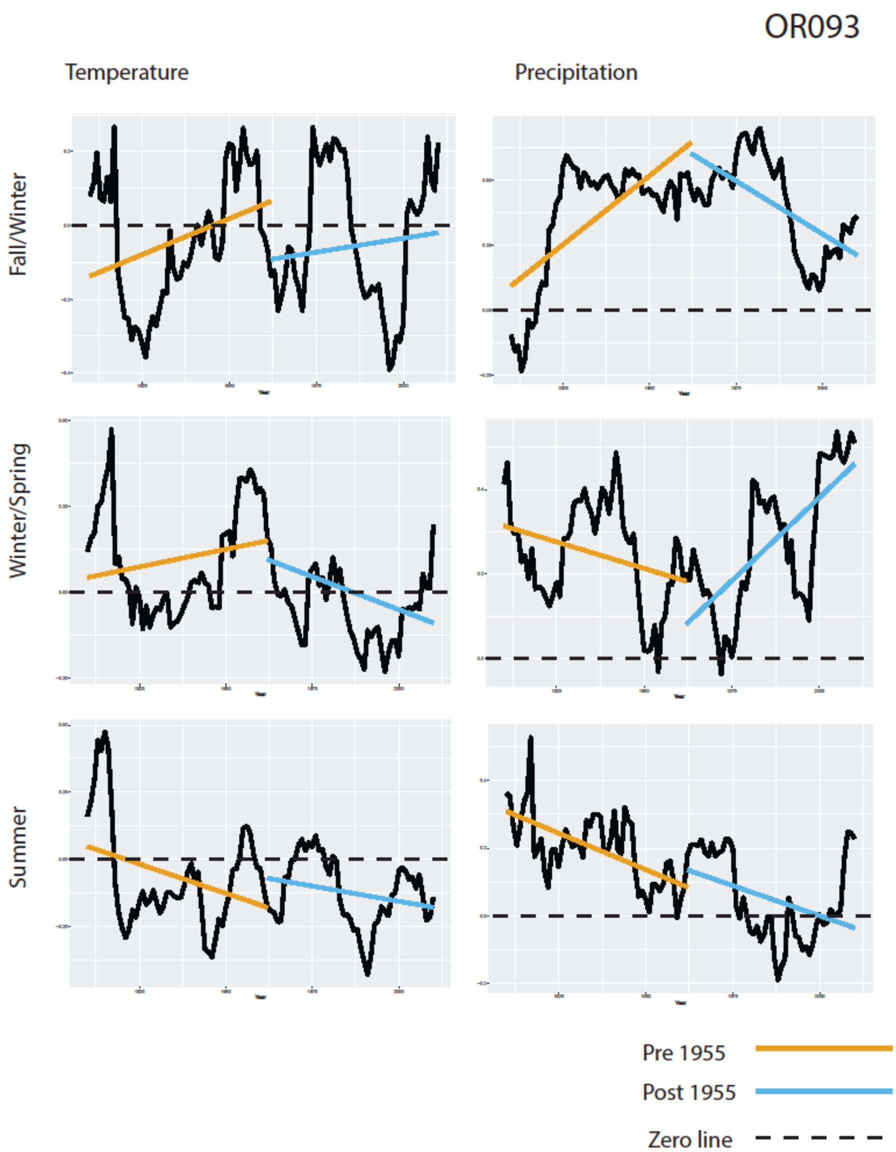

Figure 3- OR093 bootstrapped 15 year moving window response of western juniper tree-ring growth (solid black line) to three 4-month climate variables (Fall/Winter= previous year's October to current year's January, Winter/Spring= February to May, Summer= June to September) for temperature and precipitation. Solid gold and blue lines represent linear regression lines for time periods pre and post 1955. Dotted black line represents the zero line of the y-axis.

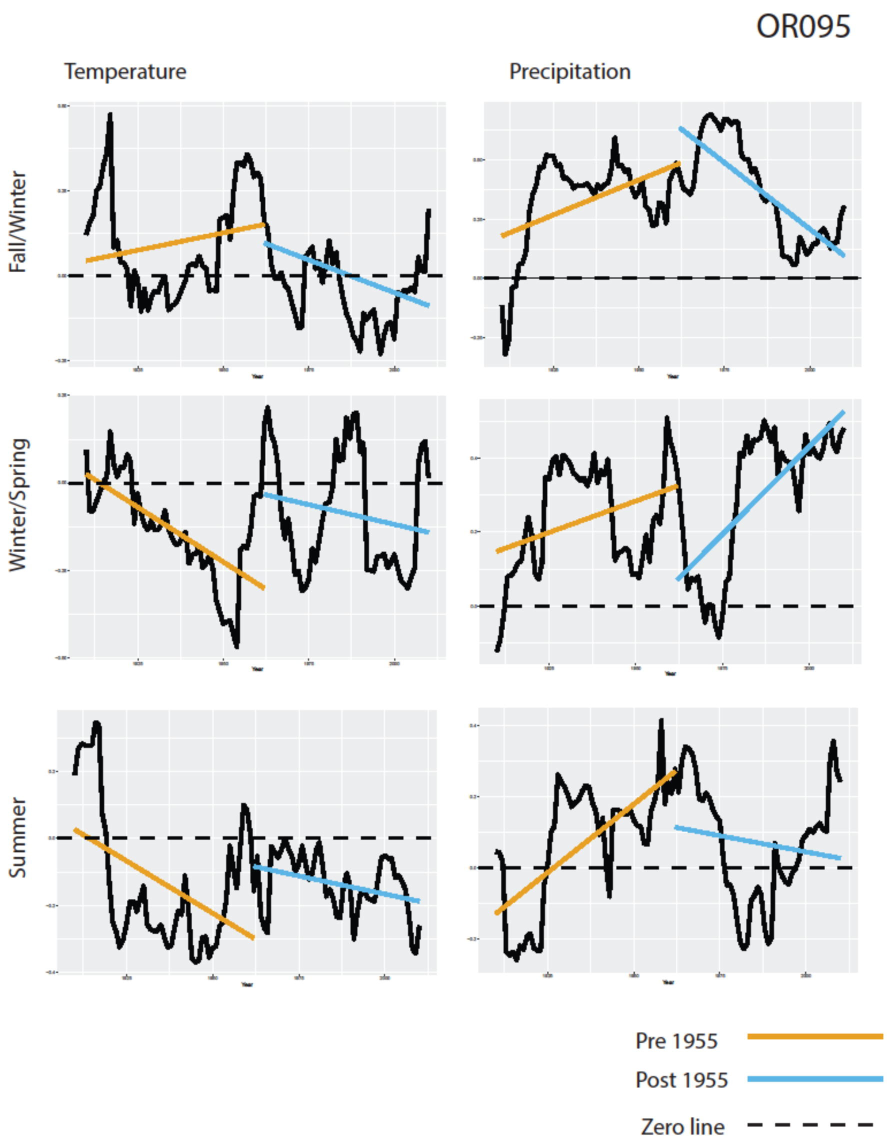

Figure 4- OR 095 bootstrapped 15 year moving window response of western juniper tree-ring growth (solid black line) to three 4-month climate variables (Fall/Winter= previous year's October to current year's January, Winter/Spring= February to May, Summer= June to September) for temperature and precipitation. Solid gold and blue lines represent linear regression lines for time periods pre and post 1955. Dotted black line represents the zero line of the y-axis.

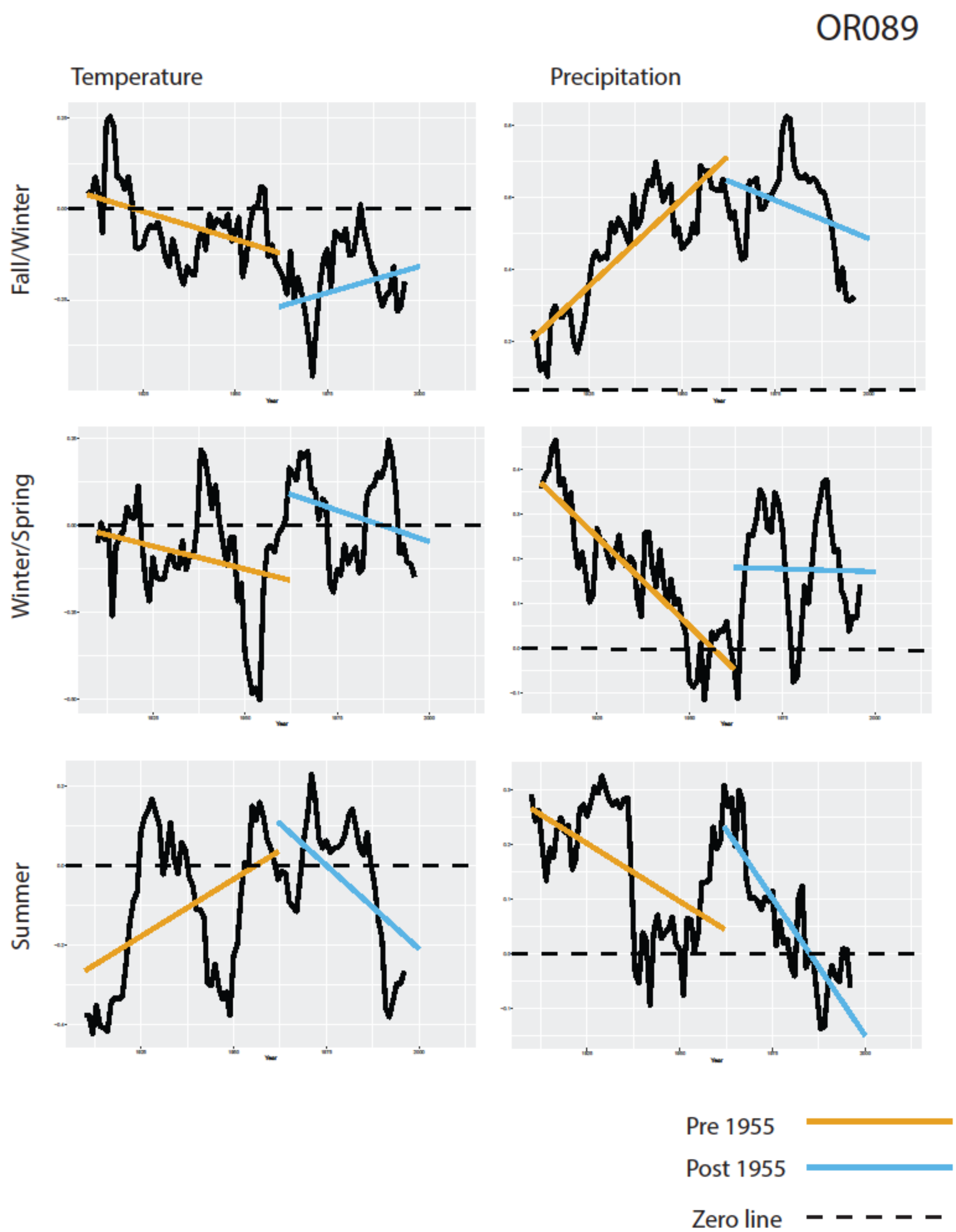

Figure 5- OR089 bootstrapped 15 year moving window response of western juniper tree-ring growth (solid black line) to three 4-month climate variables (Fall/Winter= previous year's October to current year's January, Winter/Spring= February to May, Summer= June to September) for temperature and precipitation. Solid gold and blue lines represent linear regression lines for time periods pre and post 1955. Dotted black line represents the zero line of the y-axis.

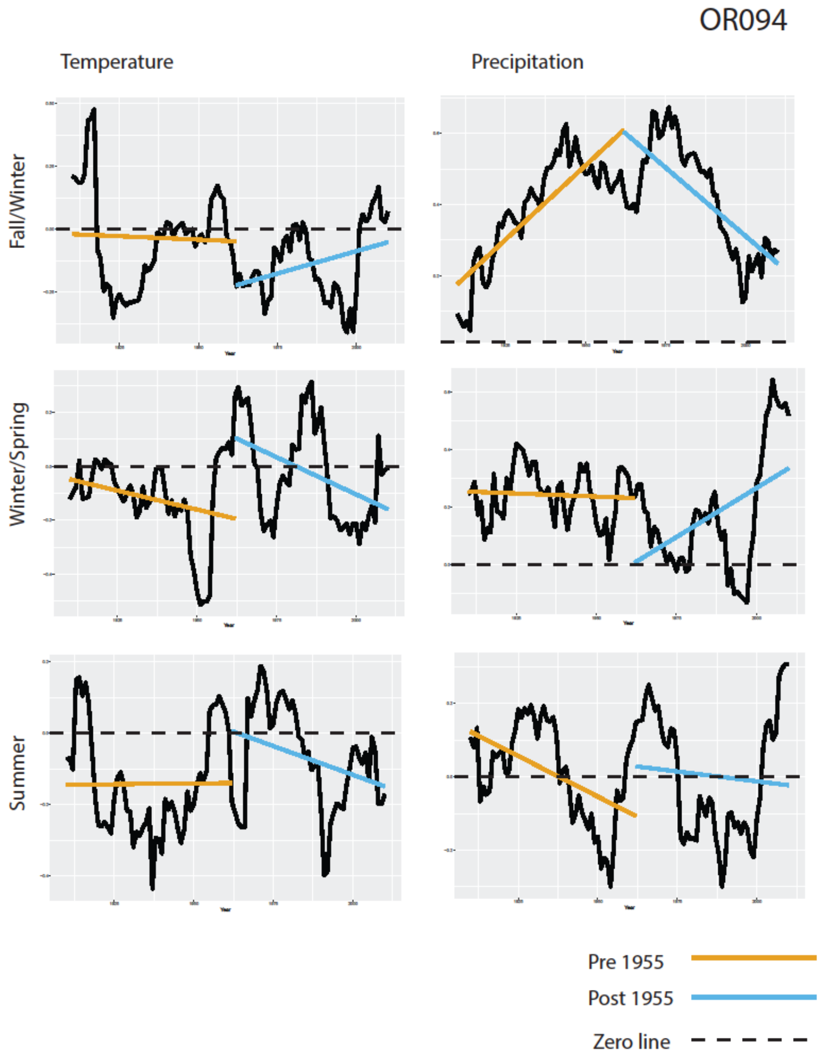

Figure 6- OR094 bootstrapped 15 year moving window response of western juniper tree-ring growth (solid black line) to three 4-month climate variables (Fall/Winter= previous year's October to current year's January, Winter/Spring= February to May, Summer= June to September) for temperature and precipitation. Solid gold and blue lines represent linear regression lines for time periods pre and post 1955. Dotted black line represents the zero line of the y-axis.

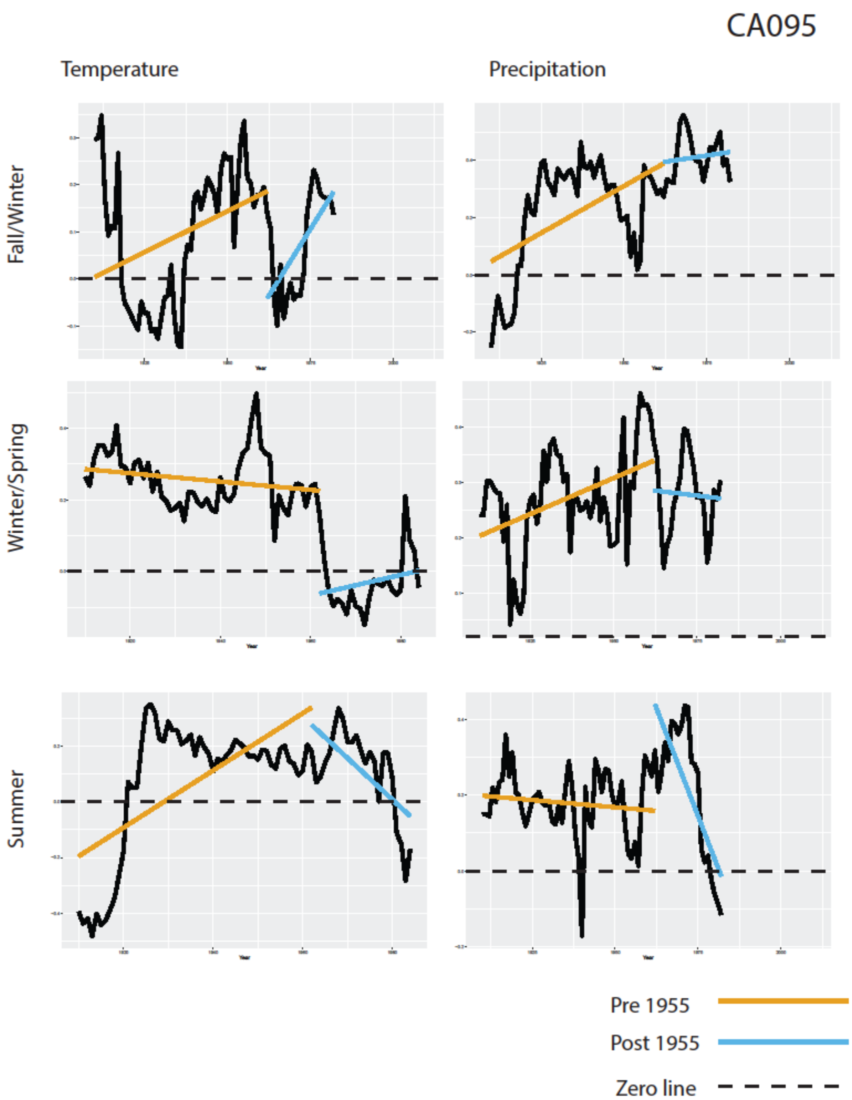

Figure 7- CA095 bootstrapped 15 year moving window response of western juniper tree-ring growth (solid black line) to three 4-month climate variables (Fall/Winter= previous year's October to current year's January, Winter/Spring= February to May, Summer= June to September) for temperature and precipitation. Solid gold and blue lines represent linear regression lines for time periods pre and post 1955. Dotted black line represents the zero line of the y-axis.

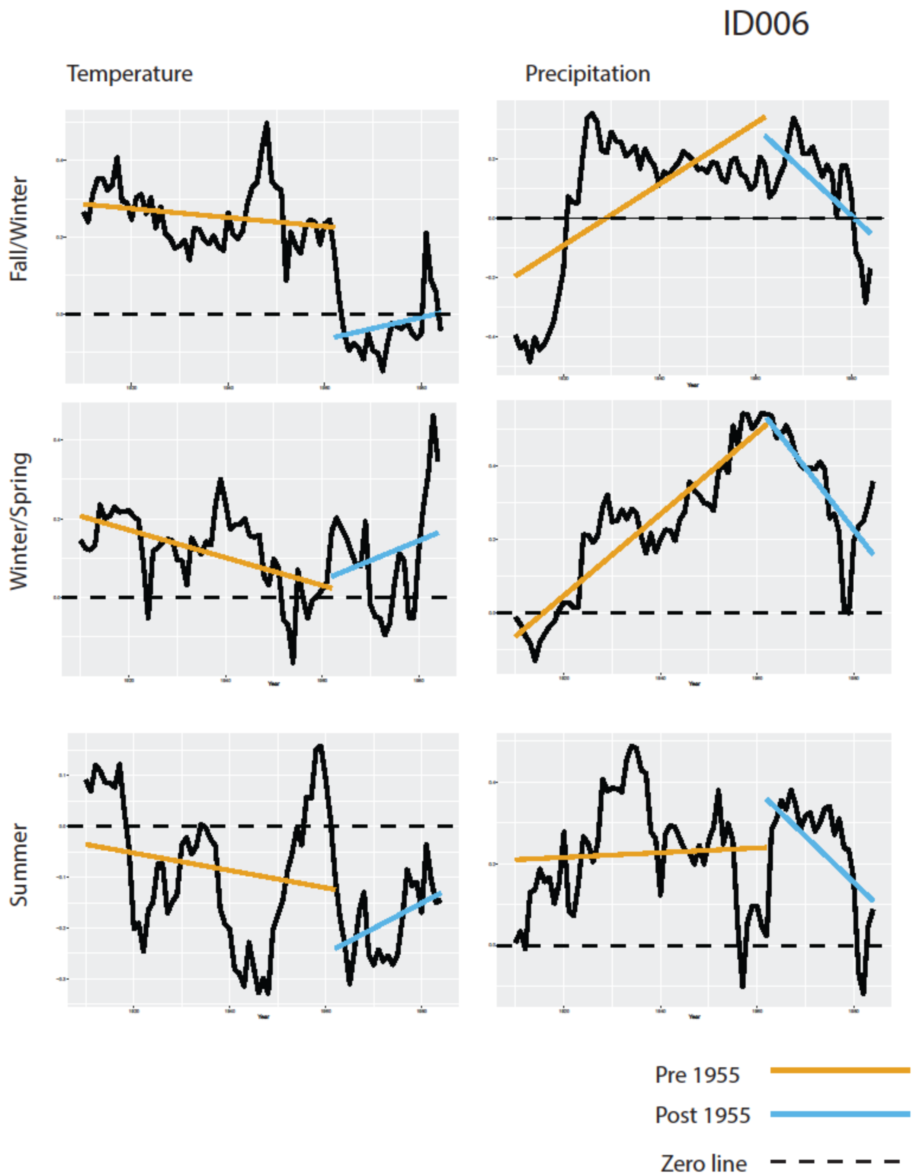

Figure 8- ID006, bootstrapped 15 year moving window response of western juniper tree-ring growth (solid black line) to three 4-month climate variables (Fall/Winter= previous year's October to current year's January, Winter/Spring= February to May, Summer= June to September) for temperature and precipitation. Solid gold and blue lines represent linear regression lines for time periods pre and post 1955. Dotted black line represents the zero line of the y-axis.

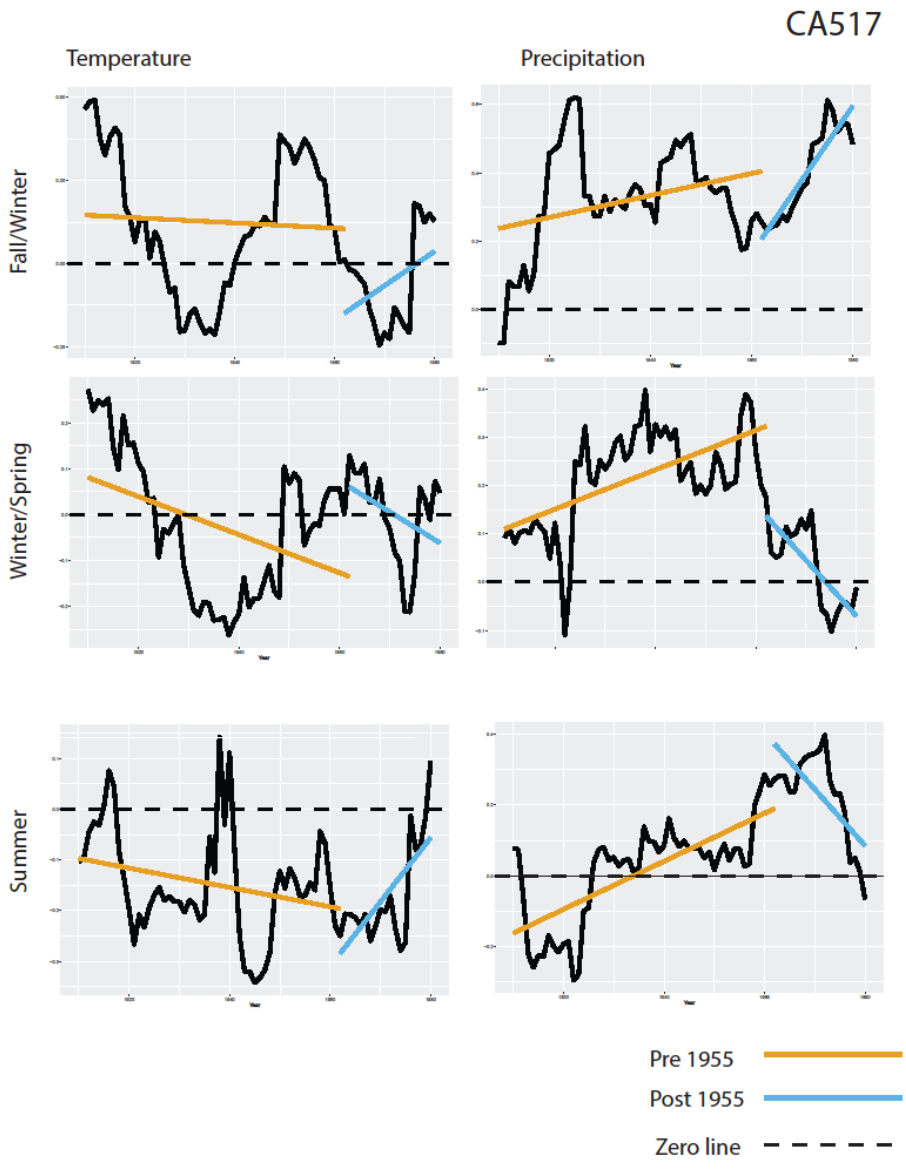

Figure 9- CA517 bootstrapped 15 year moving window response of western juniper tree-ring growth (solid black line) to three 4-month climate variables (Fall/Winter= previous year's October to current year's January, Winter/Spring= February to May, Summer= June to September) for temperature and precipitation. Solid gold and blue lines represent linear regression lines for time periods pre and post 1955. Dotted black line represents the zero line of the y-axis.

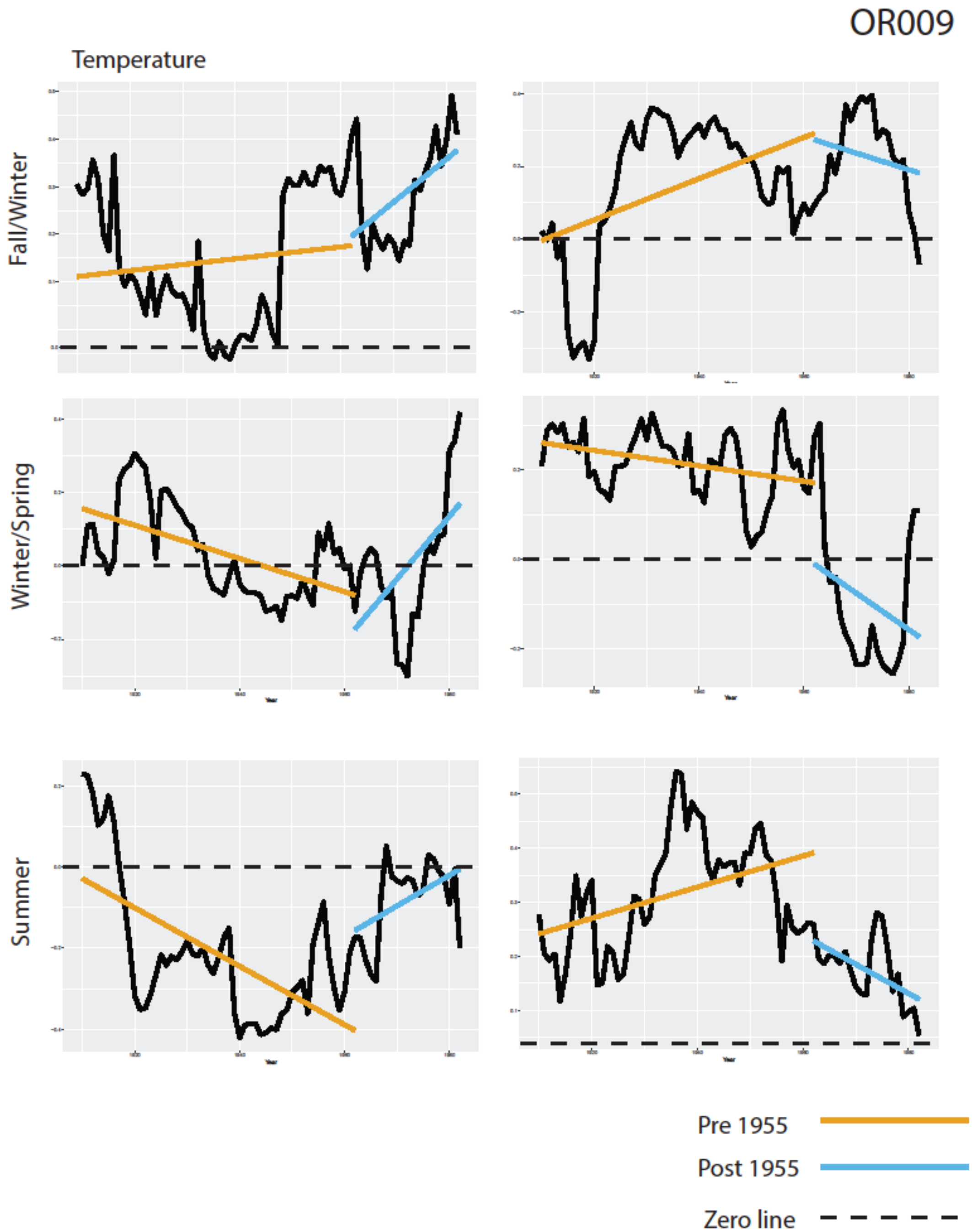

Figure 10- OR009 Bootstrapped 15 year moving window response of western juniper tree-ring growth (solid black line) to three 4-month climate variables (Fall/Winter= previous year's October to current year's January, Winter/Spring= February to May, Summer= June to September) for temperature and precipitation. Solid gold and blue lines represent linear regression lines for time periods pre and post 1955. Dotted black line represents the zero line of the y-axis.

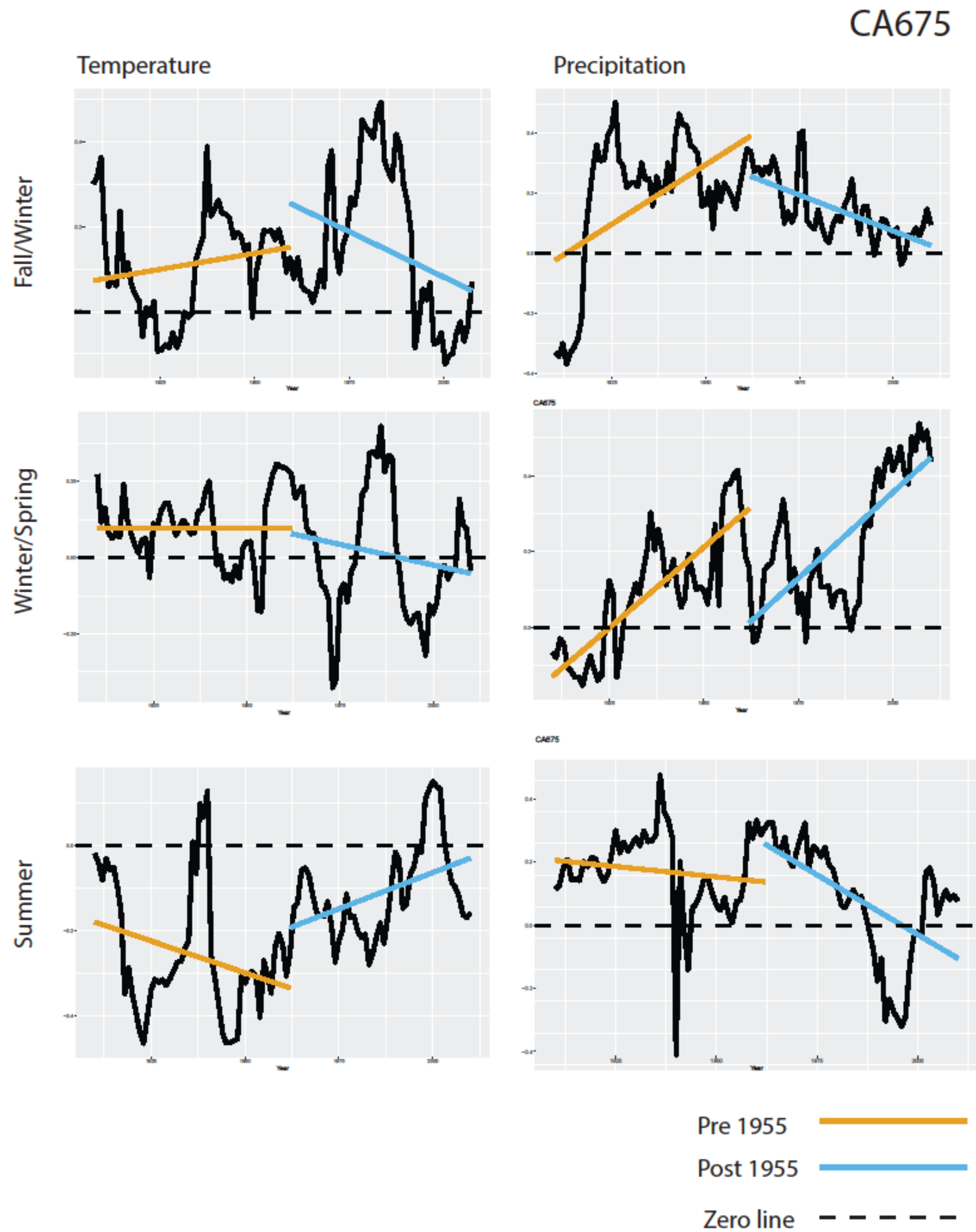

Figure 11- CA675 bootstrapped 15 year moving window response of western juniper tree-ring growth (solid black line) to three 4-month climate variables (Fall/Winter= previous year's October to current year's January, Winter/Spring= February to May, Summer= June to September) for temperature and precipitation. Solid gold and blue lines represent linear regression lines for time periods pre and post 1955. Dotted black line represents the zero line of the y-axis.

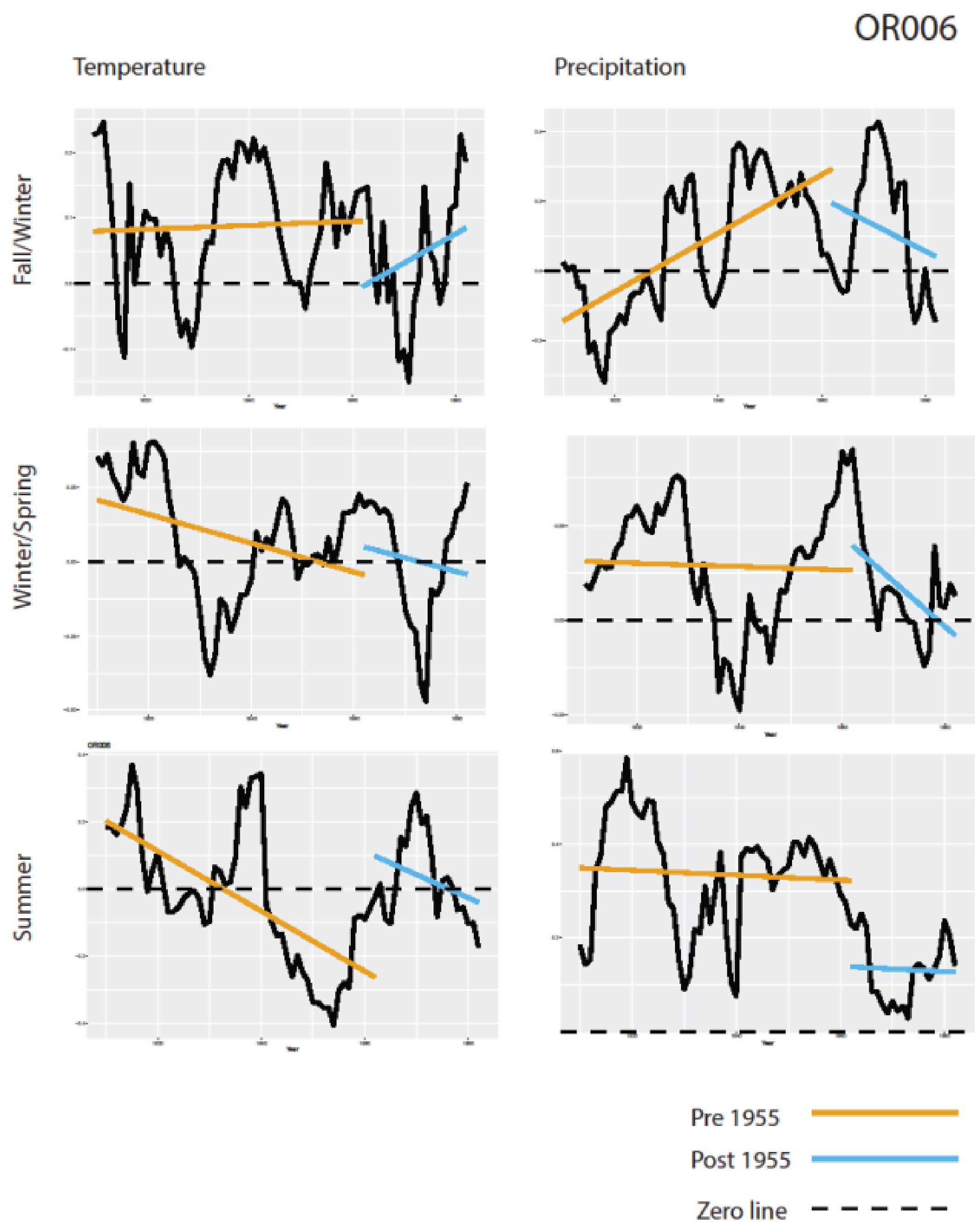

Figure 12- OR006 bootstrapped 15 year moving window response of western juniper tree-ring growth (solid black line) to three 4-month climate variables (Fall/Winter= previous year's October to current year's January, Winter/Spring= February to May, Summer= June to September) for temperature and precipitation. Solid gold and blue lines represent linear regression lines for time periods pre and post 1955. Dotted black line represents the zero line of the y-axis.

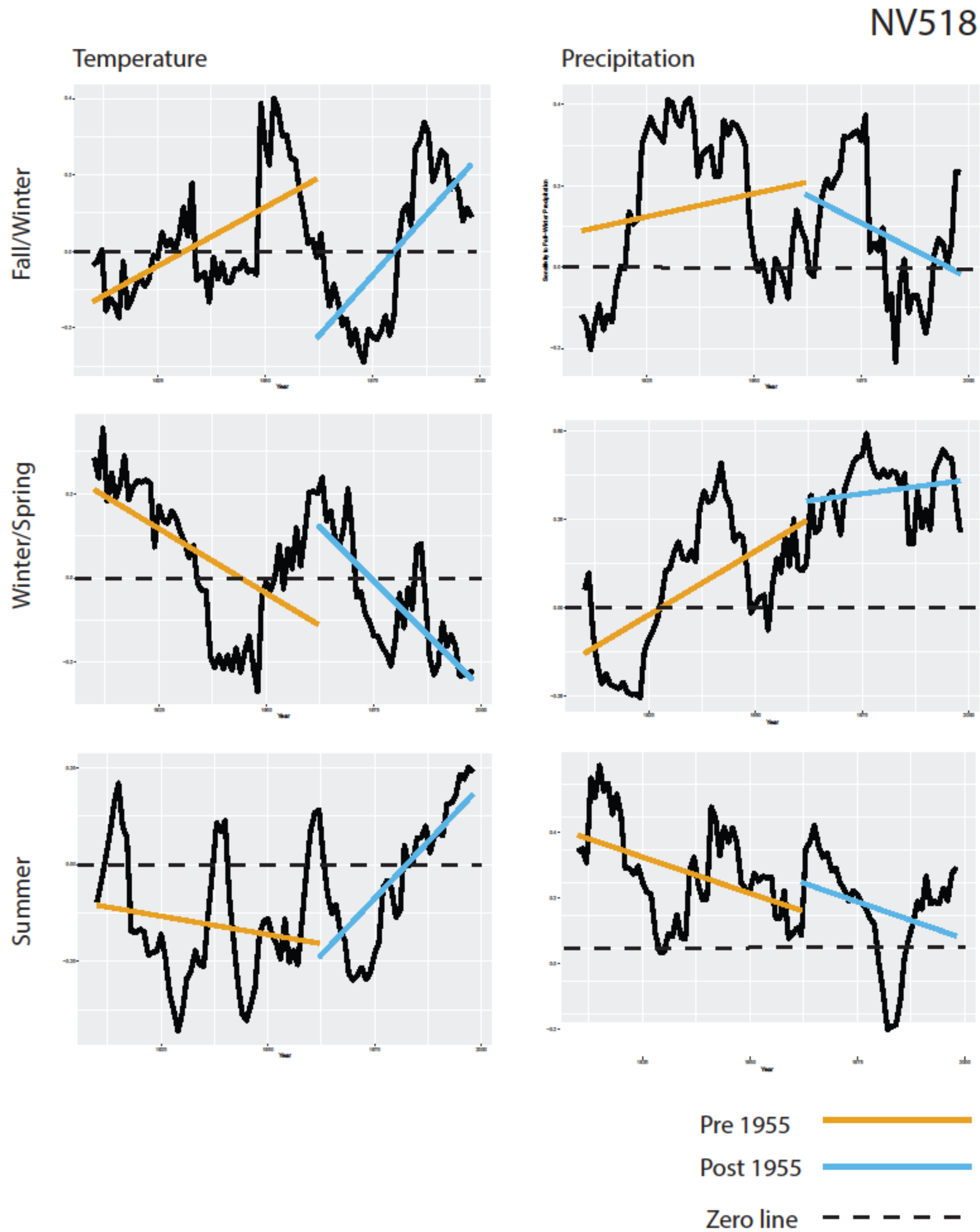

Figure 13- NV518 bootstrapped 15 year moving window response of western juniper tree-ring growth (solid black line) to three 4-month climate variables (Fall/Winter= previous year's October to current year's January, Winter/Spring= February to May, Summer= June to September) for temperature and precipitation. Solid gold and blue lines represent linear regression lines for time periods pre and post 1955. Dotted black line represents the zero line of the y-axis

Results

Results from Bootstrapped Moving Window Response Functions:

Our bootstrapped moving window response functions showed a high level of variation in tree-ring response to climate over time for all our sites and for all climate seasons (figures 2-14). Correlation of response coefficients between sites was high for all climate season with a mean Pearson's correlation coefficient of 0.594. The Winter/Fall season had the highest correlation of sensitivity between sites of 0.763, followed by Winter/Spring temperature, Summer temperature, Summer precipitation, Fall/Winter Temperature, and finally Winter/Spring precipitation (Pearson's correlation = 0.707,0.560, 0.540, 0.520, an d0.449)

Results from Linear Models:

Agreement in changes in tree-ring sensitivity to climate variables was mixed across sites and climate variables. The most agreement in sensitivity trends across sites was with Fall/Winter precipitation. Ten of 13 sites showed a significant decrease in tree-ring sensitivity to Fall/Winter precipitation post 1955. Winter/Spring precipitation had significant differences in tree-ring sensitivity trends at 9 of 13 sites, with six of those nine sites showing an increase in tree-ring sensitivity to Winter/Spring precipitation post 1955, and three of those nine sites showing a decrease in tree-ring sensitivity to Winter/Spring precipitation post 1955. Seven sites showed a significant change in tree-ring sensitivity to Summer precipitation, with all seven sites showing decreases in tree-ring sensitivity to Summer precipitation post 1955 (table 1). Additionally, CA006 had a significantly lower mean tree-ring sensitivity to Summer precipitation post 1955, but with an insignificant difference in sensitivity trend line (Figure CA006, Table CA006).

Significant changes in tree-ring sensitivity to temperature were less prevalent than changes in sensitivity to precipitation, however there was a greater degree of agreement in terms of direction of change in sensitivity, with all significant results indicating decrease in sensitivity to temperature post 1955 (table 1). Change in sensitivity to Fall/Winter temperature contained four significant values with one of them (site NV518 deemed paradoxical in nature). For Winter/Spring temperature there were six significant changes in tree-ring sensitivity post 1955 with one of them (site OR009) deemed paradoxical. Finally, for changes in sensitivity to

Summer temperatures there were seven significant changes in trends, however two of them (sites OR089 and NV518) appear paradoxical in nature.

Comparison with Regional Model from Chapter 2:

Our regional model from chapter 2 indicated three significant changes in western juniper tree-ring sensitivity to climate variables as atmospheric carbon dioxide has increased over the last century. They are a decrease in sensitivity to Fall/Winter precipitation, an increase in sensitivity to Winter/Spring precipitation, and a decrease in sensitivity to Summer precipitation. Although there may be some incongruency with comparing the site level responses from the site level analyses from this chapter with the regional level responses from chapter 2, it is worth noting that 22 of the 39 site level responses for precipitation are in agreement with the regional model a rate of 56% (table 1). One aspect that makes comparing site level responses particularly difficult is that in chapter 2 we used a dredge function to determine the most parsimonious site level and regional level models, and therefore it might be useful to recalculate the analysis of chapter 2 including all climate variables and then compare signs of sensitivity changes.

Table 1. P-values of changes in tree-ring sensitivity to climate variables; October to January precipitation (OJP), October to January temperature (OJT) February to March precipitation (FMP), February to March temperature (FMT), June to September precipitation (JSP), and June to September temperature (JST) for all 13 sites. P-values less than 0.05 are in bold, arrows indicate direction of sensitivity change, down arrows represent reductions in sensitivity, up arrows indicate increases in sensitivity, an "X" represents paradoxical sensitivity shifts.

Site	OJP	OJT	FMP	FMT	JSP	JST
OR092	↓ **0.0000**	0.1370	↑ **0.0003**	↓ **0.0009**	0.3051	0.5267
OR093	↓ **0.0000**	0.1967	↑ **0.0000**	↓ **0.0004**	0.6049	0.3520
OR095	↓ **0.0000**	↓ **0.0336**	↑ **0.0014**	↓ **0.0425**	↓ **0.0000**	0.0521
OR089	↓ **0.0000**	↓ **0.0230**	↑ **0.0002**	0.7295	↓ **0.0008**	X **0.0000**
OR094	↓ **0.0000**	0.0870	↑ **0.0005**	0.2250	0.0977	0.1003
CA095	0.3826	0.1033	0.2896	0.0962	↓ **0.0000**	↓ **0.0000**
ID006	↓ **0.0000**	0.1308	↓ **0.0000**	↓ **0.0140**	↓ **0.0078**	0.1004
CA517	X **0.0026**	0.1892	↓ **0.0000**	0.6483	X **0.0000**	↓ **0.0011**
OR063	↓ **0.0000**	0.1073	↑ **0.0003**	↓ **0.0173**	0.1476	↓ **0.0000**
OR009	0.0990	0.1239	0.1131	X **0.0000**	↓ **0.0131**	↓ **0.0029**
CA675	↓ **0.0000**	↓ **0.0060**	0.6964	0.2349	↓ **0.0020**	↓ **0.0004**
OR006	↓ **0.0085**	0.2539	0.0501	0.9734	0.9910	0.7189
NV518	↓ **0.0180**	X **0.0066**	↓ **0.0176**	0.0708	0.9638	X **0.0000**

Discussion

Key findings from this chapter are that linear trends in bootstrapped moving window response and correlation functions agree with findings from our mixed effects models from chapters 2 and 3. We have further evidence that the climate sensitivity of western juniper tree-rings have changed over the last century when compared before and after the hypothesized time period of atmospheric carbon dioxide induced increase in intrinsic water use efficiency and drought tolerance (~1955). Our results show decreases in sensitivity to Fall/Winter precipitation at 10/13 or 77% of our sites. With sensitivity to Winter/Spring precipitation increasing at 46% of our sites, and sensitivity to Summer precipitation decreasing also at 46% (albeit no the exact same sites). Additionally, the bootstrapped moving window analysis from this study indicated several trends in reduction of western juniper tree-ring response (sensitivity) to temperature that were not evident from our analysis in chapters 2 and 3. We observed changes in western juniper tree-ring sensitivity to at least one temperature season in 10 out of 13 of our study sites with only 4 out of 13 sites showing reductions in sensitivity to temperature in our analysis from chapter 2. However, overall the major findings from this chapter and chapters 2 and 3 are in agreement with each other. This begs the question of how our findings from this chapter relate to similarly methodological studies from around the world, and can our hypothesis; that these changes in tree-ring sensitivity are due to increased intrinsic water use efficiency be transferred to the results from such studies?

In a limited analysis of recent similar studies we found results that are both congruent (showing changes in tree-ring responses to climate over time) and not so (showing stability in tree-ring climate relations). The non-stationarity we observed is similar to that seen in study by Marcinkowski et al (2015) on the response of mountain hemlock (*Tsuga mertensiana*) to climate variability in the North Cascade Range in Washington state, whereas correlations with between tree-ring growth and winter precipitation became weaker over time. Additionally, Marcinkowski et al (2015) observed an increase in correlations between spring and summer temperatures and tree-ring growth with their study species.

Carrier and Urbinati (2006) found that European larch (Larix decidua) in the Alps of northern Italy were nonstationary, particularly with the most influential climate variable regarding tree-ring growth, June temperature. They observed a sharp increase then marked decrease in tree-ring growth climate correlation centered around the 1860-1959 analysis window.

In a five species (*Pinus nigra, P. sylvestris, P. uncinata, Abies alba, Fagus sylvatica*) analysis in the Mediterranean mountains, Lebourgeois et al. (2011) observed non-stationarity in tree-ring growth climate relationships from 1910-2004 for all species. Additionally, they observed that tree-ring growth response to climate varied across altitudes and climate regimes, and across species based on eco- physiological traits. Notably, they generally observed decreasing trends of correlation with precipitation and increasing trends of correlation with temperature around the 1930-1980 fifty year moving window, that would center around the 1955 proposed demarcation of enhanced water use efficiency due to increased concentration atmospheric carbon dioxide (Kienast &Luxmoore 1988, Graumlich 1991). However not all studies we explored showed such non-stationarity.

Bozkurt et al (2021) showed a stationary response to precipitation and a decrease in correlation between Scotts pine (*Pinus sylvestris*) from 1930-2013 in the Anatolian peninsula. Árvai et al. (2018) observed a stationary response of pedunculated oak (*Quercus robur L.*) in Eastern Hungary to precipitation over the past century and the response to temperature has changed from a positive relationship with dormant season temperature switching to a negative relationship in about the mid 20th century, indicating an increase in drought sensitivity for their study species in their study area.

These are only a small subset of such bootstrapped moving window tree-ring responses to climate studies that have been conducted, and although large scale multi-species dendrochronological meta analysis are becoming prevalent in the literature (Bast et al. 2018; Bauwe et al. 2016; Charney et al. 2016; Gedalof and Berg 2010; Klesse et al. 2020) to the best of our knowledge none have applied an analysis of changes in tree-ring sensitivity at a global scale, or attempted to summarize the entirety of results from bootstrapped moving window correlation and response functions. Of the previously cited studies, Gedalof and Berg (2010) is the most ambitious in terms of scope, analyzing over 2,000 sites, however, they did not directly test for changes in sensitivity of tree-rings to climate over time, but for an increasingly positive bias of residuals overtime, with a climate grid of 250 km and on a time period of analysis that started in 1950 very close to when hypothesized CO_2 is thought to have begun. Although we commend the geographic scope of their analysis we propose that a decade of advancement in analytical methods, enhancement of resolution of climatic variables, a greater time frame of analysis and recent data acquisition warrants additional studies at a global scale.

References

Árvai, M., Morgós, A., & Kern, Z. (2018). Growth-climate relations and the enhancement of drought signals in pedunculate oak (Quercus robur L.) tree-ring chronology in Eastern Hungary. *IForest - Biogeosciences and Forestry*, *11*(2), 267–274. https://doi.org/10.3832/ifor2348-011

Bauwe, A., Jurasinski, G., Scharnweber, T., Schröder, C., & Lennartz, B. (2016). Impact of climate change on tree-ring growth of Scots pine, common beech and pedunculate oak in northeastern Germany. IForest - Biogeosciences and Forestry, 9(1), 1–11. https://doi.org/10.3832/ifor1421-008

Bozkurt, A. E., Şahan, E. A., & Köse, N. (2021). Growth responses of Pinus sylvestris L. to climate from the southeastern limit of its natural distribution area, Turkey. *Dendrochronologia*, *70*, 125897. https://doi.org/10.1016/j.dendro.2021.125897

Carrer M, Urbinati C. Long-term change in the sensitivity of tree-ring growth to climate forcing in Larix decidua. New Phytol. 2006;170(4):861-71. doi: 10.1111/j.1469-8137.2006.01703.x. PMID: 16684244.

Charney, N. D., Babst, F., Poulter, B., Record, S., Trouet, V. M., Frank, D., Enquist, B. J., & Evans, M. E. K. (2016). Observed forest sensitivity to climate implies large changes in 21st century North American forest growth. *Ecology Letters*, *19*(9), 1119–1128. https://doi.org/10.1111/ele.12650

Gedalof, Z., & Berg, A. A. (2010). Tree ring evidence for limited direct CO 2 fertilization of forests over the 20th century: LIMITED CO 2 FERTILIZATION OF FORESTS. Global Biogeochemical Cycles, 24(3), n/a-n/a. https://doi.org/10.1029/2009GB003699

Graumlich, L. J. (1991). Subalpine Tree Growth, Climate, and Increasing CO_2: An Assessment of Recent Growth Trends. Ecology, 72(1), 1–11. https://doi.org/10.2307/1938895

Guiot, J. (1991). The bootstrapped response function. Tree Ring Bull.. 51.

Kienast, F., Luxmoore, R.J. Tree-ring analysis and conifer growth responses to increased atmospheric CO2 levels. Oecologia 76, 487–495 (1988). https://doi.org/10.1007/BF00397859

Lebourgeois, F., Mérian, P., Courdier, F., Ladier, J., & Dreyfus, P. (2012). Instability of climate signal in tree-ring width in Mediterranean mountains: A multi-species analysis. *Trees*, *26*(3), 715–729. https://doi.org/10.1007/s00468-011-0638-7

Lindner, M., Fitzgerald, J.B., Zimmermann, N.E., Reyer, C., Delzon, S., van der Maaten, E. et al. (2014). Climate change and European forests: what do we know, what are the uncertainties, and what are the implications for forest management? J. Environ. Manage., 146, 69–83.

Lisciandra, C., & Korbmacher, J. (2021). Multiple models, one explanation. *Journal of Economic Methodology*, *28*(2), 186–206. https://doi.org/10.1080/1350178X.2021.1892800

Marcinkowski, K., Peterson, D. L., & Ettl, G. J. (2015). Nonstationary temporal response of mountain hemlock growth to climatic variability in the North Cascade Range, Washington, USA. *Canadian Journal of Forest Research*, *45*(6), 676–688. https://doi.org/10.1139/cjfr-2014-0231

Wang, X., Zhang, M., Ji, Y., Li, Z., Li, M., & Zhang, Y. (2017). Temperature signals in tree-ring width and divergent growth of Korean pine response to recent climate warming in northeast Asia. Trees, 31(2), 415–427. https://doi.org/10.1007/s00468-015-1341-x

Zuidema, P. A., Heinrich, I., Rahman, M., Vlam, M., Zwartsenberg, S. A., & Sleen, P. (2020). Recent CO_2 rise has modified the sensitivity of tropical tree growth to rainfall and temperature. *Global Change Biology*, *26*(7), 4028–4041. https://doi.org/10.1111/gcb.15092

CHAPTER V

CONCLUSIONS

Western juniper woodlands (WJW) are a highly dynamic ecosystem at multiple spatial and temporal scales. Prehistoric climate drivers of landscape positioning of WJW are understood as such: expansion in its range at lower and upper elevations during generally wetter conditions; tree-cover decline at its upper elevational range during generally colder conditions; and/or retreat upslope during generally hotter and dryer conditions (Mehringer & Wigand, 1987; Miller & Wigand, 1994). However, since the late 19th century, western juniper woodlands have expanded in area by nearly six-fold, primarily through down slope advance and infill, and currently occupy ~3.6 million ha as of 2021 (The Gymnosperm Database, 2021; Azuma et al., 2005). This recent expansion is often attributed to reduction in fire frequency due to a reduction in fine fuels due to overgrazing by domestic livestock(Miller et al 2008; Johnson and Miller 2008; Eddleman et al 1994; Burkhardt and Tisdale 1976). However, more recent studies have attributed some of this expansion over the last century to climate and atmospheric CO_2 induced reduction in drought response via the CO_2 fertilization effect(Soulé et al., 2004; Soulé & Knapp, 2019). Indeed, studies in other ecosystems highlight the importance of accounting for the recent rise in atmospheric CO_2 when quantifying the dynamics of tree-ring climate relationships and the implications such findings could have on dynamic global vegetation models (Zuideman et al. 2020). Recent linked projection models aimed at quantifying the future dynamics and distributions of WJW are highly uncertain and incongruent (Creutzburg et al., 2015; Gibson, 2011; Zimmer et al., 2021). If we hope to manage these WJW effectively from a long-term perspective, we need to reduce this uncertainty through the refinement of our understanding of western juniper climate relations, when explicitly accounting for recent increases in atmospheric

CO_2, which my dissertation sought to address. Using *in situ* measurements and by levering past studies through meta-analysis we applied mixed effects models, linear models, and bootstrapped moving window response and correlation functions to quantify how precipitation and temperature variables impact western juniper tree-ring growth, and how the impacts of climate on tree-ring growth has changed across time and space.

Chapter II explores the relationships of western juniper tree-ring growth with three 4-month precipitation and temperature seasons and atmospheric CO_2 levels. This study leverages 13 previous dendrochronological studies from the International Tree-Ring Database across the best available representation of the geographic and climatic range of western juniper woodlands. By comparing multiple linear regression and mixed-effects models with and without CO_2 climate interactions, we were able to determine that the inclusion CO_2 as a predictor variable improved the predictive and inferential power of our models, providing further evidence that increased CO_2 has reduced the impact, i.e sensitivity, of precipitation and temperature on western juniper tree-ring growth. In addition, we observed several patterns of the climate sensitivity and changes in climate sensitivity of western juniper across the climate-space of western juniper woodlands. Whereas, generally more arid sites were more sensitive to October to January precipitation than less arid sites, and that more arid sites were experiencing a greater reduction in climate sensitivity as atmospheric CO_2 has increased over the last century. In addition, we quantified the representation of our 13 study sites within the climate space of western juniper woodlands using a novel permutation model.

Chapter III is used to validate our findings from Chapter II by testing our theories and models on tree-ring samples collected from both western juniper and ponderosa pine trees in the Chewaucan river basin located in southern central Oregon in the summer of 2017. Results from Chapter III provide evidence for our theory that increased atmospheric CO_2 have impacted the tree-ring growth climate relations of both studied tree species. Both western juniper and ponderosa pine tree rings were positively impacted by October-January precipitation, and negatively impacted by June-September temperature. However, results from our models highlighted the differences in western juniper and ponderosa pine tree-ring climate relationships, with western juniper tree-ring growth being more responsive to October-January precipitation than ponderosa pine; and ponderosa pine tree-ring growth being more response to June-

September temperate than western juniper. Furthermore, western juniper showed a reduction in precipitation sensitivity and ponderosa pine showed a reduction in temperature sensitivity as atmospheric CO_2 increased over time. In addition, we discovered that including a long-term precipitation variable improved the predictive power of our tree-ring climate growth models. Results from this chapter will improve future projection models aimed at accounting for differential future climate impacts on competing tree species within the same study area.

Chapter IV continues with the theme of model validation by comparing the results from our relatively novel (regarding changes in tree-ring climate relationships) mixed effects models from Chapter II with the more commonly used method for assessing tree-ring climate stationarity; the bootstrapped moving window response and correlation model. By comparing and contrasting trends between results from bootstrapped moving window response and correlation models and mixed effects models from Chapter II we were able to provide evidence of linkage, through shared trends, between the more commonly used bootstrapped moving window response and correlation models and our mixed effects models that explicitly contained atmospheric CO_2 as a predictor variable. We found that there was general agreement between model types and that the linear trends of bootstrapped moving window response and correlation model coefficients produced results that indicated changes in western juniper temperature sensitivity, in addition to the changes in western juniper precipitation sensitivity produced by the mixed effects models in Chapter II. Results from this chapter provide some evidence on the mechanisms behind changes in non-stationarity that has been observed but not explicitly tested at other sites/studies via bootstrapped moving window response and correlation models.

Western juniper woodlands are of great concern for land managers in the American West because of their expansion in to grass and shrub dominated rangelands. The findings from this dissertation will be useful for land mangers specifically if the findings can be incorporated into future modeling efforts aimed at determining dynamics and distributions of western juniper woodlands and adjacent ecosystems and plant community types. Understanding that CO_2 has and likely will continue to alter the relationships between WJW and climate should be considered with future projections modeling efforts, because these types of models are used to inform policy and land management actions. Furthermore, the findings from this dissertation could be used to inform scientist working in other semi-arid ecosystems around the world on how to 1) test for non-stationarity in climate relationships for their species of interest, 2) inform on why investigating such dynamics are important, and 3) inform on where to locate future study site locations via out premutation model.

Not only do we need to continue to move towards scientifically informed land management practices, we also need to move towards management informed scientific practices. Land managers are often faced with making decisions based on both limited certainty and limited resources. Liebig's law of the minimum, that plant growth is dictated not by the total resources available, but by the scarcest resource, is often acknowledged regarding the limitations of CO_2 fertilization and enhanced tree-ring growth. At a certain point the enhanced drought tolerance afforded by increased atmospheric CO_2 will no longer mitigate changes in climate or be limited by nutrient availability related to edaphic properties. The same concept could be applied to proposed land management actions and scientific research. Regarding scientific research, how important are theoretical findings with no seemingly practical application and vise versa. That being said, just because "pure" science might not seem to have a direct or immediate application does not mean its importance should be discounted. The impact of more "pure" scientific research could be considered analogous to the impact of the spline-smoothed precipitation predictor variable from Chapter III, whereas tree-ring growth is impacted by decadal and intra-annual climate variables, so is there a time delay in the practical application of more "pure" or theoretical scientific findings. Conversely, the greater global impacts of more applied science should also not be taken for granted, especially when considering the impacts of widespread management actions, based directly on that applied science, that alter ecosystem structure and function on a scale as seen under the Sage-Grouse Initiative.

On a somewhat related note I can't help but consider the vast amount of scientific knowledge that could be gained via the collection of scientific samples during widespread management actions i.e juniper treatment, as those perpetrated during the implementation of the Sage-Grouse initiative.

One example of managers, land-use practitioners, and scientist working in tandem to achieve a shared goal, is through the clipping and analysis of the wings of harvested sage-grouse. This practice has been used to tract genetics and in epidemiologic research and has been lauded as an overwhelming success (Vold, 2021). If a similar practice of citizen science-based sample acquisition could be implemented regarding tree-ring research the outcome could result in a vast improvement in our spatial coverage of sites sampled. Let us consider the 160,000 ha of confers treated by 2018 by the sage-grouse initiative. With a hypothetical average density of 75 western juniper per ha, that could mean as many as 12 million juniper trees cut in the process. For the sake of this argument, let us assume there is an average of 20 trees per dendrochronological study and there were 13 dendrochronological studies utilized in the meta-analysis from Chapter II and Chapter IV. If even one cookie (tree stem cross-section) was cut and turned in from every 50,000 juniper trees removed under that program, the amount of data we would have regarding western tree-rings would be at least doubled.

The most obvious future work that should be conducted would be the collection of additional western juniper tree-rings particularly from sites located in the more extreme portions of WJW climates space e.g. with annual temperature values greater than 9 degrees Celsius and less than 400 mm annual precipitation, and from areas with less than 6 degrees Celsius annual temperature. This would allow for further refinement of models regarding the changes in climate sensitivity of WJW as atmospheric CO_2 levels have increased. Testing our permutation model on a validation tree-ring set with more available data sets would also be a direction of further research. Furthermore the, geospatial patterns from this of climate sensitivity dynamics could be incorporated in future projection models. Results from this dissertation could be incorporated with other studies to produce a product aimed at identifying WJW areas that are likely to be more or less resilient to climate change to be used in selecting areas for intense treatment aimed at fuels reduction or conservation, or areas of likely high carbon sequestration.

REFRENCES

Azuma, D. L., Hiserote, B. A., & Dunham, P. A. (2005). *The western juniper resource of eastern Oregon, 1999.* (PNW-RB-249). U.S. Department of Agriculture, Forest Service, Pacific Northwest Research Station. https://doi.org/10.2737/PNW-RB-249

Eddleman, L., Miller, P., Miller, R. F., & Dysart, P. (1994). Western Juniper Woodlands (of the Pacific Northwest) Science Assessment. *United States Forest Servise*, *0*(0), 1–132.

Mehringer, P. J., & Wigand, P. E. (1987). *Western Juniper In the Holocene, Proceedings—Pinyon- Juniper Conference, Reno, NV, January 13-16, 1986*. https://doi.org/10.13140/2.1.1171.7442

Miller, R. F., Tausch, R. J., McArthur, E. D., Johnson, D. D., & Sanderson, S. C. (2008). *Age structure and expansion of piñon-juniper woodlands: A regional perspective in the Intermountain West*. https://sagemap.wr.usgs.gov/Docs/Miller%20et%20al%202008.PDF

Soulé, P. T., & Knapp, P. A. (2019). Radial Growth Rate Responses of Western Juniper (Juniperus occidentalis Hook.) to Atmospheric and Climatic Changes: A Longitudinal Study from Central Oregon, USA. *Forests*, *10*(12), 1127. https://doi.org/10.3390/f10121127

Soulé, P. T., Knapp, P. A., & Grissino-Mayer, H. D. (2004). HUMAN AGENCY, ENVIRONMENTAL DRIVERS, AND WESTERN JUNIPER ESTABLISHMENT DURING THE LATE HOLOCENE. *Ecological Applications*, *14*(1), 96–112. https://doi.org/10.1890/02-5300

Vold, S. (n.d.). *Oregon Department of Fish and Wildlife*. 129.

APPENDIX A

SUPPLEMENTARY MATERIAL FROM CHAPTER II

Supplementary Figures

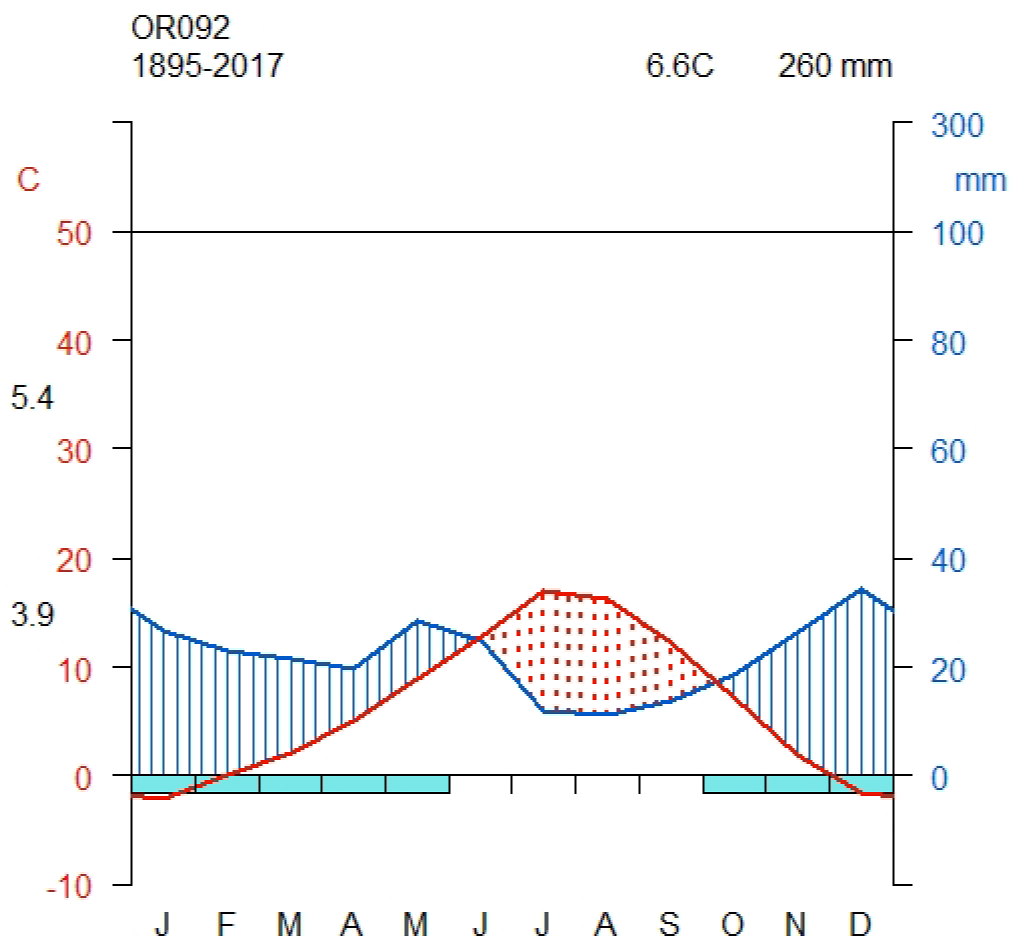

Figure S2.1.- Climograph for site OR092 derived from PRISM climate data from the years 1895-2017. Blue line represents mean monthly precipitation in millimeters. Redline represents mean monthly temperature in degrees Celsius. Red dotted area represents the dry period. Cyan colored bars under monthly abbreviations represent periods when frost can occur.

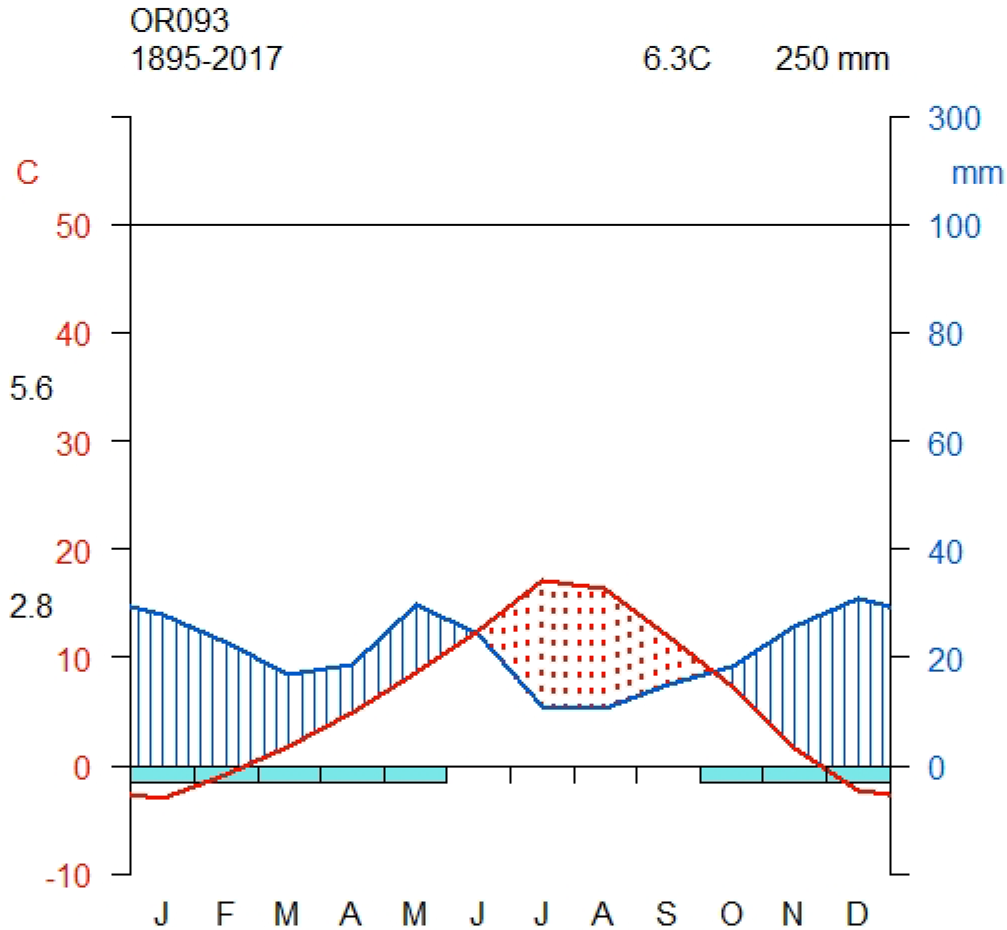

Figure S2.2.- Climograph for site OR093 derived from PRISM climate data from the years 1895-2017. Blue line represents mean monthly precipitation in millimeters. Redline represents mean monthly temperature in degrees Celsius. Red dotted area represents the dry period. Cyan colored bars under monthly abbreviations represent periods when frost can occur.

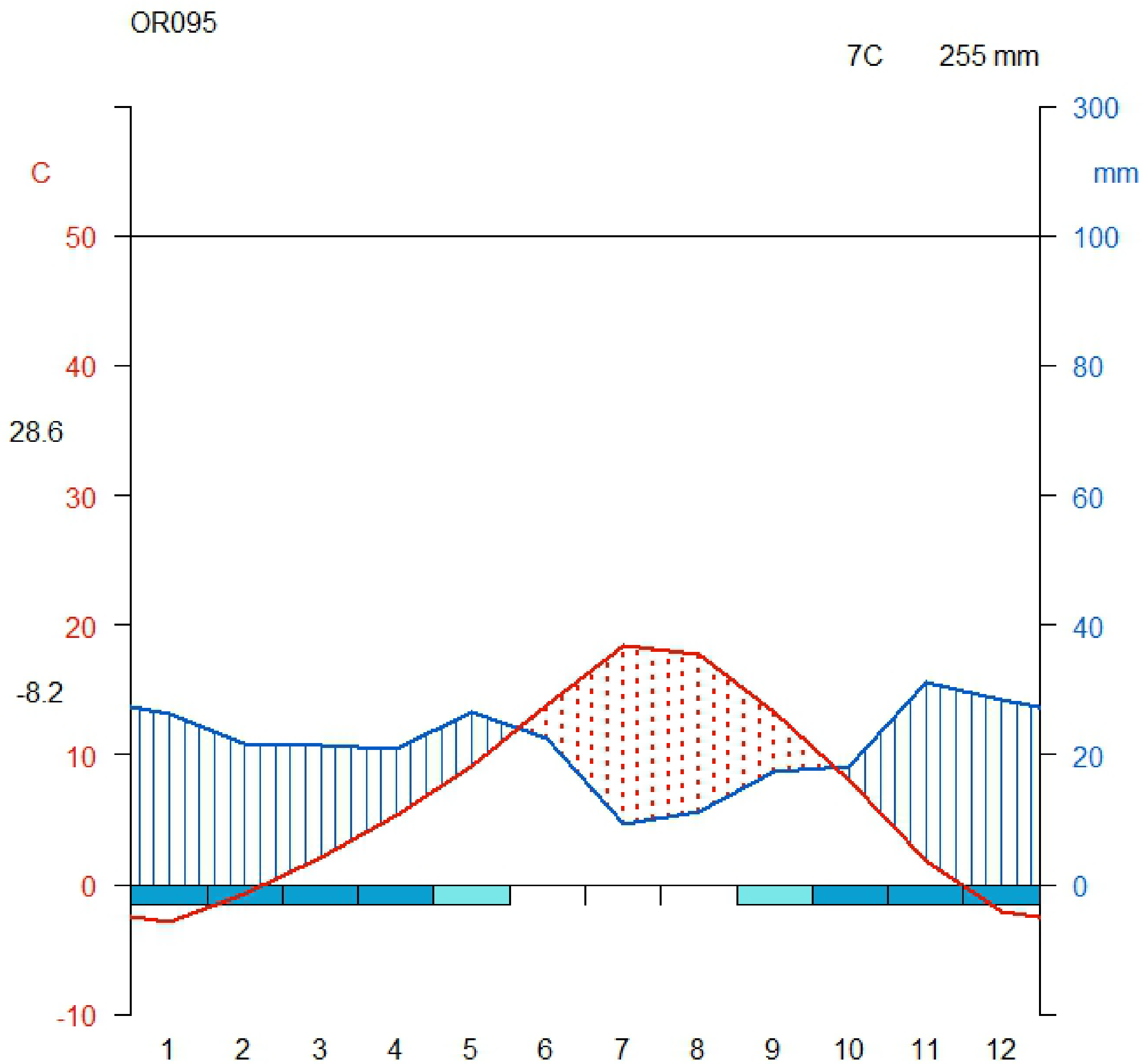

Figure S2.3.- Climograph for site OR095 derived from PRISM climate data from the years 1895-2017. Blue line represents mean monthly precipitation in millimeters. Redline represents mean monthly temperature in degrees Celsius. Red dotted area represents the dry period. Cyan colored bars under monthly abbreviations represent periods when frost can occur.

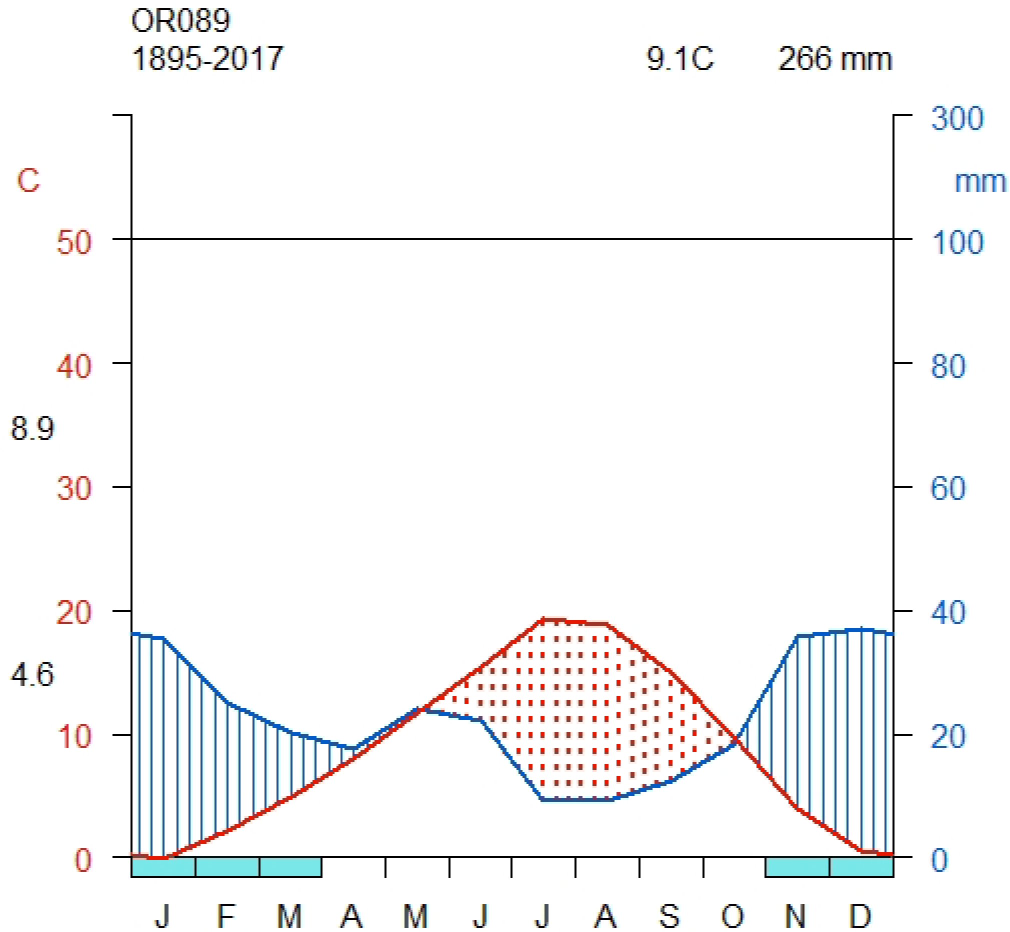

Figure S2.4.- Climograph for site OR089 derived from PRISM climate data from the years 1895-2017. Blue line represents mean monthly precipitation in millimeters. Redline represents mean monthly temperature in degrees Celsius. Red dotted area represents the dry period. Cyan colored bars under monthly abbreviations represent periods when frost can occur.

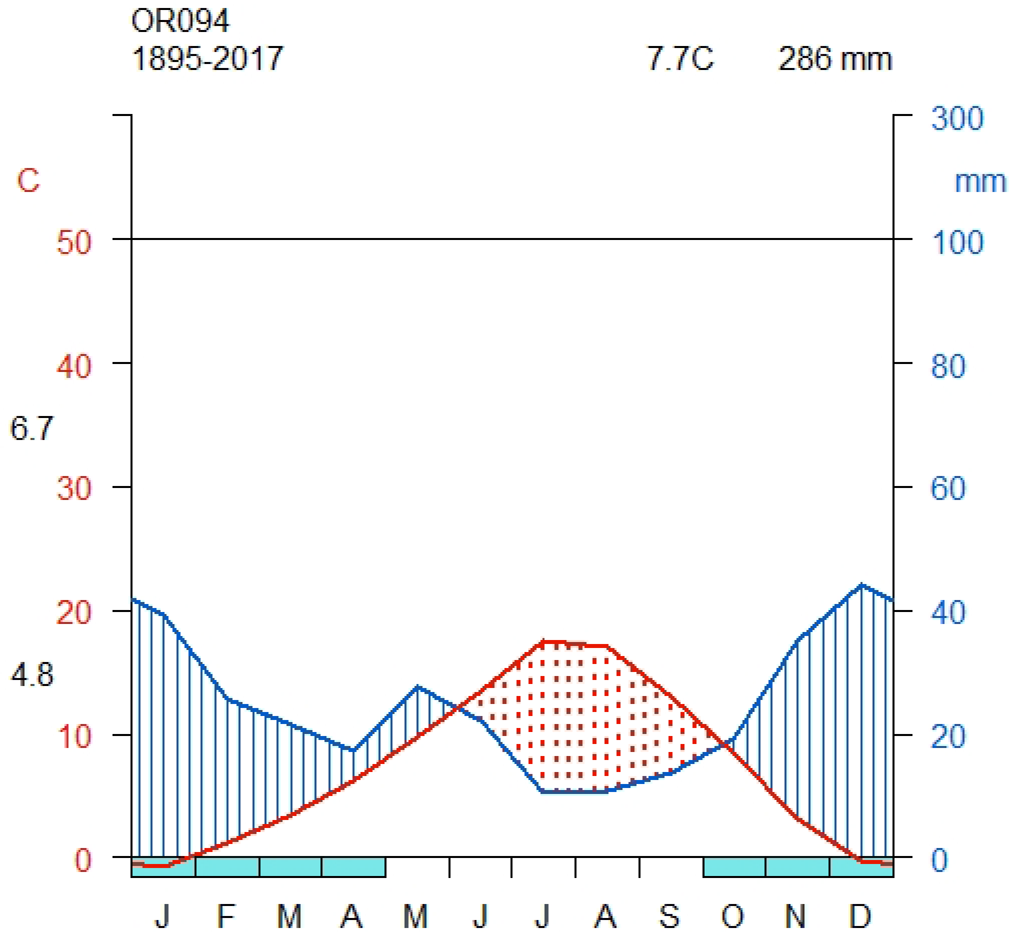

Figure S2.5.- Climograph for site OR094 derived from PRISM climate data from the years 1895-2017. Blue line represents mean monthly precipitation in millimeters. Redline represents mean monthly temperature in degrees Celsius. Red dotted area represents the dry period. Cyan colored bars under monthly abbreviations represent periods when frost can occur.

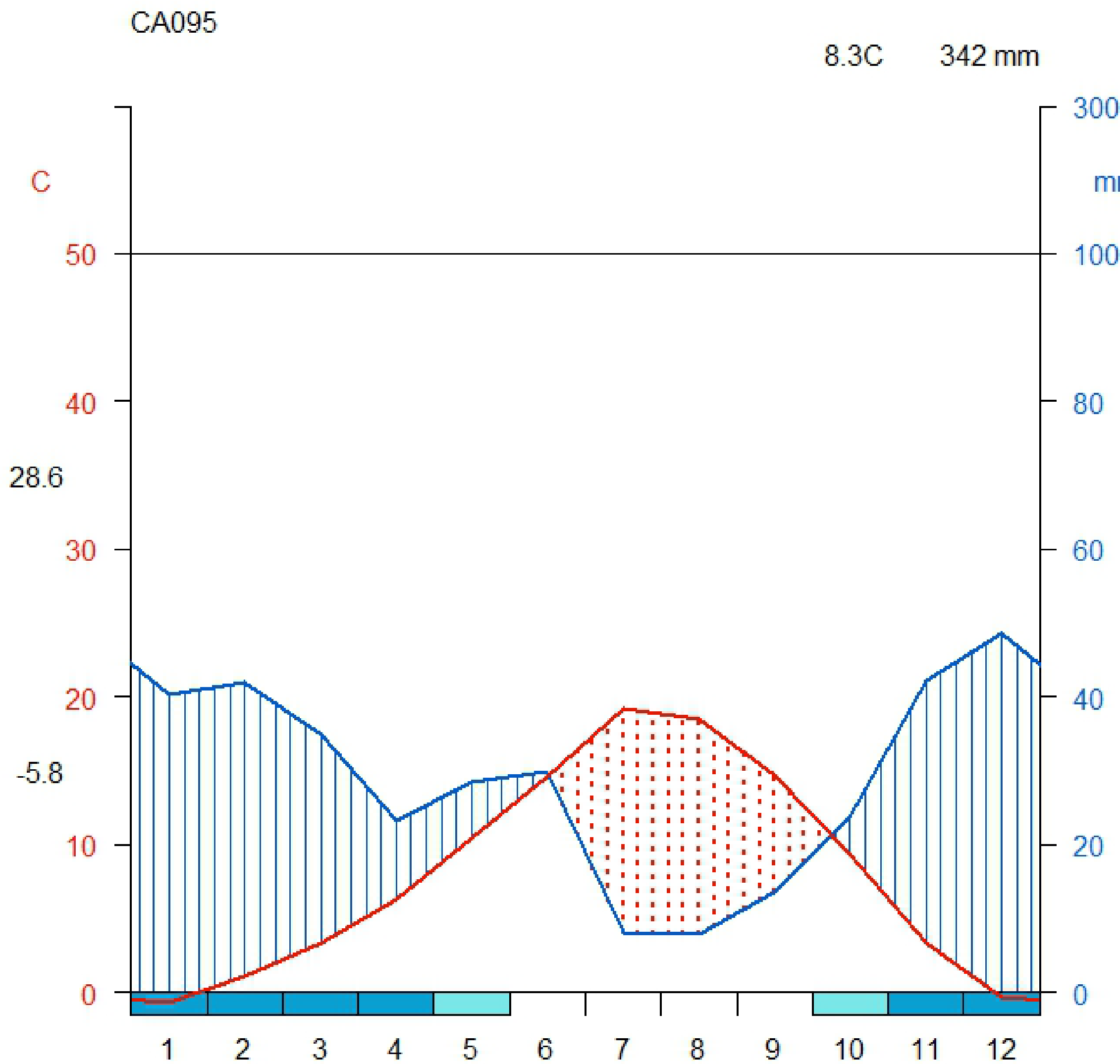

Figure S2.6.- Climograph for site CA095 derived from PRISM climate data from the years 1895-2017. Blue line represents mean monthly precipitation in millimeters. Redline represents mean monthly temperature in degrees Celsius. Red dotted area represents the dry period. Cyan colored bars under monthly abbreviations represent periods when frost can occur.

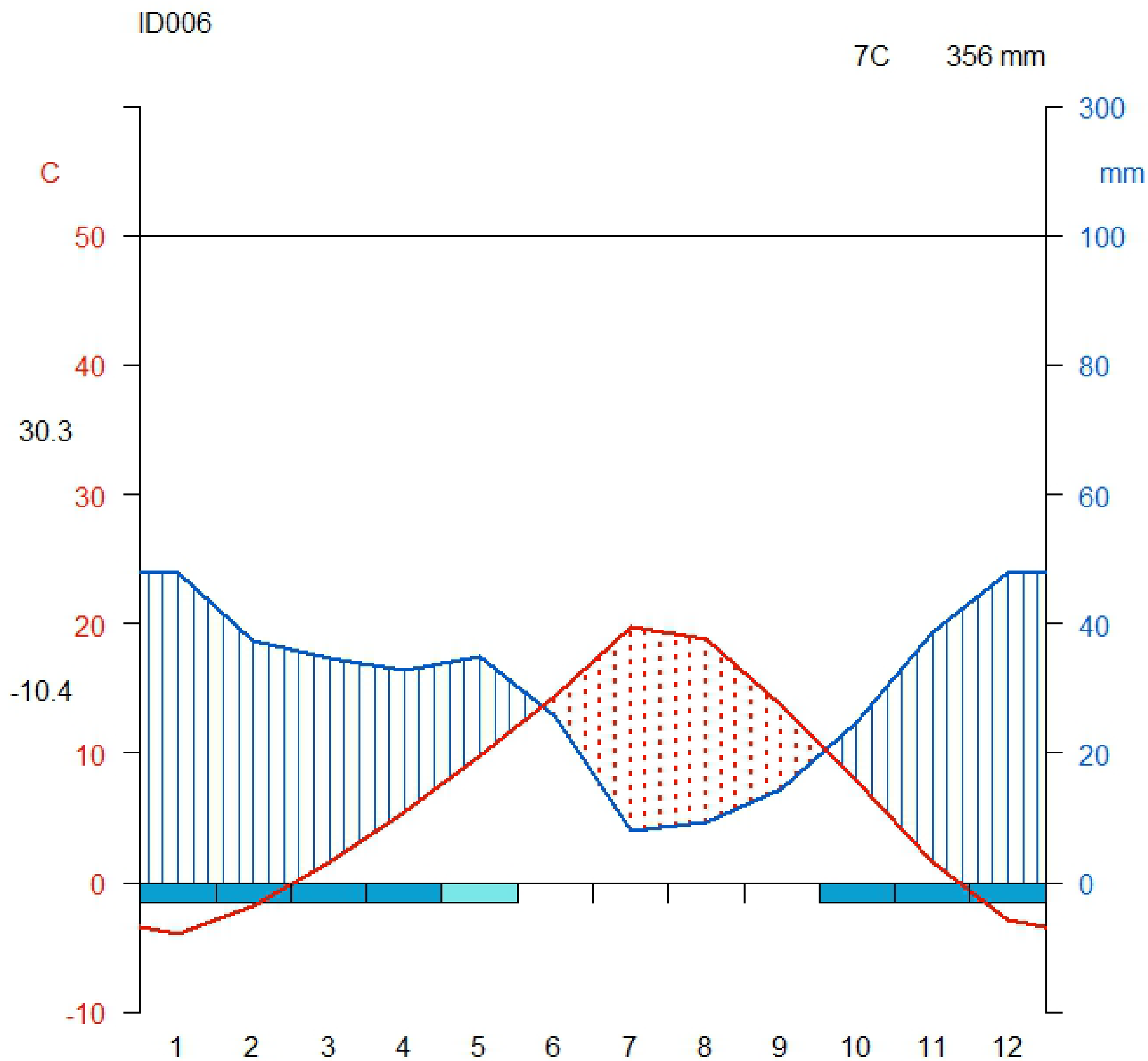

Figure S2.7.- Climograph for site ID006 derived from PRISM climate data from the years 1895-2017. Blue line represents mean monthly precipitation in millimeters. Redline represents mean monthly temperature in degrees Celsius. Red dotted area represents the dry period. Cyan colored bars under monthly abbreviations represent periods when frost can occur.

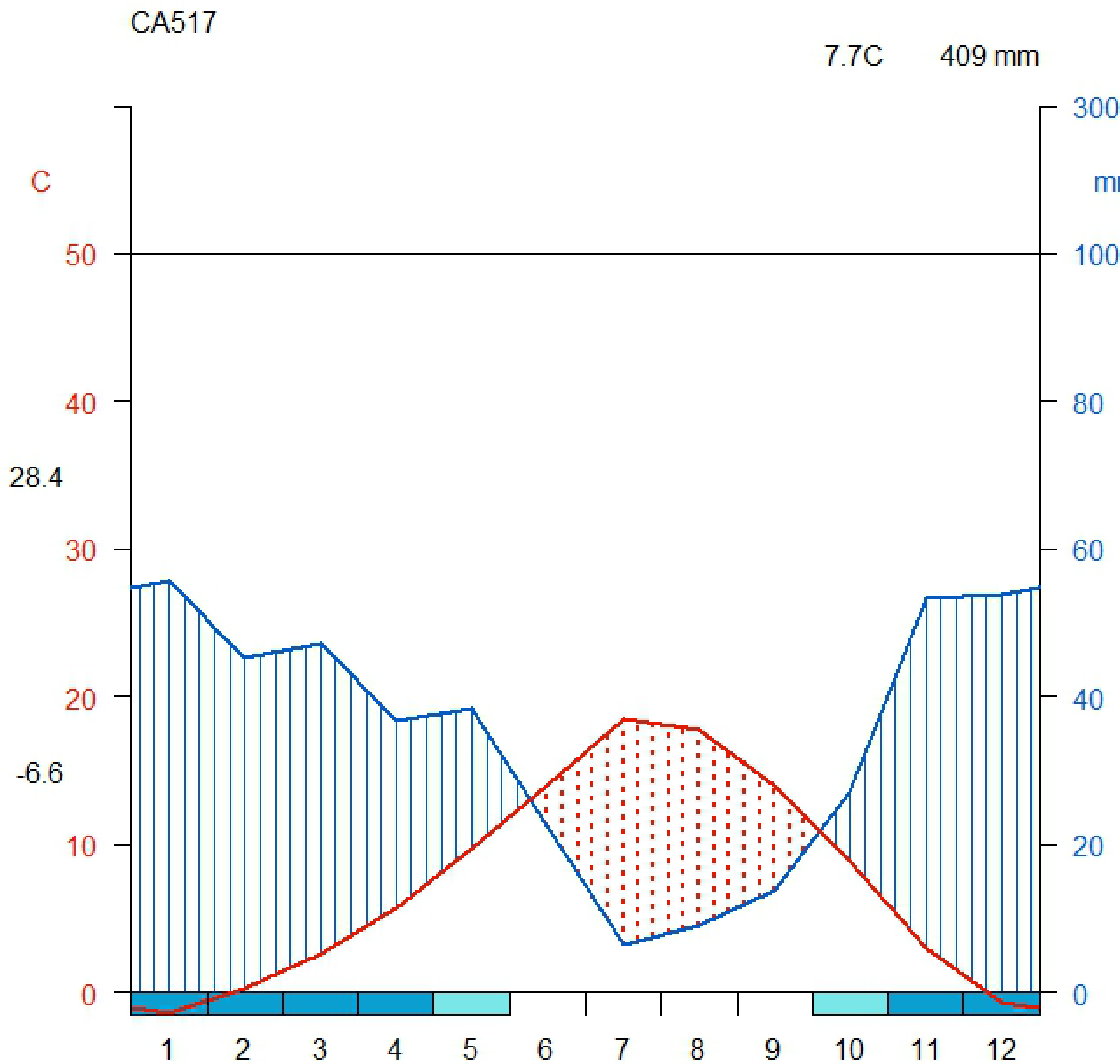

Figure S2.8.- Climograph for site CA517 derived from PRISM climate data from the years 1895-2017. Blue line represents mean monthly precipitation in millimeters. Redline represents mean monthly temperature in degrees Celsius. Red dotted area represents the dry period. Cyan colored bars under monthly abbreviations represent periods when frost can occur.

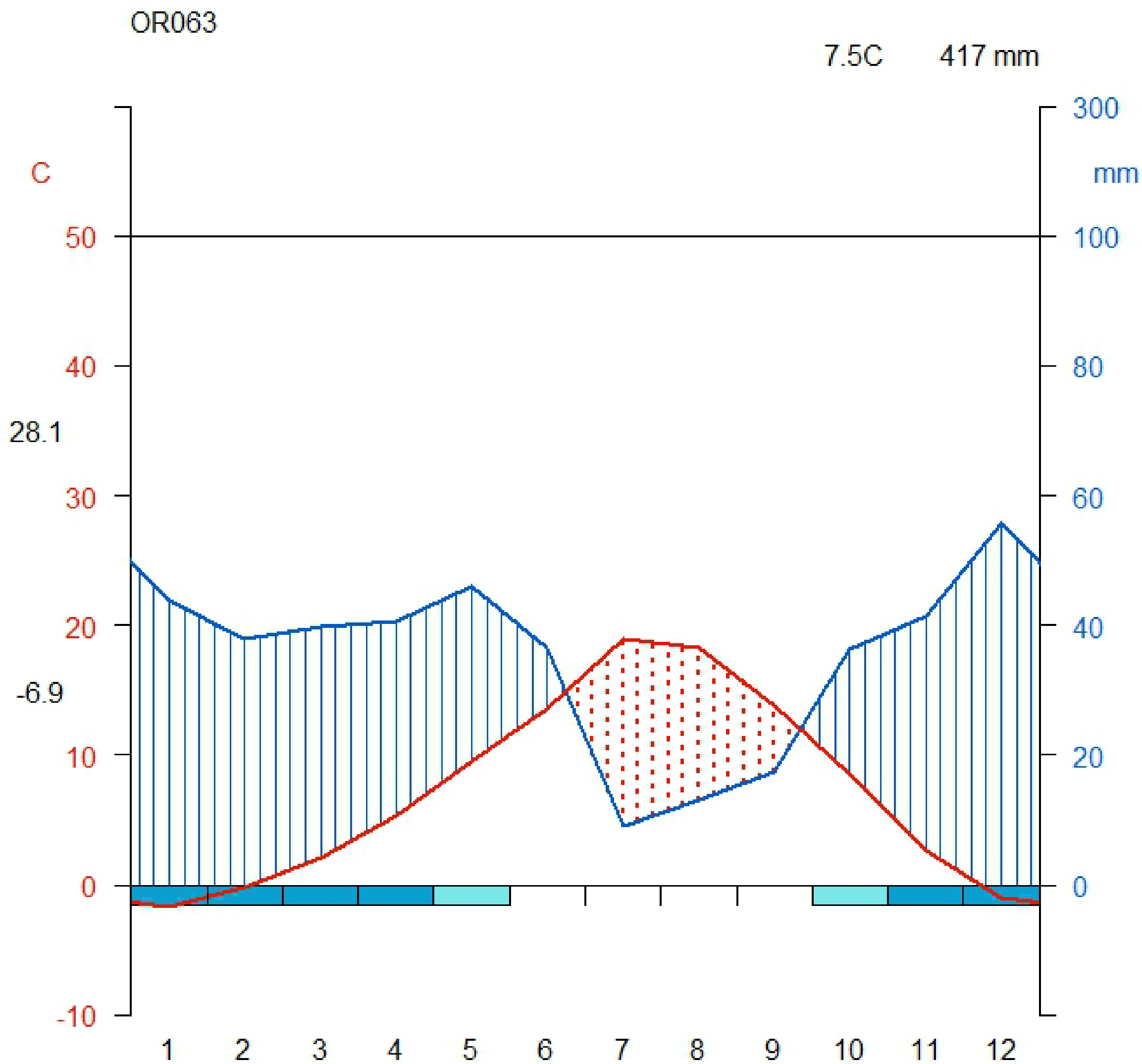

Figure S2.9.- Climograph for site OR063 derived from PRISM climate data from the years 1895-2017. Blue line represents mean monthly precipitation in millimeters. Redline represents mean monthly temperature in degrees Celsius. Red dotted area represents the dry period. Cyan colored bars under monthly abbreviations represent periods when frost can occur.

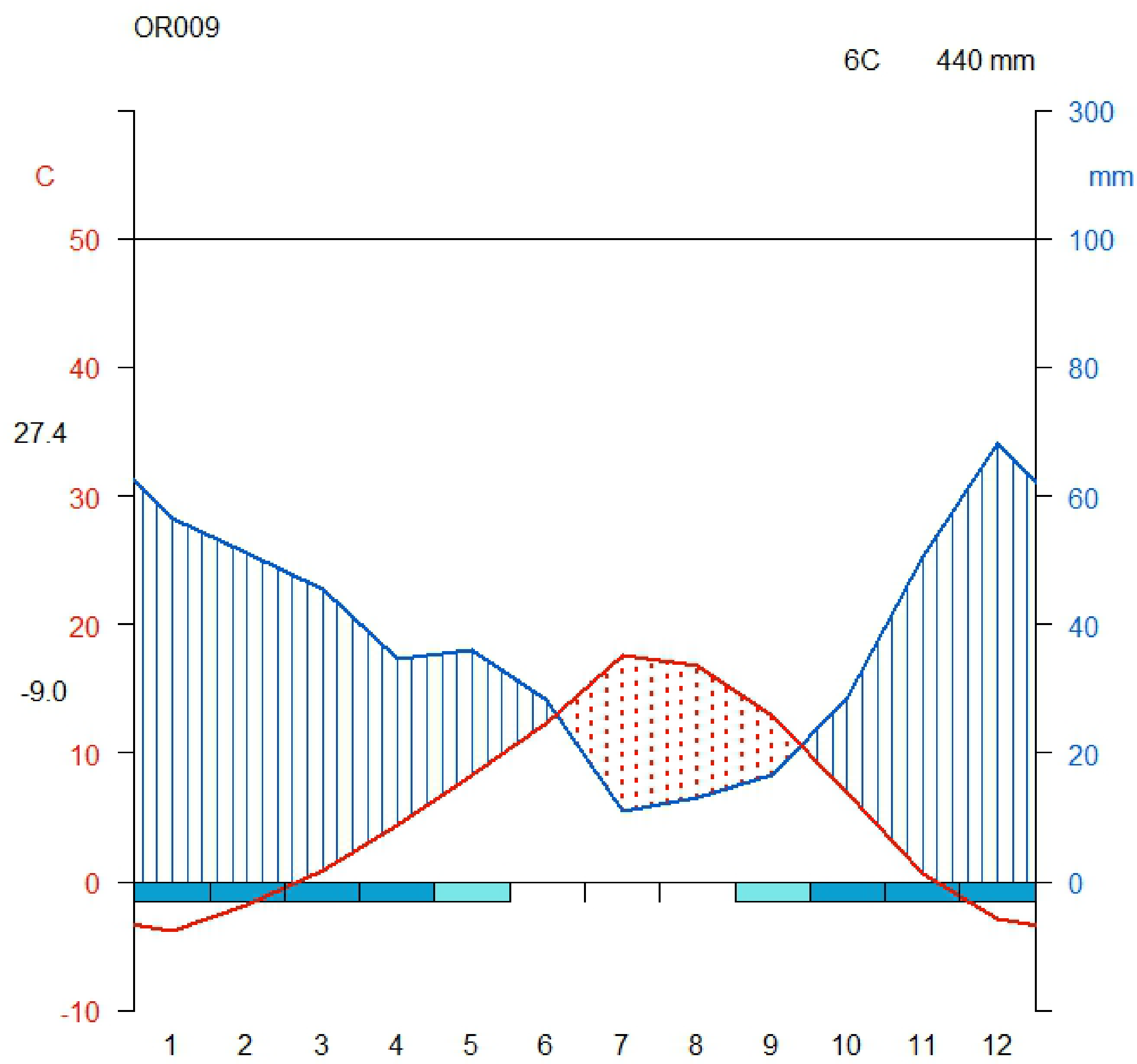

Figure S2.10.- Climograph for site OR009 derived from PRISM climate data from the years 1895-2017. Blue line represents mean monthly precipitation in millimeters. Redline represents mean monthly temperature in degrees Celsius. Red dotted area represents the dry period. Cyan colored bars under monthly abbreviations represent periods when frost can occur.

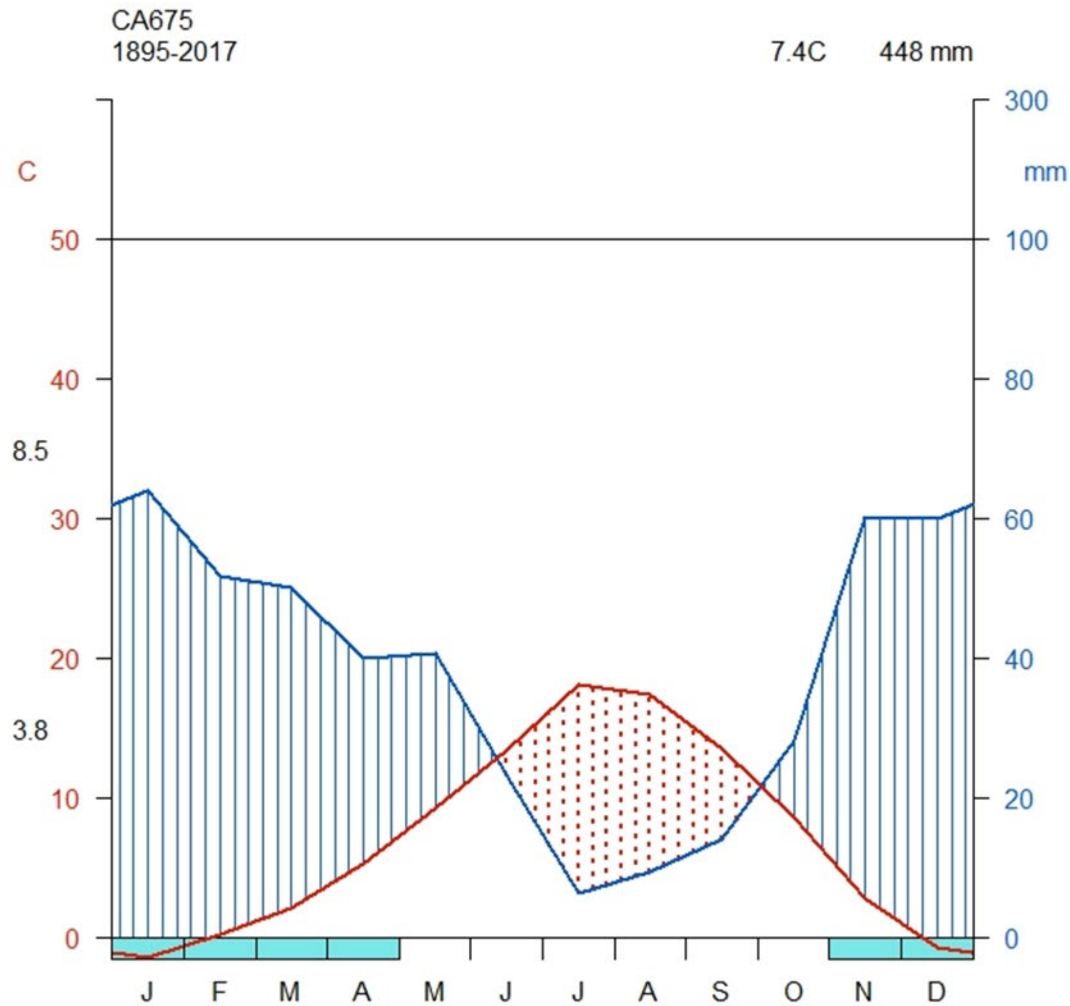

Figure S2.11.- Climograph for site CA675 for years 1895-2017. Blue line represents mean monthly precipitation in millimeters. Redline represents mean monthly temperature in degrees Celsius. Red dotted area represents the dry period. Cyan colored bars under monthly abbreviations represent periods when frost can occur.

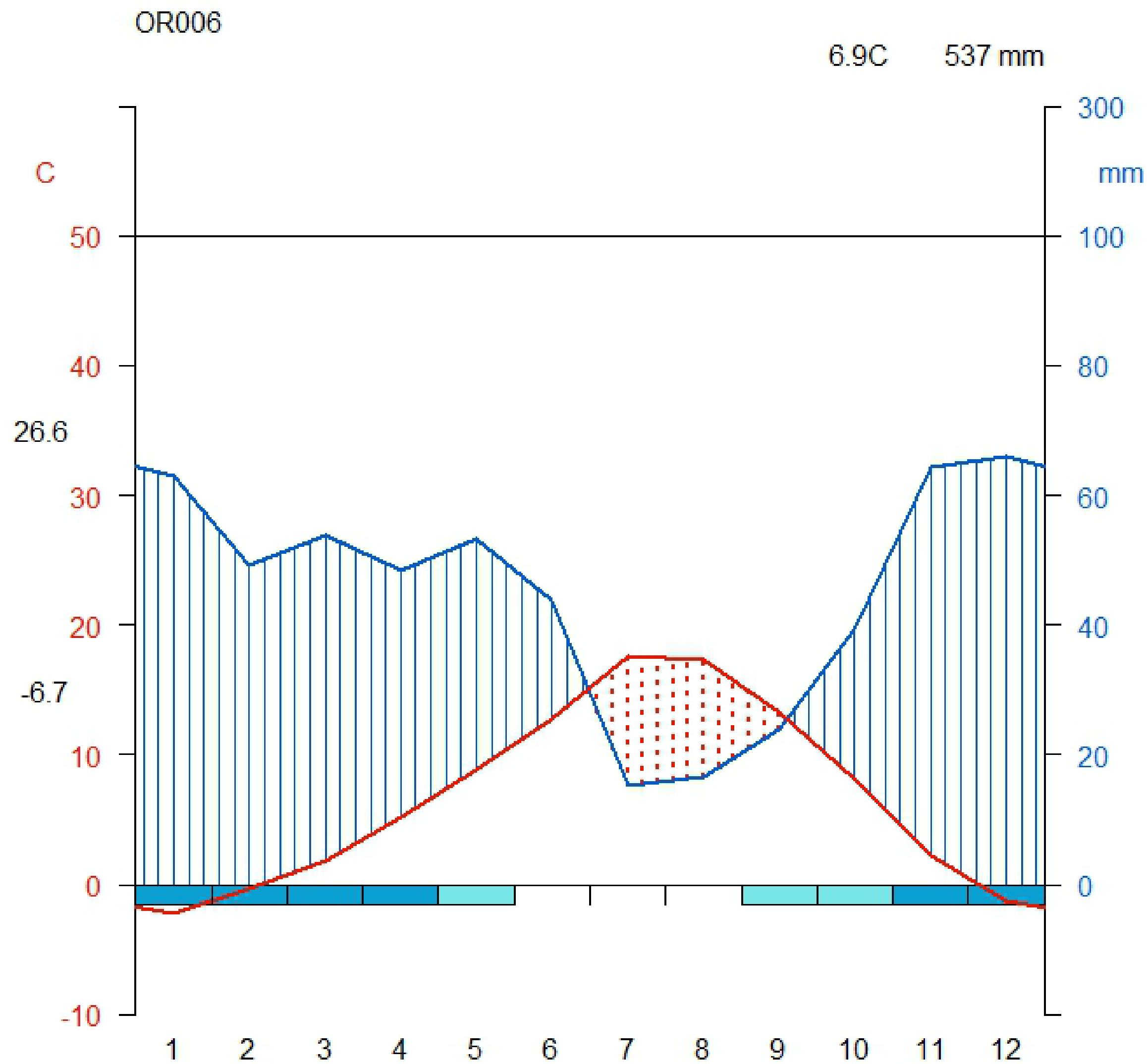

Figure S2.12.- Climograph for site OR006 derived from PRISM climate data from the years 1895-2017. Blue line represents mean monthly precipitation in millimeters. Redline represents mean monthly temperature in degrees Celsius. Red dotted area represents the dry period. Cyan colored bars under monthly abbreviations represent periods when frost can occur.

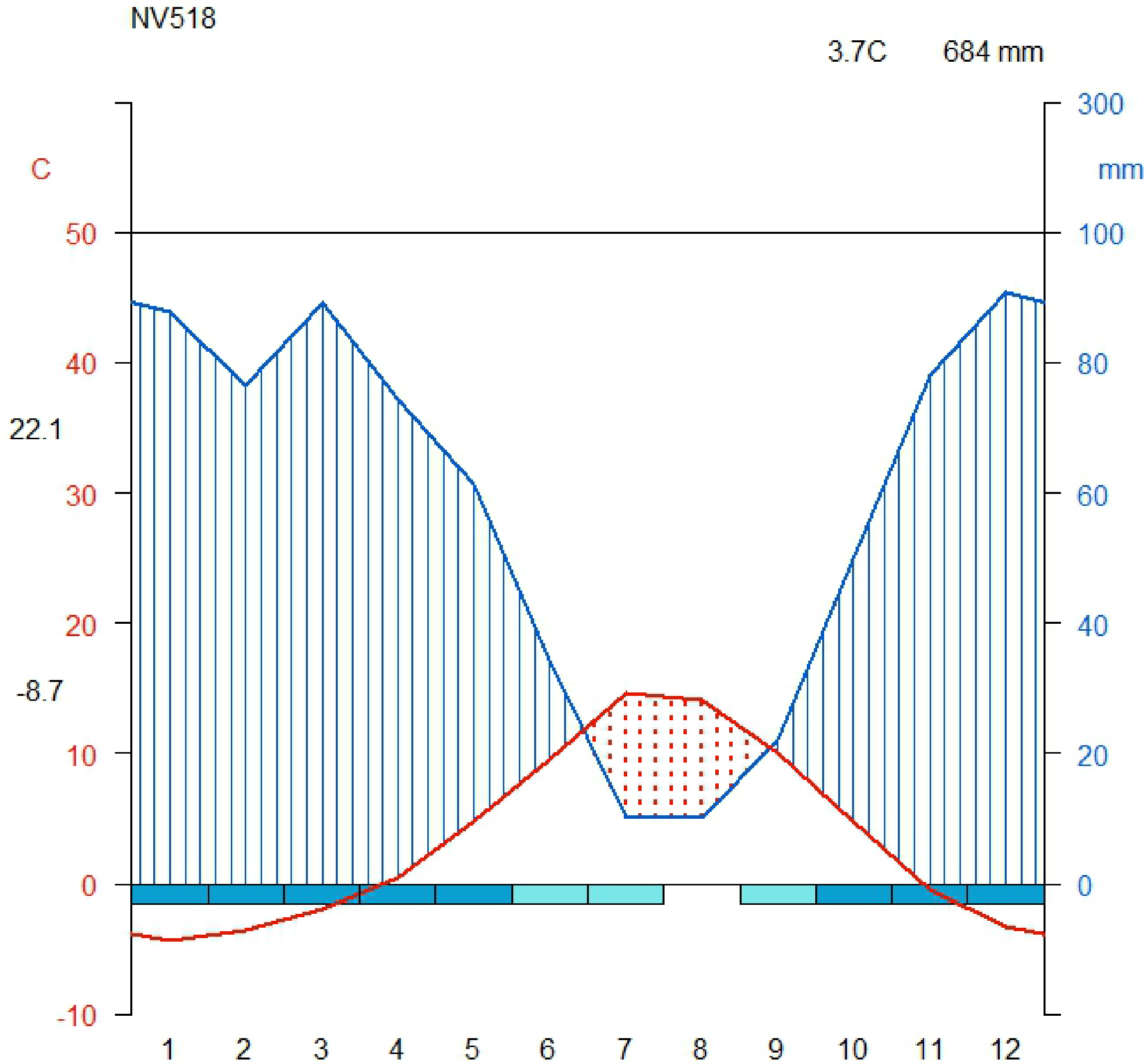

Figure S2.13.- Climograph for site NV518 derived from PRISM climate data from the years 1895-2017. Blue line represents mean monthly precipitation in millimeters. Redline represents mean monthly temperature in degrees Celsius. Red dotted area represents the dry period. Cyan colored bars under monthly abbreviations represent periods when frost can occur.

APPENDIX B

SUPPLEMENTARY MATERIAL FROM CHAPTER IV

Table S4.1.- ANVOVA tables for site OR092. Climate abbreviations for composite climate variables are as follows: June through September precipitation (JSP), June through September temperature (JST), February through March precipitation (FMP), February through March temperature (FMT), previous October through current January precipitation (OJP), previous October through current January temperature (OJT).

OR092

```
JSP
             Df Sum Sq Mean Sq F value Pr(>F)
Year          1 0.1337 0.13365   5.058 0.0268 *
CO2fert       1 0.0217 0.02173   0.822 0.3668
Year:CO2fert  1 0.0281 0.02809   1.063 0.3051
Residuals    97 2.5632 0.02643

JST

             Df Sum Sq Mean Sq F value   Pr(>F)
Year          1 0.0159  0.0159   0.907    0.343
CO2fert       1 0.3408  0.3408  19.440 2.68e-05 ***
Year:CO2fert  1 0.0071  0.0071   0.404    0.527
Residuals    97 1.7002  0.0175

FMP
             Df Sum Sq Mean Sq F value   Pr(>F)
Year          1 0.9350  0.9350  43.380 2.33e-09 ***
CO2fert       1 0.0335  0.0335   1.554 0.215583
Year:CO2fert  1 0.3005  0.3005  13.943 0.000318 ***
Residuals    97 2.0906  0.0216

FMT
             Df Sum Sq Mean Sq F value   Pr(>F)
Year          1 0.0514  0.0514   2.509 0.116421
CO2fert       1 0.4423  0.4423  21.580 1.07e-05 ***
Year:CO2fert  1 0.2426  0.2426  11.835 0.000859 ***
Residuals    97 1.9880  0.0205

OJP
             Df Sum Sq Mean Sq F value  Pr(>F)
Year          1 0.1269  0.1269   7.835 0.00618 **
CO2fert       1 0.0039  0.0039   0.243 0.62349
Year:CO2fert  1 0.8433  0.8433  52.057 1.2e-10 ***
Residuals    97 1.5714  0.0162

OJT
             Df Sum Sq Mean Sq F value   Pr(>F)
Year          1 0.1424 0.14244   8.601 0.004191 **
CO2fert       1 0.2211 0.22109  13.351 0.000419 ***
Year:CO2fert  1 0.0372 0.03724   2.249 0.136950
Residuals    97 1.6063 0.01656
---
Signif. codes:  0 '***' 0.001 '**' 0.01 '*' 0.05 '.' 0.1 ' ' 1
```

Table S4.2.- ANVOVA tables for site OR093. Climate abbreviations for composite climate variables are as follows: June through September precipitation (JSP), June through September temperature (JST), February through March precipitation (FMP), February through March temperature (FMT), previous October through current January precipitation (OJP), previous October through current January temperature (OJT).

```
OR093

JSP
             Df Sum Sq Mean Sq F value Pr(>F)
Year          1 0.1337 0.13365   5.058 0.0268 *
CO2fert       1 0.0217 0.02173   0.822 0.3668
Year:CO2fert  1 0.0281 0.02809   1.063 0.3051
Residuals    97 2.5632 0.02643
JST
             Df Sum Sq Mean Sq F value  Pr(>F)
Year          1 0.2648 0.26483   9.724 0.00239 **
CO2fert       1 0.0666 0.06662   2.446 0.12107
Year:CO2fert  1 0.0196 0.01963   0.721 0.39798
Residuals    97 2.6419 0.02724

FMP
             Df Sum Sq Mean Sq F value   Pr(>F)
Year          1 0.9350  0.9350  43.380 2.33e-09 ***
CO2fert       1 0.0335  0.0335   1.554 0.215583
Year:CO2fert  1 0.3005  0.3005  13.943 0.000318 ***
Residuals    97 2.0906  0.0216

FMT
             Df Sum Sq Mean Sq F value   Pr(>F)
Year          1 0.0514  0.0514   2.509 0.116421
CO2fert       1 0.4423  0.4423  21.580 1.07e-05 ***
Year:CO2fert  1 0.2426  0.2426  11.835 0.000859 ***
Residuals    97 1.9880  0.0205

OJP
             Df Sum Sq Mean Sq F value  Pr(>F)
Year          1 0.1269  0.1269   7.835 0.00618 **
CO2fert       1 0.0039  0.0039   0.243 0.62349
Year:CO2fert  1 0.8433  0.8433  52.057 1.2e-10 ***
Residuals    97 1.5714  0.0162

OJT
             Df Sum Sq Mean Sq F value   Pr(>F)
Year          1 0.1424 0.14244   8.601 0.004191 **
CO2fert       1 0.2211 0.22109  13.351 0.000419 ***
Year:CO2fert  1 0.0372 0.03724   2.249 0.136950
Residuals    97 1.6063 0.01656
---
Signif. codes:  0 '***' 0.001 '**' 0.01 '*' 0.05 '.' 0.1 ' ' 1
```

Table S4.3.- ANVOVA tables for site OR095. Climate abbreviations for composite climate variables are as follows: June through September precipitation (JSP), June through September temperature (JST), February through March precipitation (FMP), February through March temperature (FMT), previous October through current January precipitation (OJP), previous October through current January temperature (OJT).

OR095

```
JSP
             Df Sum Sq Mean Sq F value   Pr(>F)    
Year          1 0.0676  0.0676   2.991  0.08691 .  
CO2fert       1 0.1753  0.1753   7.760  0.00642 ** 
Year:CO2fert  1 0.4827  0.4827  21.363 1.17e-05 ***
Residuals    97 2.1916  0.0226                     

JST
             Df Sum Sq Mean Sq F value  Pr(>F)    
Year          1 0.1124 0.11236   4.930 0.02873 *  
CO2fert       1 0.3008 0.30081  13.198 0.00045 ***
Year:CO2fert  1 0.0882 0.08816   3.868 0.05207 .  
Residuals    97 2.2108 0.02279                    

FMP
             Df Sum Sq Mean Sq F value   Pr(>F)    
Year          1 0.5329  0.5329   29.41 4.29e-07 ***
CO2fert       1 0.3873  0.3873   21.38 1.17e-05 ***
Year:CO2fert  1 0.1972  0.1972   10.88  0.00136 ** 
Residuals    97 1.7577  0.0181                     

FMT
             Df Sum Sq Mean Sq F value   Pr(>F)    
Year          1 0.0138  0.0138   0.679   0.4121    
CO2fert       1 0.4691  0.4691  23.004 5.84e-06 ***
Year:CO2fert  1 0.0862  0.0862   4.226   0.0425 *  
Residuals    97 1.9779  0.0204                     

OJP
             Df Sum Sq Mean Sq F value   Pr(>F)    
Year          1 0.0002  0.0002   0.009    0.923    
CO2fert       1 0.1098  0.1098   4.334    0.040 *  
Year:CO2fert  1 1.5694  1.5694  61.932 5.07e-12 ***
Residuals    97 2.4580  0.0253                     

OJT
             Df Sum Sq Mean Sq F value  Pr(>F)    
Year          1 0.3467  0.3467  19.901 2.2e-05 ***
CO2fert       1 0.1500  0.1500   8.610 0.00417 ** 
Year:CO2fert  1 0.0810  0.0810   4.648 0.03357 *  
Residuals    97 1.6901  0.0174                    
---
Signif. codes:  0 '***' 0.001 '**' 0.01 '*' 0.05 '.' 0.1 ' ' 1
```

Table S4.4.- ANVOVA tables for site OR089. Climate abbreviations for composite climate variables are as follows: June through September precipitation (JSP), June through September temperature (JST), February through March precipitation (FMP), February through March temperature (FMT), previous October through current January precipitation (OJP), previous October through current January temperature (OJT).

OR089

```
JSP
             Df Sum Sq Mean Sq F value   Pr(>F)    
Year          1 0.5452  0.5452   71.72 7.54e-13 ***
CO2fert       1 0.1264  0.1264   16.62 0.000104 ***
Year:CO2fert  1 0.0926  0.0926   12.18 0.000776 ***
Residuals    83 0.6310  0.0076                     

JST
             Df Sum Sq Mean Sq F value   Pr(>F)    
Year          1 0.2373  0.2373   9.087  0.00341 ** 
CO2fert       1 0.0028  0.0028   0.107  0.74385    
Year:CO2fert  1 0.5476  0.5476  20.966 1.63e-05 ***
Residuals    83 2.1676  0.0261                     
FMP

             Df Sum Sq Mean Sq F value   Pr(>F)    
Year          1 0.1303  0.1303   11.92 0.000876 ***
CO2fert       1 0.4582  0.4582   41.94 6.27e-09 ***
Year:CO2fert  1 0.1642  0.1642   15.03 0.000211 ***
Residuals    83 0.9068  0.0109                     

FMT
             Df Sum Sq Mean Sq F value   Pr(>F)    
Year          1 0.0705  0.0705   3.418 0.068055 .  
CO2fert       1 0.3400  0.3400  16.475 0.000111 ***
Year:CO2fert  1 0.0025  0.0025   0.120 0.729474    
Residuals    83 1.7127  0.0206                     

OJP
             Df Sum Sq Mean Sq F value   Pr(>F)    
Year          1 0.7898  0.7898   71.19 8.73e-13 ***
CO2fert       1 0.1483  0.1483   13.37 0.000448 ***
Year:CO2fert  1 0.5333  0.5333   48.07 8.25e-10 ***
Residuals    83 0.9208  0.0111                     

OJT

             Df Sum Sq Mean Sq F value  Pr(>F)    
Year          1 0.4862  0.4862  51.459 2.8e-10 ***
CO2fert       1 0.0175  0.0175   1.855   0.177    
Year:CO2fert  1 0.0507  0.0507   5.365   0.023 *  
Residuals    83 0.7842  0.0094                    
---
Signif. codes:  0 ‘***’ 0.001 ‘**’ 0.01 ‘*’ 0.05 ‘.’ 0.1 ‘ ’ 1
```

Table S4.5.- ANVOVA tables for site OR094. Climate abbreviations for composite climate variables are as follows: June through September precipitation (JSP), June through September temperature (JST), February through March precipitation (FMP), February through March temperature (FMT), previous October through current January precipitation (OJP), previous October through current January temperature (OJT).

OR094

```
JSP
             Df Sum Sq Mean Sq F value Pr(>F)
Year          1 0.0599 0.05988   2.801 0.0974 .
CO2fert       1 0.1215 0.12153   5.684 0.0191 *
Year:CO2fert  1 0.0598 0.05981   2.797 0.0977 .
Residuals    97 2.0741 0.02138

JST
             Df Sum Sq Mean Sq F value Pr(>F)
Year          1 0.0409 0.04087   1.919 0.1691
CO2fert       1 0.1278 0.12781   6.002 0.0161 *
Year:CO2fert  1 0.0586 0.05861   2.752 0.1003
Residuals    97 2.0655 0.02129

FMP
             Df Sum Sq Mean Sq F value   Pr(>F)
Year          1 0.0105 0.01045   0.474 0.492613
CO2fert       1 0.2986 0.29855  13.548 0.000382 ***
Year:CO2fert  1 0.2822 0.28216  12.804 0.000542 ***
Residuals    97 2.1375 0.02204

FMT
             Df Sum Sq Mean Sq F value   Pr(>F)
Year          1 0.0113  0.0113   0.432    0.513
CO2fert       1 0.5563  0.5563  21.199 1.26e-05 ***
Year:CO2fert  1 0.0391  0.0391   1.491    0.225
Residuals    97 2.5456  0.0262

OJP

             Df Sum Sq Mean Sq F value Pr(>F)
Year          1 0.0438  0.0438   4.661 0.0333 *
CO2fert       1 0.0030  0.0030   0.318 0.5739
Year:CO2fert  1 1.3770  1.3770 146.607 <2e-16 ***
Residuals    97 0.9111  0.0094

OJT
             Df Sum Sq Mean Sq F value Pr(>F)
Year          1 0.1246 0.12462   4.118 0.0452 *
CO2fert       1 0.1843 0.18426   6.088 0.0154 *
Year:CO2fert  1 0.0905 0.09046   2.989 0.0870 .
Residuals    97 2.9358 0.03027
---
Signif. codes:  0 ‘***’ 0.001 ‘**’ 0.01 ‘*’ 0.05 ‘.’ 0.1 ‘ ’ 1
```

Table S4.6.- ANVOVA tables for site CA095. Climate abbreviations for composite climate variables are as follows: June through September precipitation (JSP), June through September temperature (JST), February through March precipitation (FMP), February through March temperature (FMT), previous October through current January precipitation (OJP), previous October through current January temperature (OJT).

```
CA095

JSP
             Df Sum Sq Mean Sq F value   Pr(>F)
Year          1 0.0019  0.0019   0.192   0.6629
CO2fert       1 0.0711  0.0711   7.119   0.0095 **
Year:CO2fert  1 0.3460  0.3460  34.654 1.29e-07 ***
Residuals    69 0.6890  0.0100

JST

             Df Sum Sq Mean Sq F value   Pr(>F)
Year          1 0.2360  0.2360   15.24 0.000217 ***
CO2fert       1 0.7090  0.7090   45.78 3.52e-09 ***
Year:CO2fert  1 0.3902  0.3902   25.20 3.87e-06 ***
Residuals    69 1.0685  0.0155

FMP
             Df Sum Sq Mean Sq F value Pr(>F)
Year          1 0.0369 0.03687   5.230 0.0253 *
CO2fert       1 0.0366 0.03658   5.188 0.0259 *
Year:CO2fert  1 0.0080 0.00803   1.139 0.2896
Residuals    69 0.4865 0.00705

FMT
             Df Sum Sq Mean Sq F value   Pr(>F)
Year          1 0.3023 0.30226  31.473 3.89e-07 ***
CO2fert       1 0.0717 0.07168   7.464  0.00799 **
Year:CO2fert  1 0.0273 0.02732   2.845  0.09617 .
Residuals    69 0.6627 0.00960

OJP
             Df Sum Sq Mean Sq F value   Pr(>F)
Year          1 1.0632  1.0632  49.049 1.31e-09 ***
CO2fert       1 0.0060  0.0060   0.278    0.600
Year:CO2fert  1 0.0167  0.0167   0.772    0.383
Residuals    69 1.4956  0.0217

OJT
             Df Sum Sq Mean Sq F value  Pr(>F)
Year          1 0.0441 0.04405   2.754 0.10155
CO2fert       1 0.1609 0.16087  10.058 0.00226 **
Year:CO2fert  1 0.0436 0.04359   2.725 0.10332
Residuals    69 1.1036 0.01599
---
Signif. codes:  0 '***' 0.001 '**' 0.01 '*' 0.05 '.' 0.1 ' ' 1
```

Table S4.7.- ANVOVA tables for site ID006. Climate abbreviations for composite climate variables are as follows: June through September precipitation (JSP), June through September temperature (JST), February through March precipitation (FMP), February through March temperature (FMT), previous October through current January precipitation (OJP), previous October through current January temperature (OJT).

ID006

```
JSP
             Df Sum Sq Mean Sq F value  Pr(>F)
Year          1 0.0000 0.00001   0.001 0.97938
CO2fert       1 0.0031 0.00305   0.174 0.67761
Year:CO2fert  1 0.1313 0.13129   7.497 0.00781 **
Residuals    71 1.2434 0.01751

JST
             Df Sum Sq Mean Sq F value   Pr(>F)
Year          1 0.1767 0.17666  11.794 0.000996 ***
CO2fert       1 0.0227 0.02271   1.516 0.222270
Year:CO2fert  1 0.0415 0.04151   2.771 0.100365
Residuals    71 1.0634 0.01498

FMP
             Df Sum Sq Mean Sq F value   Pr(>F)
Year          1 1.0044  1.0044  151.17  < 2e-16 ***
CO2fert       1 0.2491  0.2491   37.49 4.55e-08 ***
Year:CO2fert  1 0.7287  0.7287  109.67 4.78e-16 ***
Residuals    71 0.4717  0.0066

FMT
             Df Sum Sq Mean Sq F value Pr(>F)
Year          1 0.0477 0.04767   4.459 0.0382 *
CO2fert       1 0.0553 0.05535   5.178 0.0259 *
Year:CO2fert  1 0.0678 0.06784   6.346 0.0140 *
Residuals    71 0.7590 0.01069

OJP
             Df Sum Sq Mean Sq F value   Pr(>F)
Year          1 0.5038  0.5038   16.66 0.000115 ***
CO2fert       1 0.4054  0.4054   13.41 0.000479 ***
Year:CO2fert  1 0.5931  0.5931   19.62 3.36e-05 ***
Residuals    71 2.1466  0.0302

OJT
             Df Sum Sq Mean Sq F value  Pr(>F)
Year          1 0.9392  0.9392 144.371 < 2e-16 ***
CO2fert       1 0.3741  0.3741  57.501 9.9e-11 ***
Year:CO2fert  1 0.0152  0.0152   2.336   0.131
Residuals    71 0.4619  0.0065
---
Signif. codes:  0 â€˜***â€™ 0.001 â€˜**â€™ 0.01 â€˜*â€™ 0.05 â€˜.â€™ 0.1
â€˜ â€™ 1
```

Table S4.8.- ANVOVA tables for site CA517. Climate abbreviations for composite climate variables are as follows: June through September precipitation (JSP), June through September temperature (JST), February through March precipitation (FMP), February through March temperature (FMT), previous October through current January precipitation (OJP), previous October through current January temperature (OJT).

CA517

```
JSP
             Df Sum Sq Mean Sq F value   Pr(>F)    
Year          1 1.0661  1.0661 110.632 7.96e-16 ***
CO2fert       1 0.0012  0.0012   0.129     0.72    
Year:CO2fert  1 0.2821  0.2821  29.270 9.10e-07 ***
Residuals    67 0.6456  0.0096                     

JST
             Df Sum Sq Mean Sq F value  Pr(>F)   
Year          1 0.0248 0.02476   2.514 0.11754   
CO2fert       1 0.0021 0.00209   0.212 0.64656   
Year:CO2fert  1 0.1153 0.11533  11.710 0.00106 **
Residuals    67 0.6599 0.00985                   

FMP
             Df Sum Sq Mean Sq F value   Pr(>F)    
Year          1 0.0771  0.0771   12.36 0.000793 ***
CO2fert       1 0.5146  0.5146   82.45 2.75e-13 ***
Year:CO2fert  1 0.1324  0.1324   21.21 1.89e-05 ***
Residuals    67 0.4182  0.0062                     

FMT
             Df Sum Sq Mean Sq F value  Pr(>F)   
Year          1 0.0552 0.05525   3.100 0.08287 . 
CO2fert       1 0.1776 0.17762   9.966 0.00239 **
Year:CO2fert  1 0.0037 0.00374   0.210 0.64833   
Residuals    67 1.1941 0.01782                   

OJP
             Df Sum Sq Mean Sq F value   Pr(>F)    
Year          1 0.2754 0.27540  14.670 0.000285 ***
CO2fert       1 0.0225 0.02247   1.197 0.277825    
Year:CO2fert  1 0.1834 0.18338   9.769 0.002624 ** 
Residuals    67 1.2577 0.01877                     

OJT
             Df Sum Sq Mean Sq F value  Pr(>F)   
Year          1 0.2907 0.29071   7.661 0.00729 **
CO2fert       1 0.1702 0.17017   4.485 0.03792 * 
Year:CO2fert  1 0.0668 0.06678   1.760 0.18916   
Residuals    67 2.5424 0.03795                   
---
Signif. codes:  0 '***' 0.001 '**' 0.01 '*' 0.05 '.' 0.1 ' ' 1
```

Table S4.9.- ANVOVA tables for site OR063. Climate abbreviations for composite climate variables are as follows: June through September precipitation (JSP), June through September temperature (JST), February through March precipitation (FMP), February through March temperature (FMT), previous October through current January precipitation (OJP), previous October through current January temperature (OJT).

OR063

```
JSP
             Df Sum Sq Mean Sq F value   Pr(>F)    
Year          1 0.2061 0.20608  12.586 0.000636 ***
CO2fert       1 0.0874 0.08744   5.340 0.023258 *  
Year:CO2fert  1 0.0350 0.03496   2.135 0.147621    
Residuals    85 1.3918 0.01637

JST
             Df Sum Sq Mean Sq F value   Pr(>F)    
Year          1 0.0000  0.0000   0.001    0.977    
CO2fert       1 0.5196  0.5196  60.863 1.42e-11 ***
Year:CO2fert  1 0.7904  0.7904  92.592 2.97e-15 ***
Residuals    85 0.7256  0.0085

FMP
             Df Sum Sq Mean Sq F value   Pr(>F)    
Year          1 0.3670  0.3670   46.89 1.10e-09 ***
CO2fert       1 0.3306  0.3306   42.24 5.24e-09 ***
Year:CO2fert  1 0.1121  0.1121   14.32 0.000286 ***
Residuals    85 0.6652  0.0078

FMT
             Df Sum Sq Mean Sq F value Pr(>F)  
Year          1 0.1052 0.10519   4.357 0.0398 *
CO2fert       1 0.0483 0.04826   1.999 0.1610  
Year:CO2fert  1 0.1423 0.14229   5.894 0.0173 *
Residuals    85 2.0519 0.02414

OJP
             Df Sum Sq Mean Sq F value   Pr(>F)    
Year          1 0.0033  0.0033   0.130    0.719    
CO2fert       1 0.0542  0.0542   2.157    0.146    
Year:CO2fert  1 1.4696  1.4696  58.488 2.88e-11 ***
Residuals    85 2.1357  0.0251

OJT
             Df Sum Sq Mean Sq F value   Pr(>F)    
Year          1 0.5271  0.5271   28.49  7.7e-07 ***
CO2fert       1 0.2855  0.2855   15.43 0.000173 ***
Year:CO2fert  1 0.0490  0.0490    2.65 0.107251    
Residuals    85 1.5725  0.0185
---
Signif. codes:  0 '***' 0.001 '**' 0.01 '*' 0.05 '.' 0.1 ' ' 1
```

Table S4.10.- ANVOVA tables for site OR009. Climate abbreviations for composite climate variables are as follows: June through September precipitation (JSP), June through September temperature (JST), February through March precipitation (FMP), February through March temperature (FMT), previous October through current January precipitation (OJP), previous October through current January temperature (OJT).

OR009

```
JSP
             Df Sum Sq Mean Sq F value   Pr(>F)
Year          1 0.0683 0.06831   8.954  0.00384 **
CO2fert       1 0.2963 0.29629  38.837 3.18e-08 ***
Year:CO2fert  1 0.0495 0.04946   6.483  0.01313 *
Residuals    69 0.5264 0.00763

JST
             Df Sum Sq Mean Sq F value   Pr(>F)
Year          1 0.0014  0.0014   0.085  0.77210
CO2fert       1 0.7502  0.7502  45.613 3.71e-09 ***
Year:CO2fert  1 0.1572  0.1572   9.558  0.00287 **
Residuals    69 1.1349  0.0164

FMP
             Df Sum Sq Mean Sq F value   Pr(>F)
Year          1 1.1736  1.1736 101.579 3.38e-15 ***
CO2fert       1 0.3091  0.3091  26.758 2.15e-06 ***
Year:CO2fert  1 0.0298  0.0298   2.576    0.113
Residuals    69 0.7972  0.0116

FMT
             Df Sum Sq Mean Sq F value   Pr(>F)
Year          1 0.1217  0.1217   8.034  0.00602 **
CO2fert       1 0.0323  0.0323   2.135  0.14847
Year:CO2fert  1 0.3390  0.3390  22.382 1.15e-05 ***
Residuals    69 1.0451  0.0151

OJP
             Df Sum Sq Mean Sq F value   Pr(>F)
Year          1 0.3725  0.3725  13.835 0.000403 ***
CO2fert       1 0.0542  0.0542   2.012 0.160555
Year:CO2fert  1 0.0753  0.0753   2.797 0.098955 .
Residuals    69 1.8581  0.0269

OJT

             Df Sum Sq Mean Sq F value   Pr(>F)
Year          1 0.3049 0.30487  16.986 0.000103 ***
CO2fert       1 0.0365 0.03647   2.032 0.158548
Year:CO2fert  1 0.0436 0.04355   2.427 0.123859
Residuals    69 1.2384 0.01795
---
Signif. codes:  0 '***' 0.001 '**' 0.01 '*' 0.05 '.' 0.1 ' ' 1
```

Table S.4.11.- ANVOVA tables for site CA675. Climate abbreviations for composite climate variables are as follows: June through September precipitation (JSP), June through September temperature (JST), February through March precipitation (FMP), February through March temperature (FMT), previous October through current January precipitation (OJP), previous October through current January temperature (OJT).

```
CA675

JSP
             Df Sum Sq Mean Sq F value   Pr(>F)    
Year          1 0.5227  0.5227  25.379 2.18e-06 ***
CO2fert       1 0.0825  0.0825   4.007  0.04811 *  
Year:CO2fert  1 0.2081  0.2081  10.104  0.00199 ** 
Residuals    97 1.9977  0.0206                     

JST
             Df Sum Sq Mean Sq F value   Pr(>F)    
Year          1 0.3858  0.3858  23.718 4.33e-06 ***
CO2fert       1 0.1380  0.1380   8.485 0.004445 ** 
Year:CO2fert  1 0.2171  0.2171  13.351 0.000419 ***
Residuals    97 1.5777  0.0163                     

FMP
             Df Sum Sq Mean Sq F value   Pr(>F)    
Year          1 1.5770  1.5770 138.688  < 2e-16 ***
CO2fert       1 0.5723  0.5723  50.333 2.13e-10 ***
Year:CO2fert  1 0.0017  0.0017   0.153    0.696    
Residuals    97 1.1029  0.0114                     

FMT
             Df Sum Sq Mean Sq F value Pr(>F)   
Year          1 0.2027 0.20270   7.216 0.0085 **
CO2fert       1 0.0028 0.00277   0.099 0.7543   
Year:CO2fert  1 0.0401 0.04013   1.428 0.2349   
Residuals    97 2.7250 0.02809                  

OJP
             Df Sum Sq Mean Sq F value   Pr(>F)    
Year          1 0.0001  0.0001   0.004   0.9482    
CO2fert       1 0.1354  0.1354   5.768   0.0182 *  
Year:CO2fert  1 0.8686  0.8686  36.998 2.35e-08 ***
Residuals    97 2.2774  0.0235                     

OJT

             Df Sum Sq Mean Sq F value  Pr(>F)   
Year          1 0.0090 0.00903   0.397 0.52997   
CO2fert       1 0.0606 0.06059   2.665 0.10581   
Year:CO2fert  1 0.1792 0.17916   7.881 0.00604 **
Residuals    97 2.2052 0.02273                   
---
Signif. codes:  0 ‘***’ 0.001 ‘**’ 0.01 ‘*’ 0.05 ‘.’ 0.1 ‘ ’ 1
```

Table S4.12.- ANVOVA tables for site OR006. Climate abbreviations for composite climate variables are as follows: June through September precipitation (JSP), June through September temperature (JST), February through March precipitation (FMP), February through March temperature (FMT), previous October through current January precipitation (OJP), previous October through current January temperature (OJT).

OR006

```
JSP
             Df Sum Sq Mean Sq F value   Pr(>F)    
Year          1 0.4314  0.4314   34.87  1.2e-07 ***
CO2fert       1 0.1976  0.1976   15.97 0.000159 ***
Year:CO2fert  1 0.0000  0.0000    0.00 0.990969    
Residuals    69 0.8535  0.0124                     

JST
             Df Sum Sq Mean Sq F value   Pr(>F)    
Year          1 0.1978  0.1978   8.667  0.00441 ** 
CO2fert       1 0.8176  0.8176  35.828 8.65e-08 ***
Year:CO2fert  1 0.0030  0.0030   0.131  0.71894    
Residuals    69 1.5746  0.0228                     

FMP
             Df Sum Sq Mean Sq F value Pr(>F)  
Year          1 0.0766 0.07664   3.272 0.0748 .
CO2fert       1 0.0031 0.00309   0.132 0.7177  
Year:CO2fert  1 0.0931 0.09311   3.976 0.0501 .
Residuals    69 1.6160 0.02342                 
FMT
             Df Sum Sq Mean Sq F value  Pr(>F)   
Year          1 0.3373  0.3373   8.796 0.00414 **
CO2fert       1 0.0532  0.0532   1.388 0.24276   
Year:CO2fert  1 0.0000  0.0000   0.001 0.97337   
Residuals    69 2.6461  0.0383                   

OJP
             Df Sum Sq Mean Sq F value   Pr(>F)    
Year          1 0.4283  0.4283  17.047 0.000101 ***
CO2fert       1 0.2858  0.2858  11.374 0.001224 ** 
Year:CO2fert  1 0.1843  0.1843   7.335 0.008518 ** 
Residuals    69 1.7337  0.0251                     

OJT
             Df Sum Sq Mean Sq F value Pr(>F)  
Year          1 0.0111 0.01107   1.162 0.2848  
CO2fert       1 0.0267 0.02668   2.799 0.0988 .
Year:CO2fert  1 0.0126 0.01261   1.324 0.2539  
Residuals    69 0.6575 0.00953                 
---
Signif. codes:  0 '***' 0.001 '**' 0.01 '*' 0.05 '.' 0.1 ' ' 1
```

Table S4.13.- ANVOVA tables for site NV518. Climate abbreviations for composite climate variables are as follows: June through September precipitation (JSP), June through September temperature (JST), February through March precipitation (FMP), February through March temperature (FMT), previous October through current January precipitation (OJP), previous October through current January temperature (OJT).

NV518

```
JSP
            Df Sum Sq Mean Sq F value   Pr(>F)    
Year         1 0.5462  0.5462  26.840 1.47e-06 ***
CO2fert      1 0.0430  0.0430   2.114    0.150    
Year:CO2fert  1 0.0000  0.0000   0.002    0.964    
Residuals    85 1.7297  0.0203                     
---

JST
             Df Sum Sq Mean Sq F value   Pr(>F)    
Year          1 0.3638  0.3638  17.094 8.31e-05 ***
CO2fert       1 0.0136  0.0136   0.637    0.427    
Year:CO2fert  1 0.5710  0.5710  26.827 1.47e-06 ***
Residuals    85 1.8091  0.0213                     
---

FMP
             Df Sum Sq Mean Sq F value Pr(>F)    
Year          1 2.1462  2.1462 128.008 <2e-16 ***
CO2fert       1 0.0024  0.0024   0.140 0.7088    
Year:CO2fert  1 0.0983  0.0983   5.865 0.0176 *  
Residuals    85 1.4251  0.0168                   
```

```
FMT
             Df Sum Sq Mean Sq F value   Pr(>F)    
Year          1 0.8355  0.8355  54.903 8.60e-11 ***
CO2fert       1 0.2591  0.2591  17.025 8.57e-05 ***
Year:CO2fert  1 0.0510  0.0510   3.348   0.0708 .  
Residuals    85 1.2936  0.0152                     
---

OJP
             Df Sum Sq Mean Sq F value Pr(>F)  
Year          1 0.0602 0.06019   1.913  0.170  
CO2fert       1 0.0346 0.03458   1.099  0.297  
Year:CO2fert  1 0.1831 0.18314   5.821  0.018 *
Residuals    85 2.6743 0.03146                 
---


OJT
             Df Sum Sq Mean Sq F value   Pr(>F)    
Year          1 0.1722  0.1722  10.271   0.0019 ** 
CO2fert       1 0.8279  0.8279  49.378 4.91e-10 ***
Year:CO2fert  1 0.1300  0.1300   7.756   0.0066 ** 
Residuals    85 1.4251  0.0168                     
---
Signif. codes:  0 '***' 0.001 '**' 0.01 '*' 0.05 '.' 0.1 ' ' 1
```